ALPHA LYRAE/SUN FLUX RATIOS FOR USE IN STANDARD STAR CALIBRATIONS: RESULTS OF THREE TECHNIQUES

by

SUSAN NYGARD

B.A., Wellesley College
1974

SUBMITTED IN PARTIAL FULFILLMENT

OF THE REQUIREMENTS FOR THE

DEGREE OF MASTER OF

SCIENCE

at the

MASSACHUSETTS INSTITUTE OF

TECHNOLOGY

September, 1975

Signature of Author.....
Department of Earth and Planetary Sciences,
August, 1975

Certified by....
Thesis Supervisor

Accepted by.....
Chairman, Departmental Committee on Graduate
Students, Earth and Planetary Sciences

ALPHA LYRAE/SUN FLUX RATIOS

FOR USE IN

STANDARD STAR CALIBRATIONS:

RESULTS OF THREE TECHNIQUES

by

SUSAN NYGARD

Submitted to the Department of Earth and Planetary Sciences on September, 1975 in partial fulfillment of the requirements for the degree of Master of Science.

ABSTRACT

Three techniques were used to improve the relative calibration of Alf Lyr/Sun for filters in the spectral region of 0.33-1.10μM. These methods were:

(1) To use an Apollo 16 lunar soil sample as an object of known reflectivity
(2) To use absolute calibrations of Alpha Lyrae and the sun
(3) To compare the sun with solar-type stars.

Method (1) was the most reliable. It indicated that the model Alf Lyr/Sun flux ratios currently used by the MIT Remote Sensing Laboratory had systematic errors. The flux ratio of the 0.40μM filter in the old calibration was too low by 7-11% and the flux ratio for the 0.87μM filter was too high by 6-10%. Systematic errors of 1-3% existed throughout the region. The results of methods (2) and (3) were less reliable.

Thesis Supervisor: Thomas B. McCord
Title: Associate Professor of Planetary Physics

Acknowledgements

I wish to thank Dr. Thomas B. McCord for his help and support during this thesis. I would also like to thank Ms. Carlè Pieters and Dr. Michael J. Gaffey for suggesting this problem to me and for much moral support and professional advice. I especially wish to thank Dr. Robert L. Kurucz, Visiting Astronomer from Kitt Peak National Observatory, presently at the Center for Astrophysics, Cambridge, Mass., for providing me with his new Alpha Lyrae model spectrum in advance of publication. My thanks also to the MIT Remote Sensing Laboratory computer programmers George Fawcett and Paul Kinnucan for programming assistance and to the summer employees who provided me with data in several areas and who did much Calcomp plotting for me. My thanks to my roommate and office partner and to all of my other student colleagues and friends who saw me through this trying time.

This research was supported by an Amelia Earhart Fellowship awarded by Zonta International and by NASA grant NGR22-009-473.

Table of Contents

List of Figures

Note: Many of these figures were made using the program Dataplot (see Appendix A). All star/star graphs should be labelled "flux ratio normalized at 0.57μM" rather than spectral reflectance. Many of these figures also appearon sheets that have two page numbers. No pages are missing.

List of Tables

I. Introduction

For many years Alpha Lyrae, also known as Vega, has been the primary standard star used by astronomers for atmospheric and instrumental calibration when making their telescopic observations. The electromagnetic radiation of a solar system object consists of two parts: (1) a component of reflected solar radiation defined as spectral reflectance and (2) solar radiation which has been absorbed, converted to heat, and reemitted as thermal radiation. Thus planetary astronomers studying spectral reflectance also need to know the Alf Lyr/Sun flux ratio for specific wavelengths precisely. Secondary standard stars can then be calibrated relative to Alf Lyr.

In 1972 Elias calculated a relative Alf Lyr/Sun calibration from absolute calibrations of the two stars. He used the solar calibration of Arvesen, Griffin, and Pearson (3) and the model Alpha Lyrae spectrum of Schild, Peterson, and Oke (25). He then calculated the ratios of the effective fluxes of the sun and Alpha Lyrae for various filter wavelengths. Such an effective flux is given by:
$F_c = \int T_f(\lambda) F(\lambda) T_a(\lambda) R(\lambda) d\lambda$, $F(\lambda)$ defined as the absolute energy spectrum of the star, T_f defined as the filter response, T_a defined as the atmospheric transmission function, and R defined as the instrument response (5). Since that time, however, errors in this calibration have been dis-

covered. For example, the 0.87μM filter is too high in the Alf Lyr/Sun flux ratio, giving unreasonable discontinuities between adjacent filters in subsequent reflectance measurements of solar system objects. Similarly, the Alf Lyr/Sun flux ratio for the 0.40μM filter in the Balmer region is too low. Hence the need existed for a new Alf Lyr/Sun relative calibration to be calculated.

The methods attempted in this thesis to better determine the Alf Lyr/Sun flux ratios for the 25 filters of the photometer data system were:

(1) Using an object of known reflectivity--The reflectance of Apollo soil samples measured in the laboratory were taken as representative of the telescopic reflectance of standard Apollo lunar areas. Fluxes of the following type were measured and multiplied:

$$\left(\frac{\text{Alf Lyr}}{\text{Apollo Site}}\right)_{\text{Telescope}} \cdot \left(\frac{\text{Apollo Lunar Sample}}{\text{MgO}}\right)_{\text{Lab}} \approx \frac{\text{Alf Lyr}}{\text{Sun}}$$

(2) Using absolute calibrations of Alpha Lyrae and the sun--An Alpha Lyrae spectrum from an improved theoretical model by Kurucz (12) which better agreed with the improved absolute calibration of Hayes, Latham, and Hayes (9) was ratioed versus the observational solar spectrum of Arvesen, Griffin, and Pearson (3).

(3) Using solar-type stars--Telescopically measured ratios of Alf Lyr versus solar-type stars were averaged.

In actuality, however, the major effort was directed towards completion of method 1. Method 2 should be attempted again after the entire Alpha Lyrae model spectrum of Kurucz becomes available. Very little data existed for method 3.

The observational data used in this thesis were gathered during four observing runs: Run II at Mt. Wilson Observatory, Pasadena, California on the 24-inch telescope, August 29-September 5, 1974; Run III at the Cerro Tololo Inter-American Observatory, La Serena, Chile on the 36-inch telescope, September 26-October 8, 1974; Run IV at Cerro Tololo on the 36-inch telescope, January 26-31, 1975; Run V at Cerro Tololo on the 36-inch telescope, March 6-11, 1975. A dual-beam photometer with an ITT fw-118 photomultiplier tube with S-1 photocathode was used for data gathering. Two similar but different filter sets were used, called "Wallace" and "Spectrum" or "25*". The filters ranged in wavelength coverage from 0.33μM to 1.10μM spaced at intervals of 0.3μM. A "run" was defined as a complete sequence of measurements using the 25 filters and requiring about two minutes.

The theoretical data used in the Alf Lyr/Sun calibration via absolute calibrations (method 2) came from two sources. For the wavelength region 0.33-o.82μM the Alpha Lyrae spectrum of Schild, Peterson, and Oke (25) was used. This model used the parameters of effective temperature,

T_{eff}=9650°K, and gravity, log g=4.05. The model agreed well with the continuum indicators and the H_α, H_β, H_γ profiles made at that time by Oke and Schild (23). It disagreed with the observations of Hayes (7), however, by 7% across the Paschen discontinuity. Since then Hayes and Latham (8) have corrected the Oke and Schild observations and have added some observations of their own to calculate a new energy distribution for Alpha Lyrae. A correction in calculating extinction coefficients helped lead to improved results. Kurucz (12) has used these observations to compute a theoretical model (T_{eff}=9400°K; log g=3.95) which is quite consistent ($\pm$2-$\pm$3% at worse) with the new Hayes, Latham, and Hayes absolute flux calibration. This model was used for the wavelength region 0.82-2.00μM and is shown in Figure (III-1). (The data for the 0.33-0.82μM region was not yet available at the time these calculations were done.)

II. Relative Calibration via Lunar Sample

A. Introduction

The major efforts of the author were directed towards this technique of calculating Alf Lyr/Sun flux ratios for the 25 narrow-band interference filters evenly spaced between 0.33μM and 1.10μM. The main assumption made was that the spectral reflectance of an Apollo landing site (eg. Apollo 16) as seen at the telescope was the same as that measured in the laboratory of a returned lunar soil sample. The laboratory standard, MgO, approximated a perfect Lambert surface so that MgO/Sun ≈ 1. Thus:

$$\left(\frac{\text{Alf Lyr}}{\text{Apollo 16}}\right)_{\text{Telescope}} \cdot \left(\frac{\text{Apollo 16 soil sample}}{\text{MgO}}\right)_{\text{Lab}} \approx \frac{\text{Alf Lyr}}{\text{Sun}}$$

Mare Serenitatis, labelled "MS2," is a standard lunar telescopic spot in Mare Serenitatis located at $18^{\circ}40'$N, $21^{\circ}25'$E. During Run II and Run IV the Apollo 16 spot observed was labelled "Ap 16." During Run III the Apollo 16 spot observed was labelled "Ap 16B" or "Ap 16'." The Ap 16 spot is shown in Figure (II-1); the Ap 16B spot is located ¼ inch to the upper left of the Ap 16 spot. This picture was taken when Ap 16 was near the terminator; the data was not taken at this time. Since MS2 was the standard lunar area to which all other lunar observations were compared, ratios of the following form entered into the calculation:

$$\left(\frac{\text{Alf Lyr}}{\text{MS2}}\right) \cdot \left(\frac{\text{MS2}}{\text{Ap 16 or Ap 16B}}\right)$$

If Alpha Lyrae (Alf Lyr) was not observed for a particular night, then other star/star ratios also entered into the computation in order to obtain the desired Alf Lyr/MS2 ratio. Thus, in its most complicated form the factors in the multiplication were:

$$\underbrace{\left(\frac{\text{Alf Lyr}}{\text{Star 1}}\right)\left(\frac{\text{Star 1}}{\text{Star 2}}\right)}_{\text{previously measured at telescope}}\underbrace{\left(\frac{\text{Star 2}}{\text{MS2}}\right)\left(\frac{\text{MS2}}{\text{Ap 16 or Ap 16B}}\right)\left(\frac{\text{Ap 16 sample}}{\text{MgO or Sun}}\right)}_{\text{telescope}} \approx \frac{\text{Alf Lyr}}{\text{Sun}}$$

Thus, Steps 1,2,3, and 4 of the data reduction program consisted of:

Step (1) Measure (telescope) Alf Lyr/MS2

Step (2) Measure (telescope) MS2/Ap 16 or MS2/Ap 16B

Step (3) Measure (laboratory) Ap 16 soil sample/Sun

Step (4) Calculate Alf Lyr/Sun from Steps 1-3.

The results of applying the above steps was an Alf Lyr/Sun flux ratio for each of 17 nights with different phases of the moon. It has been shown by Lane and Irvine (18) and others that the slope of the spectral reflectance of the moon changes with phase and that the amount of change is dependent upon the wavelength region being observed. Thus, the next step, Step 5, was to reduce all the Alf Lyr/Sun flux ratios to one reference phase. This required deriving a phase function for our lunar observations. A phase function is defined as a function which describes how the ab-

solute intensity of the moon's reflected light varies with phase angle for various wavelength regions. As used here a phase function will describe how the relative intensity, rather than absolute intensity, varies with phase angle and wavelength region. Alf Lyr/Sun flux ratios for the 17 nights were plotted versus phase angle for each of the 22 filters for the region 0.37μM to 1.06μM. The deletion of the 0.33, 0.35, and 1.10μM filters will be discussed in section II.B.4. Linear and cubic fits were then applied to the 22 graphs and a phase function derived. The application of this phase function to the 17 nights to obtain 17 Alf Lyr/Sun flux ratios for a standard phase completed Step 5. The details of this computation will be discussed in section II. B.5.

Step 6 consisted of averaging the individual Alf Lyr/Sun flux ratios reduced to the reference phase to obtain a final new Alf Lyr/Sun flux ratio for the 22 filters covering the 0.37μM to 1.06μM wavelength region.

A description of the data reduction programs can be found in Appendix A. Referral should also be made to the Tables and Figures at the end of this section.

B. Data Reduction

1. Step 1--Calculation of $(MS2/Alf\ Lyr)^{-1}$ from telescopic measurements

During Run II the Wallace filter set was used on August 30 and September 1. The Spectrum filter set was used for all other nights. The 0.86μM filter was later discovered to be leaky. Corrections were made for this leak in subsequent data reduction. Alf Lyr was the standard star observed each night. Ratios of the form $(MS2/Alf\ Lyr)^{-1}$ were calculated. The phase angle, defined as the angle formed by the sun-moon-observer, varied from -28° before full moon, to a minimum of -6°, to $+41^{\circ}$ after full moon. Although there were lunar observations available for September 2 and 3, no stellar observations were made. Thus, it was not possible to calculate Alf Lyr/Sun flux ratios for these nights.

Standard errors for each filter for the MS2/Alf Lyr flux ratios were generally less than $\pm 0.5\%$; the largest error of $\pm 1.9\%$ occurred for the 0.33μM filter for August 30 (see Appendix A "Mushkin" for definition of standard error).

During Run III the Wallace filter set was used on September 30 while the Spectrum filter set was used on all other nights. The 1.10μM filter of the Spectrum filter set was later discovered to be faulty for this run. The standard for all Run III nights except September 27 and 30 was Alpha Aquarii (Alf Aqr). Thus, ratios of the following form were calculated: $(MS2/Alf\ Aqr)^{-1}(Alf\ Aqr/Alf\ Lyr)^{-1}$. The phase

coverage for this run varied from -56^{o} to a minimum of -5^{o} to $+59^{o}$. This was the largest phase coverage for a single observing Run. The addition of the Alf Aqr/Alf Lyr flux ratio in the above multiplication presented another source of error in the calculation. The Alf Aqr/Alf Lyr flux ratio used was determined by averaging individual ratios measured during the nights of September 4, 5, and 6 during Run II at Mt. Wilson. A total of 47 independent runs were averaged. The largest standard error for this average was $\pm$0.9% for the 0.33μM filter; the error was even smaller ($\pm$0.3%) for the other filters.

For September 30, the only Run III night for which the Wallace filters were used, the Alf Lyr/Sun flux ratio was calculated in two ways. One method used Xi^{2} Ceti (Xi2 Cet) as the standard and the Xi2 Cet/Alf Lyr flux ratio determined from 15 independent runs on August 30 and September 1 (RunII) using the Wallace filter set, i.e. $(MS2/Xi2Cet)^{-1}(Xi2Cet/AlfLyr)^{-1}$ The second method used Alf Aqr as the standard and the Alf Aqr/Alf Lyr flux ratio mentioned above, although this ratio was determined using the Spectrum or 25* filter set. The Xi2 Cet/Alf Lyr ratio had standard errors approximately 0.5% larger than the Alf Aqr/Alf Lyr ratio. Also the MS2/Xi2 Cet flux ratio was slightly noisier than the MS2/Alf Aqr ratio. A comparison of the same star ratios for several spectral types measured by both filter sets in-

dicated that there were no systematic differences in flux ratios as determined by the two different sets. Thus, the Alf Lyr/Sun flux ratio computed using Alf Aqr as the standard was used in subsequent data reduction.

On September 26 there was insufficient air mass coverage to compute any extinction curves for use in ratioing MS2/Star or Star/MS2. There was also insufficient air mass coverage to compute any stellar extinction curves for September 27. However, in this case, the air mass coverage did permit MS2 to be used as a standard and 10 Tau/MS2 and Xi2 Cet/MS2 flux ratios to be calculated. The 10 Tau/Alf Aqr link determined from 34 runs for September 28 and 29 and October 1 had its largest standard error of 1.5% for the 1.06μM filter, but had typical errors of ±0.5%-±0.7% for the other filters. The Xi2 Cet/Alf Aqr flux ratio, determined from 30 runs for September 29 and October 6 and 7, had larger standard errors, being ±1.0% at 0.89μM and increasing to ±2.6% at 1.06μM. The Xi2 Cet/MS2 ratio was also noisier than the 10 Tau/MS2 ratio. Thus, the Alf Lyr/Sun calculated using 10 Tau as the standard was used in further data reduction.

The MS2/Alf Aqr flux ratios for September 28 and 29, October 1, 4, and 5 were all quite good, having errors averaging ±0.5%. October 6 was noisier with ±1.4% errors.

For Run IV only the Spectrum filter set was used. The 1.10μM filter was replaced by a second 0.86μM filter; this

second 0.86μM filter was later discovered to be leaky and corrections were made. During this Run the standard stars were Omicron Tauri (Omi Tau) and Gamma Geminorum (Gam Gem). The phase angle varied from -19° to a minimum of $+11^{\circ}$ to $+54^{\circ}$. Omi Tau and Gam Gem were both suitable for standards for the night of January 28. Both MS2/Omi Tau and MS2/Gam Gem flux ratios had standard errors of less than $\pm$0.5%. However, the Gam Gem/Alf Aqr link determined from 14 independent runs on October 1 and 8 had statistical errors about 1% larger than the Omi Tau/Alf Aqr link determined from 42 independent runs on September 28 and 29 and October 7 and 8 ($\pm$0.6-$\pm$0.7%). Thus, the MS2/Omi Tau flux ratio was used to calculate Alf Lyr/Sun for this night. The standard for January 29 was Omi Tau; MS2/Omi Tau had standard errors of $\pm$0.2-$\pm$0.3%. The standard for January 30 was Gam Gem; MS2/Gam Gem had errors of $\pm$0.3-$\pm$0.4%. And the standard for January 31 was Omi Tau with the MS2/Omi Tau flux ratio having $\pm$0.2-$\pm$0.3% errors.

2. Step 2--Calculation of $(Ap\ 16/MS2)^{-1}$ or $(Ap\ 16B/MS2)^{-1}$ from telescopic measurements

Two methods were tested for calculating Ap 16/MS2 flux ratios. In one method the individual Ap 16 runs were ratioed versus the individual MS2 runs which were near in time (<15 minutes) to the Ap 16 observations. These individual flux ratios were then averaged. The second method was to compute a lunar extinction curve using the same MS2 observations used in method 1. The Ap 16 observations were then ratioed versus this standard and averaged. The purpose of calculating an extinction curve is so that an individual object run at a specific air mass can be ratioed versus the standard at the same air mass (as derived from the extinction formula). This procedure also resulted in a smoothing factor being applied to the MS2 component of the ratio. It is known from laboratory work (19) that such lunar reflectance curves should be smooth. Thus, the second method which gave smoother spectral reflectance curves for Ap 16/MS2 was chosen for all moon/moon data reduction (see Figure (II-2) for examples of these two methods).

For Run II standard errors for the Ap 16B/MS2 flux ratios were largest for August 30 and 31 and September 2, reaching approximately $\pm$2% for some filters. Typical errors for the other nights were $\pm$0.5-$\pm$1.0%. Most of this error was attributed to the poor guiding of the telescope on the lunar area due to a lack of declination tracking rate.

The Ap 16/MS2 flux ratios for Run III were quite good with ±0.5% errors for all nights except October 5 and 6 which had standard errors of approximately ±1.0%. On October 6 our MS2 telescopic spot was very close to the terminator. As a result, the photon counts/second were abnormally low requiring no subtraction of scattered light (see Appendix A "Subtract"). For all Run IV nights the Ap 16B/MS2 flux ratios had standard errors of about ±0.5%.

There were a total of 21 nights for which Ap 16/MS2 or Ap 16B/MS2 flux ratios were calculated. These nights gave a total phase angle coverage of a maximum of -56° and a minimum of -5° before full moon, and a maximum of $+59^{\circ}$ and a minimum of $+8^{\circ}$ after full moon. The 21 spectral reflectance curves were then analyzed to determine whether systematic differences existed (1) for Ap 16/MS2 flux ratios compared to Ap 16B/MS2 flux ratios, (2) for flux ratios before full moon compared to flux ratios after full moon for equivalent phase angles, and (3) for changes in general shape and slope of the curves with changing phase angle. It was determined that there were no systematic differences for Ap 16/MS2 versus Ap 16B/MS2; the two spots were telescopically the same. Thus, it was not necessary to select two lunar samples, one for each Ap 16 site, for use in further data reduction (see section II.B.3.). It was also determined that the sign of the phase angle, i.e. before or after full

moon, did not affect the flux ratios. Thus, the absolute value of the phase angle could be used when the Alf Lyr/Sun flux ratios for each night were reduced to a single reference phase (see section II.B.5.). The 21 spectral reflectance curves were analyzed for systematic changes in shape and slope with changes in the absolute value of the phase angle. As stated previously, we know from laboratory work (19) that the relative reflectance curves should be smooth. It is therefore justifiable to smooth the observed relative reflectance curves to eliminate discontinuities. (For example, one large discontinuity of 8% between the 0.89μM filter and the 0.93μM filter for the September 30 data could have been smoothed.) The Alf Lyr/Sun calibration was continued using the uncorrected Ap 16/MS2 or Ap 16B/MS2 flux ratios. An analysis of the derived phase functions for each filter (see section II.B.5.) indicated that enough data existed for such errors to cancel out. Hence, the tedious task of smoothing the Ap 16/MS2 or Ap 16B/MS2 flux ratios was not required.

3.Step 3--Calculation of (Ap 16 soil sample/Sun) from laboratory measurements

The major assumption made in this analysis was that the spectral reflectance of an Apollo landing site received at the telescope was the same as that measured in the laboratory of a returned lunar soil sample from that site. Apollo 16 was a complicated landing site since there were two relatively fresh craters nearby which could have contaminated the surrounding area with their ejecta. Care had to be taken to choose a sample which was representative of the lunar soil in the areas of our telescopic spots. From Step 2 it has been shown that the two Ap 16 telescopic spots were similar, thus only one lunar sample needed to be selected for use in further data reduction.

The following criteria were used to select the lunar sample: (1) particle size of the returned sample, (2) weight percentage of agglutinates in the sample, and (3) station location in relation to our telescopic spots. The sample chosen needed to be a surface soil sample; this particle size ($<$ 1mm) is representative of the lunar surface, whereas large rocks and boulders are not representative (19). The two Ap 16 spots appeared homogeneous photographically and when viewed through the telescope (no rays, small bright craters, etc.) implying that the areas consisted of a mature soil. It has also been shown that as a lunar soil matures, the

percentage of dark, glass-welded agglutinates increases. The agglutinates are believed to be produced by micrometeoroid-impact melts which weld particles together (2). It has also been suggested that the immature soils in this Descartes area are derived from two rock types: those rich in light breccias, those rich in dark breccias, and their mixtures (2). However, the spectral reflectivities of all Apollo 16 soils are lowered and approach the same values for specific wavelengths as they mature. Thus, the lunar sample selected needed to be high in weight percentage of agglutinates to insure that it was a mature, homogeneous soil. The sample station location relative to our telescopic spots was also considered. The station area had to be homogeneous and clear of crater ejecta. Lunar sample 62230, from station 2, fulfilled these criteria the best. This surface soil sample was located near the southeast rim of Buster Crater approximately equidistant from our telescopic spots. It had 55% weight percentage agglutinates and was therefore a mature soil in the area (see Figure (II-1) for location of Ap 16 and Ap 16B spots).

The Beckman DK-2A ratio recording spectroreflectometer at the Caribbean Research Institute Laboratory was used to measure the diffuse reflectance of sample 62230 for wavelengths of 0.35μM to 2.5μM at intervals of 0.005μM. The sample was positioned inside an MgO-lined integrating sphere.

(Sandblasted gold and freshly smoked MgO are usual standards.) Light then entered the sphere through an aperture, hit the sample, was diffusely reflected from the sides of the sphere, and was measured through a second aperture located 90 degrees from the source aperture and sample. The sample was oriented so that unwanted specular components of the measurements from glasses, etc. were removed, leaving only the diffuse component of reflectivity (1). In order to calculate the sample reflectance at the specific wavelengths of the Wallace and Spectrum filters, an interpolation program was used (6). This program did a lunar interpolation for each desired wavelength using the reflectance measurements for the nearestpoint to the specific filter wavelength and the closest two points on both sides of this measurement. Since there were no measurements made below 0.36μM, the 0.33μM and 0.35μM filters were omitted from further data reduction. The reflectance of the lunar sample could be measured to within ±0.1%, thus no standard error of the mean was associated with these measurements. A graph of spectral reflectance versus wavelength for sample 62230 normalized at 0.57μM for the Wallace and Spectrum filter sets can be seen in Figures (II-3) and (II-4).

To verify that the Alf Lyr/Sun flux ratio calculated via this lunar sample method was not a function of the particular Apollo landing site or sample selected, the procedure

was also carried out using a different lunar sample and telescopic spot. From many previous studies (19) it has been found that the telescopic reflectance of MS2 is approximately the same as the reflectance measured in the laboratory for lunar sample 12070 taken from an Apollo 12 landing site. The spectral reflectance curves exhibit a difference of approximately 2% in the near infrared. The following calculations were done for the nights of September 28 and 29 and October 1, 4, 5, and 6 during Run III:

$$\left(\frac{\text{MS2}}{\text{Alf Aqr}}\right)^{-1} \cdot \left(\frac{\text{Alf Aqr}}{\text{Alf Lyr}}\right)^{-1} \cdot \left(\frac{\text{Lunar sample 12070}}{\text{Sun}}\right) = \frac{\text{Alf Lyr}}{\text{Sun}}$$

These flux ratios were then divided by the Alf Lyr/Sun flux ratios derived by Elias and modified by Gaffey for the Spectrum filter set. The results when using the Apollo 12 sample showed the same systematic changes as those when the Apollo 16 sample was used. (see Figures (II-5,6,41-45)--The error bars in these figures are those of the lunar Alf Lyr/Sun calibration; errors were not assigned to the model calibration.) The exact values differed by $\pm$1.5-$\pm$2.0% in most cases and by no more than $\pm$4.0% for a few isolated filters for particular nights. Thus, it was safe to conclude that the Apollo landing site and sample selected gave accurate results and did not systematically affect the Alf Lyr/Sun flux ratio calibration.

4. Step 4--Calculation of Alf Lyr/Sun from Steps 1-3

The measured fluxes were then multiplied in the following form to obtain Alf Lyr/Sun flux ratios for each of the 17 nights:

$$\left(\frac{\text{MS2}}{\text{Star 1}}\right)^{-1} \cdot \left(\frac{\text{Star 1}}{\text{Star 2}}\right)^{-1} \cdot \left(\frac{\text{Star 2}}{\text{Alf Lyr}}\right)^{-1} \cdot \left(\frac{\text{Ap 16,16B}}{\text{MS2}}\right)^{-1} \cdot \left(\frac{\text{Ap sample}}{\text{Sun}}\right) \approx \frac{\text{Alf Lyr}}{\text{Sun}}$$

The main variation was a slope change from one phase to the next. For Run II August 30 and 31 had the largest standard errors, averaging about 2%. September 4, 5, and 6 averaged about $\pm$0.7% standard errors. For Run III September 28 and 29 and October 1 all had errors averaging about $\pm$0.8%. October 4 and 5 had about $\pm$1.0% errors. And September 27 and October 6 had the largest standard errors averaging about $\pm$1.5%. January 30 of Run IV also had errors averaging $\pm$1.5% while January 28,29, and 31 had errors of about $\pm$1.0%. (see Fig7-40)

Thus, using less well determined intermediary standards in order to calculate MS2/Alf Lyr flux ratios (see section II.B.1.) for Run IV resulted in slightly larger standard errors of the means. The nights were all weighted equally in subsequent data reduction, however, since the differences were not large.

These flux ratios were divided by the Alf Lyr/Sun flux ratios derived by Elias and modified by Gaffey for the Spectrum filter set. The resulting plots (see Figures (II-41-45)) showed the systematic differences between the two. In these

plots the 0.40μM filter in the Balmer region was observed to be too high, the 0.87μM filter was observed to be too low, and the entire region appeared snake-like. The amplitudes of the curves showed 4-8% deviations. The differences are believed to be due to systematic errors in the model Alf Lyr/Sun calibration resulting from errors in the stellar fluxes used. An alternative, but unlikely, explanation is that the instrumental response of the spectroreflectometer used to measure the spectral reflectance of the lunar sample was such that MgO/Sun was not equal to unity at all wavelengths.

5. Step 5--Reduction of Alf Lyr/Sun flux ratios to a reference phase

The slope of the spectral reflectance of the moon varies with phase, and the amount of variation is dependent upon the wavelength being observed (18). Thus it was necessary to reduce the 17 Alf Lyr/Sun flux ratios to a reference phase before averaging the results. A phase function, as defined here, describes how the relative intensity varies with phase angle and wavelength. The 17 Alf Lyr/Sun flux ratios were plotted against the absolute value of the phase angle for each of the 22 filters, 0.37μM to 1.06μM. (Note that the 0.33μM and 0.35μM filters were deleted because the lunar sample laboratory measurements were not done for these wavelengths (see section II.B.3.). Also the 1.10μM filter was deleted because it was faulty during Run III and omitted for Run IV.) Linear and cubic fits were then done for each plot. The scatter of points was such that either fit was suitable. The linear fits were used to determine the change in the Alf Lyr/Sun flux ratio per degree phase angle for each of the 22 filters. Typical phase function graphs are shown in Figure (II-46). These phase coefficients were then plotted versus wavelength. It can be seen (see Figure (II-47) that there is a very large, steep rise in the rate of change of the flux ratio for the ultraviolet region. The change in color per degree of phase angle is approximately constant for

the wavelength region 0.60-1.10μM.

The next step was to determine which phase angle should be used as the reference phase for comparison with the lunar sample. The original idea was to calculate the effective phase angle that the spectroreflectometer measeured in the laboratory for lunar sample 62230. The MgO-lined integrating sphere was treated as a Lambert surface. Thus, the reflectance was not a function of wavelength. However, as discussed above, the phase function was observed to be a function of phase and wavelength. Hence, a single effective phase angle could not be equated to a lunar phase angle for all wavelengths. The author next tried to match the Alf Lyr/Sun flux ratios to the Alf Lyr/Sun flux ratio derived in section III using absolute calibrations of the sun and Alpha Lyrae. As discussed in section III, the best known wavelength region is the Paschen discontinuity (0.80-1.04μM). However, the Alpha Lyrae model used had it largest discrepancy with the observations in this area. Each of the 17 Alf Lyr/Sun flux ratios were divided by the calibration of section III. The results, shown in Figures (II-48,49), were not conclusive.

It was decided to use reference phase angles of 20°,25°, 30°,35°, and 40° and calculate Alf Lyr/Sun flux ratios for each of these angles. This region was selected because it is known that observations at large phase angles have a high degree of polarization which implies a large specular com-

ponent of the reflectance. The spectroreflectometer, as mentioned previously, measured only the diffuse component of the reflectance of sample 62230. Hence, a small phase angle, which has a largercomponent of diffuse reflectance than a large phase angle, was a more suitable choice for the reference phase angle.

The difference between the phase angle at the time of observation and the reference phase angle times the phase coefficient for a particular filter gave the correction that was added to the flux ratio for that filter. The Alf Lyr/Sun flux ratios for each filter and each night were corrected in this manner.

6. Step 6--Calculation of the final Alf Lyr/Sun flux ratios

The set of flux ratios for each reference phase angle of 20°, 25°, 30°, 35°, and 40° were averaged together to give final Alf Lyr/Sun flux ratios. The results are shown in Figures(II-50-59). Standard errors of the mean of $\pm$2% were typical. These values were divided by the Alf Lyr/Sun flux ratios calculated by Gaffey for the Spectrum filter set using the absolute calibration method of Elias. The results are shown in Figure (V-1) and are discussed in section V.

Table II-1

Standards for Data Reduction

Key: W is defined as Wallace filter set

25*-1 is defined as Spectrum filter set but with leaky 0.86μM filter

25* is defined as Spectrum filter set

25*? is defined as Spectrum filter set but with suspicious 1.10μM filter

1-24* is defined as Spectrum filter set for 0.33μM to 18 1k 1.06μM; 1.10μM filter replaced by leaky 0.86μM filter

1-24* is defined as Spectrum filter set for 0.33μM to 1.06μM; 1.10μM filter omitted

**See Appendix A "Mumpit"

Name	Date	Filter Set	Numb. of Indp. Runs	Minimum Airmass	Maximum Airmass
Run II					
Alf Lyr	8/30	W	4	1.25	2.06
Alf Lyr	8/31	25*-1	5	1.17	2.21
Alf Lyr	9/01	W	6	1.04	2.01
Alf Lyr	9/04	25*-1	11	1.09	2.00
Alf Lyr	9/05	25*-1	6	1.23	2.07
Alf Lyr	9/06	25*-1	9	1.22	1.77
Run III					
MS2	9/27	25*?	20	1.06	2.73
Alf Aqr	9/28	25*?	12	1.21	2.55
Alf Aqr	9/29	25*?	18	1.16	3.50
Alf Aqr	9/30	W	13	1.17	1.76
Xi^2 Cet	9/30	W	20	1.28	1.42
Alf Aqr	10/1	25*?	13	1.16	1.97
Alf Aqr	10/4	25*?	21	1.16	2.04
Alf Aqr	10/5	25*?	15	1.16	1.80
Alf Aqr	10/6	25*?	11	1.16	1.62

Table II-1
(Cont.)

Name	Date	**Max. ln $\frac{I}{I_o}$ for 1 Airmass	Weather Conditions	Subj. Qual. Ratings 1:Excel. 5:Poor
Run II				
Alf Lyr	8/30	+0.003	Clear	3
Alf Lyr	8/31	+0.02	Visible seeing	2
Alf Lyr	9/01	-0.07	Clear	2
Alf Lyr	9/04	-0.14	Clear	1
Alf Lyr	9/05	-0.003	Clear	1
Alf Lyr	9/06	-0.01	Turbulent seeing	1
Run III				
MS2	9/27	-0.41	Clouds	1
Alf Aqr	9/28	+0.03	Fair	1
Alf Aqr	9/29	+0.07	Fair	1
Alf Aqr	9/30	-0.004	Clouds	2
Xi^2 Cet	9/30	+0.25	Clouds	Small airmass coverage
Alf Aqr	10/1	+0.04	High thin clouds	1
Alf Aqr	10/4	+0.01	Hazy	1
Alf Aqr	10/5	-0.03	Hazy	2
Alf Aqr	10/6	+0.04	Hazy	2

Table II-1
(Cont.)

Name	Date	Filter Set	Numb. of Indp. Runs	Minimum Airmass	Maximum Airmass
Run IV					
Omi Tau	1/28	1-24*, 18 1k	14	1.31	1.80
Gam Gem	1/28	1-24*, 18 1k	14	1.48	1.78
Omi Tau	1/29	1-24*, 18 1k	18	1.36	2.02
Gam Gem	1/29	1-24*, 18 1k	18	1.54	1.65
Gam Gem	1/30	1-24*, 18 1k	13	1.50	1.66
Omi Tau	1/31	1-24*, 18 1k	23	1.39	2.30
Run V					
Gam Gem	3/10	1-24	10	1.68	2.48
Gam Gem	3/11	1-24	8	1.60	2.04

Table II-1
(Cont.)

Name	Date	**Max. $\ln \frac{I}{I_o}$ for 1 Airmass	Weather Conditions	Subj. Qual. Ratings 1:Excel. 5:Poor
Run IV				
Omi Tau	1/28	+0.05	Hazy/Clouds	2
Gam Gem	1/28	-0.06	Hazy/Clouds	2
Omi Tau	1/29	-0.00	Thin clouds	1
Gam Gem	1/29	+0.09	Thin clouds	3
Gam Gem	1/30	+0.43	Fair	Small airmass coverage
Omi Tau	1/31	-0.01	Clear	1
Run V				
Gam Gem	3/10	+0.05	Clear	2
Gam Gem	3/11	-0.01	Clear	1

Table II-2

Ratios used to Calculate $\frac{\text{Alf Lyr}}{\text{MS2}}$

Key: See Table I

Ratio	Date	Filter Set	No. Ind. Runs	Lg. Std. Error (%)	Filter (μM)	Typical Error (%)
Run II						
MS2/Alf Lyr	8/30	W	8	1.90	0.33	0.6
MS2/Alf Lyr	8/31	25*-1	11	1.68	0.33	0.5
MS2/Alf Lyr	9/01	W	15	1.23	0.34	0.4
MS2/Alf Lyr	9/04	25*-1	11	0.83	0.35	0.3
MS2/Alf Lyr	9/05	25*-1	11	0.80	0.40	0.4
Run III						
10Tau/MS2	9/27	25*?	4	2.01	1.06	1.0
Xi^2Cet/MS2	9/27	25*?	3	4.82	1.06	2.0
MS2/Alf Aqr	9/28	25*?	11	0.28	0.33	0.2
MS2/Alf Aqr	9/29	25*?	19	1.10	0.33	0.4
MS2/Alf Aqr	9/30	W	13	1.02	0.40	0.4
MS2/Xi^2 Cet	9/30	W	13	3.28	1.06	0.7
MS2/Alf Aqr	10/1	25*?	16	1.02	0.93	0.5

Table II-2
(Cont.)

Ratio	Date	Filter Set	No. Ind. Runs	Lg. Std. Error (%)	Filter (μM)	Typical Error (%)
MS2/Alf Aqr	10/4	25*?	21	0.77	0.33	0.4
MS2/Alf Aqr	10/5	25*?	11	1.27	0.93	0.5
MS2/Alf Aqr	10/6	25*?	4	2.92	1.00	1.4
10Tau/ Alf Aqr	9/28,29, 10/1	25*?	34	1.54	1.06	0.7
Xi^{2}Cet/ Alf Aqr	9/29, 10/6	25*?	30	2.59	1.03	1.1
Xi^{2}Cet/ Alf Aqr	8/30, 9/01	W	15	1.33	1.06	0.7
Alf Aqr/ Alf Lyr	9/04,05 ,06	25*-1	47	0.95	0.33	0.3
Run IV						
MS2/Omi Tau	1/28	1-24*, 18 1k	14	0.46	0.33	0.2
MS2/Gam Gem	1/28	1-24*, 18 1k	14	0.52	0.93	0.2
MS2/Omi Tau	1/29	1-24*, 18 1k	15	0.79	0.33	0.3
MS2/Gam Gem	1/30	1-24*, 18 1k	9	0.60	1.00	0.4

Table II-2
(Cont.)

Ratio	Date	Filter Set	No. Ind. Runs	Lg. Std. Error (%)	Filter (μM)	Typical Error (%)
MS2/Omi Tau	1/31	1-24*, 18 1k	9	0.62	0.33	0.3
Omi Tau/ Alf Aqr	9/28,29, 10/07,08	25*?	42	1.14	0.35	0.7
Gam Gem/ Alf Aqr	10/01,08	25*?	14	3.93	0.33	1.8

Table II-3

Ratios for $\frac{MS2}{Ap16}$ or $\frac{MS2}{Ap16B}$

Key: See Table II-1

Ratio	Date	Filter Set	No. Ind. Runs	Lg. Std. Error (%)	Filter (μM)	Typical Error (%)
Run II						
Ap16B/MS2	8/31	W	3	2.24	0.90	1.2
Ap16B/MS2	8/31	25*-1	3	2.85	0.76	1.4
Ap16B/MS2	9/01	W	3	1.07	0.33	0.3
Ap16B/MS2	9/02	25*-1	3	1.90	0.96	1.2
Ap16B/MS2	9/03	25*-1	3	1.24	0.37	0.5
Ap16B/MS2	9/04	25*-1	3	0.78	0.35	0.4
Ap16B/MS2	9/05	25*-1	3	1.25	1.10	0.4
Run III						
Ap16/MS2	9/26	25*?	3	1.18	0.35	0.6
Ap16/MS2	9/27	25*?	3	0.93	0.40	0.5
Ap16/MS2	9/28	25*?	3	1.21	0.35	0.5
Ap16/MS2	9/29	25*?	3	0.73	0.93	0.5
Ap16/MS2	9/30	W	3	1.12	0.36	0.5

Table II-3
(Cont.)

Ratio	Date	Filter Set	No. Ind. Runs	Lg. Std. Error (%)	Filter (μM)	Typical Error (%)
Ap16/MS2	10/1	25*?	3	1.19	0.33	0.5
Ap16/MS2	10/4	25*?	3	1.32	1.03	0.7
Ap16/MS2	10.5	25*?	3	1.74	0.35	0.8
Ap16/MS2	10/6	25*?	3	2.45	0.33	1.0
Run IV						
Ap16B/MS2	1/26	1-24*, 18 1k	3	1.22	0.33	0.5
Ap16B/MS2	1/28	1-24*, 18 1k	3	0.98	0.33	0.4
Ap16B/MS2	1/29	1-24*, 18 1k	3	1.62	0.33	0.6
Ap16B/MS2	1/30	1-24*, 18 1k	3	0.98	0.33	0.4
Ap16B/MS2	1/31	1-24*, 18 1k	3	0.91	0.33	0.5

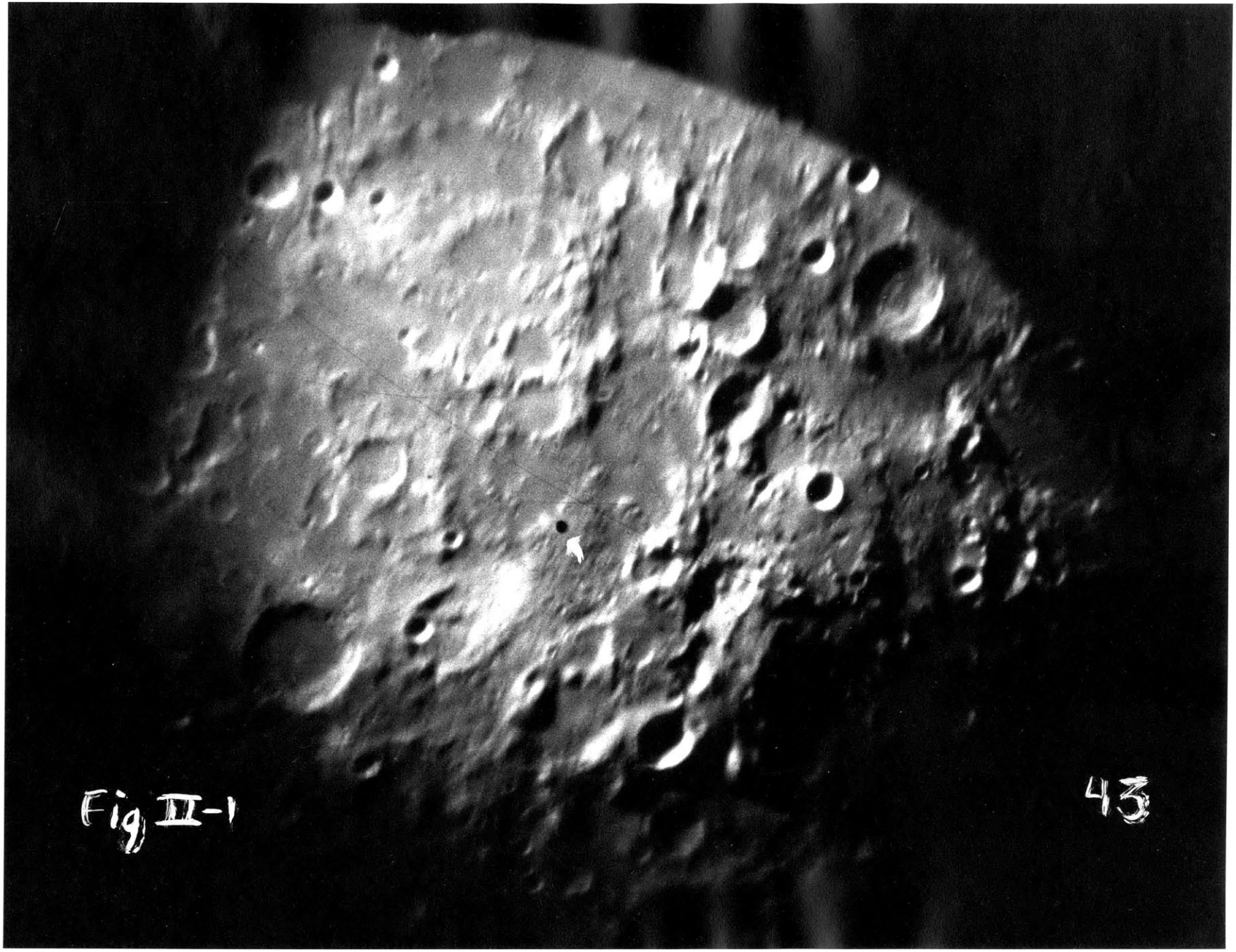

Fig III-1

Figure II-2

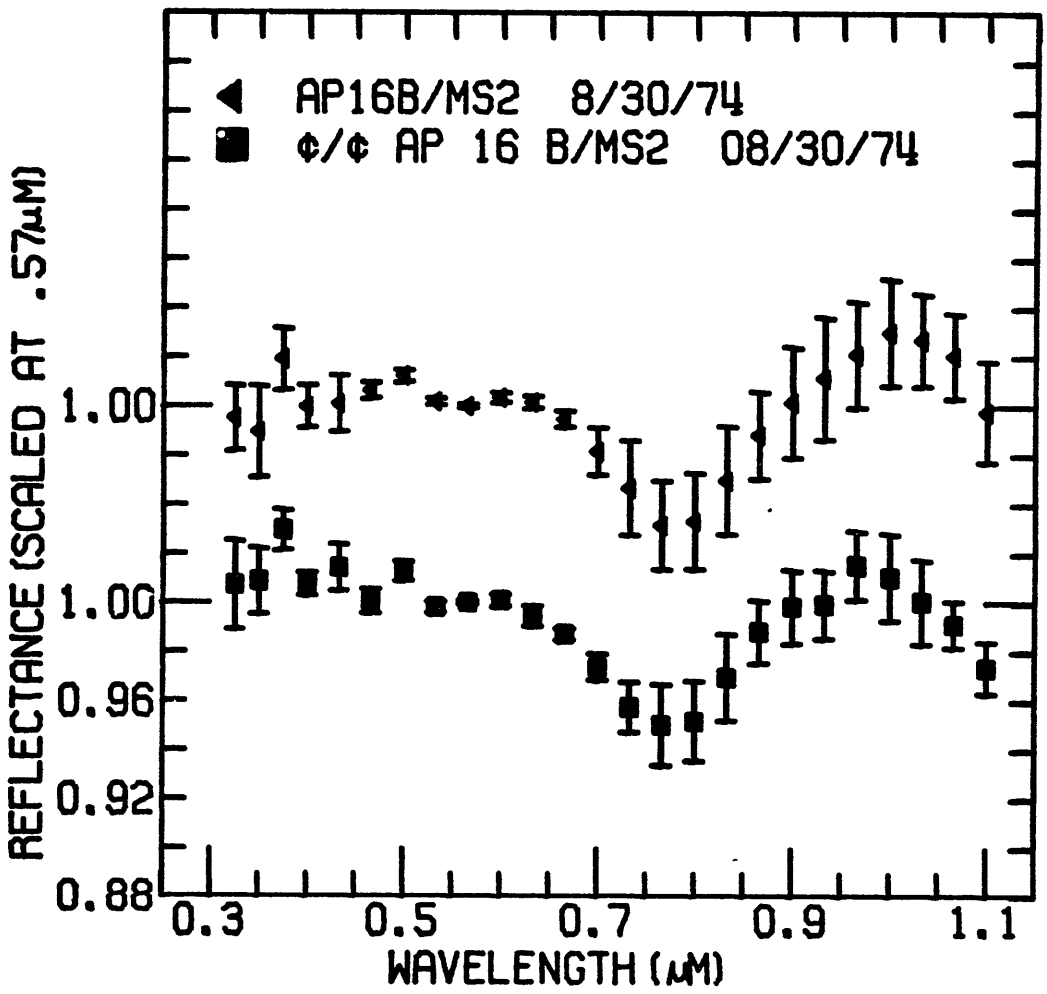
AP16B/MS2 8/30/74
¢/¢ AP 16 B/MS2 08/30/74
REFLECTANCE (SCALED AT .57μM)
1.00
1.00
0.96
0.92
0.88
0.3
0.5
0.7
0.9
1.1
WAVELENGTH (μM)

Table II-4

62230 Wallace		62230 Spectrum	
Wavelength	Reflectance	Wavelength	Reflectance
0.36260	0.60689	0.37840	0.63651
0.40370	0.69175	0.40410	0.69175
0.43700	0.76381	0.42990	0.74299
0.47160	0.83667	0.46770	0.82786
0.50330	0.88551	0.50190	0.88551
0.53830	0.94956	0.53660	0.94956
0.56590	1.00000	0.56740	1.00000
0.60500	1.06165	0.60410	1.05524
0.63760	1.10568	0.63120	1.09928
0.66960	1.14892	0.66790	1.14892
0.70100	1.19375	0.69860	1.18815
0.73480	1.23139	0.73390	1.23139
0.76850	1.26261	0.76450	1.25861
0.80060	1.27862	0.79990	1.27622
0.83480	1.29864	0.83100	1.29864
0.86790	1.31545	0.86530	1.31545
0.90200	1.33867	0.89870	1.33467
0.93360	1.37470	0.93290	1.37470
0.96670	1.41073	0.96600	1.41073
0.99800	1.44115	1.00080	1.44676
1.03050	1.48119	1.03300	1.48119
1.06310	1.51401	1.06370	1.51401
1.09810	1.54364	1.09910	1.54364

Figure II-3,4

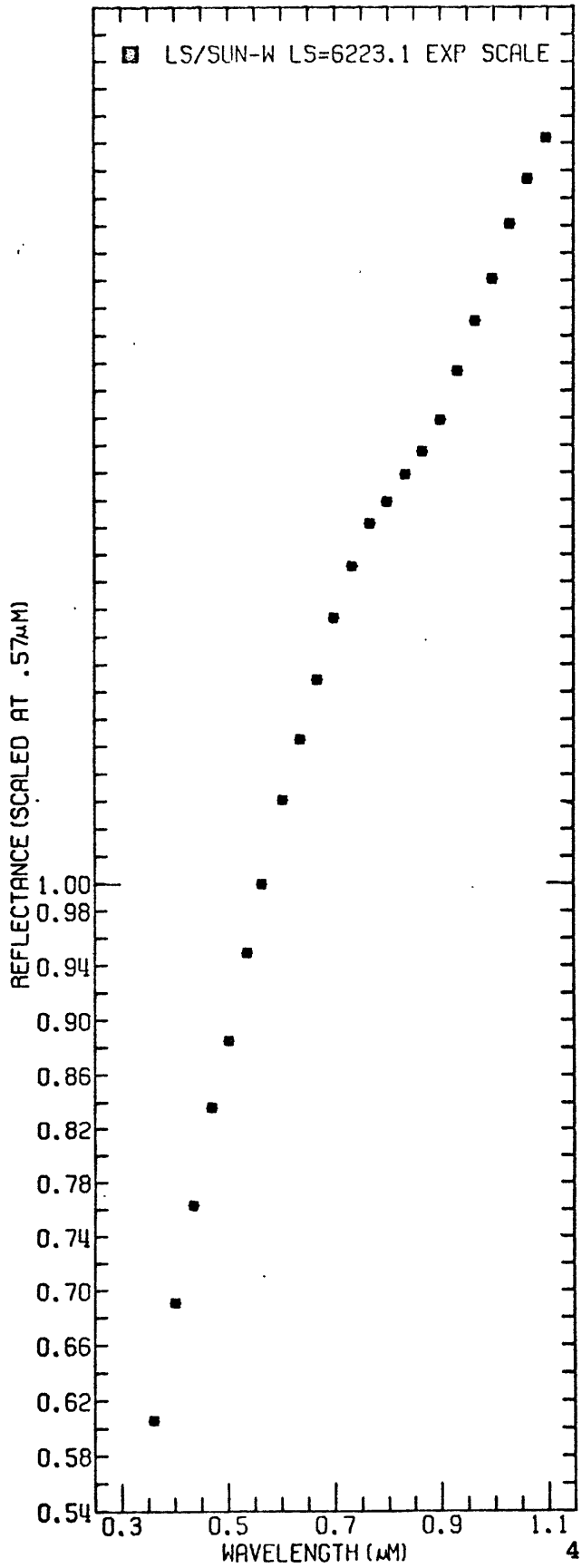
LS/SUN-W LS=6223.1 EXP SCALE
REFLECTANCE (SCALED AT .57μM)
1.00
0.98
0.94
0.90
0.86
0.82
0.78
0.74
0.70
0.66
0.62
0.58
0.54
0.3
0.5
0.7
0.9
1.1
WAVELENGTH (μM)

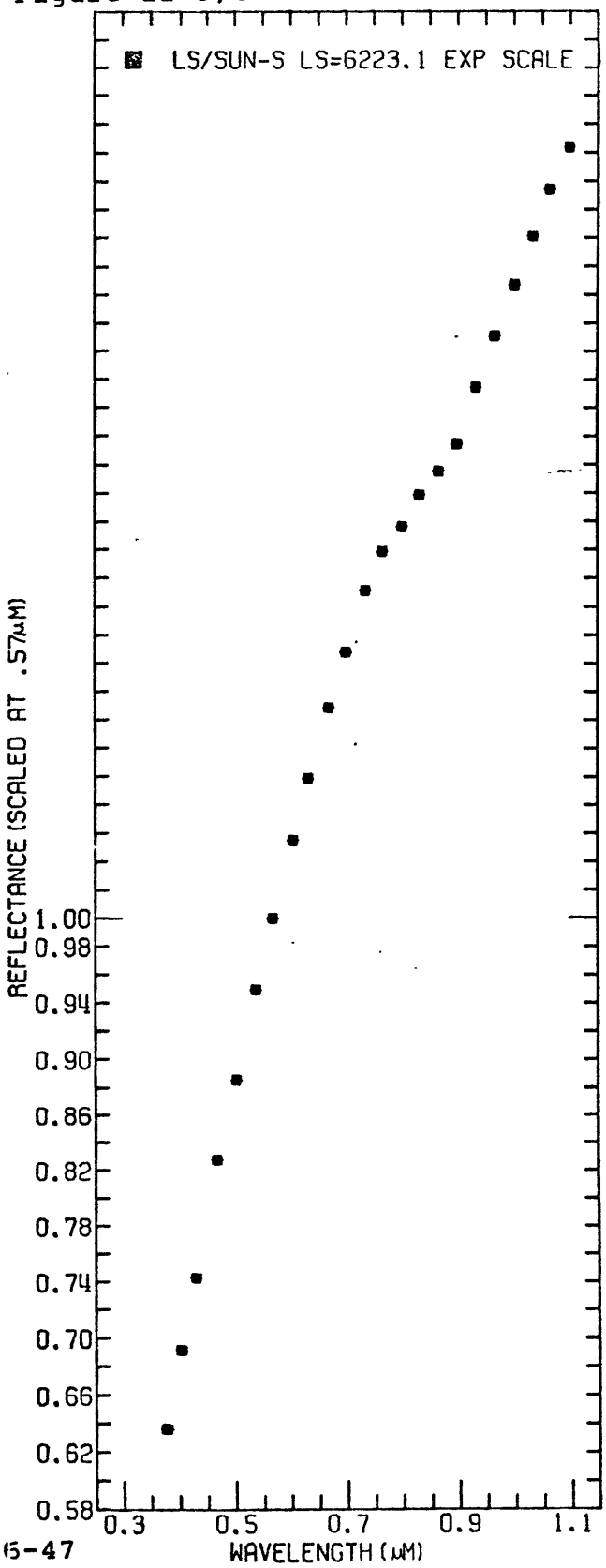
LS/SUN-S LS=6223.1 EXP SCALE
REFLECTANCE (SCALED AT .57μM)
1.00
0.98
0.94
0.90
0.86
0.82
0.78
0.74
0.70
0.66
0.62
0.58
0.3
0.5
0.7
0.9
1.1
WAVELENGTH (μM)

Figure II-5,6

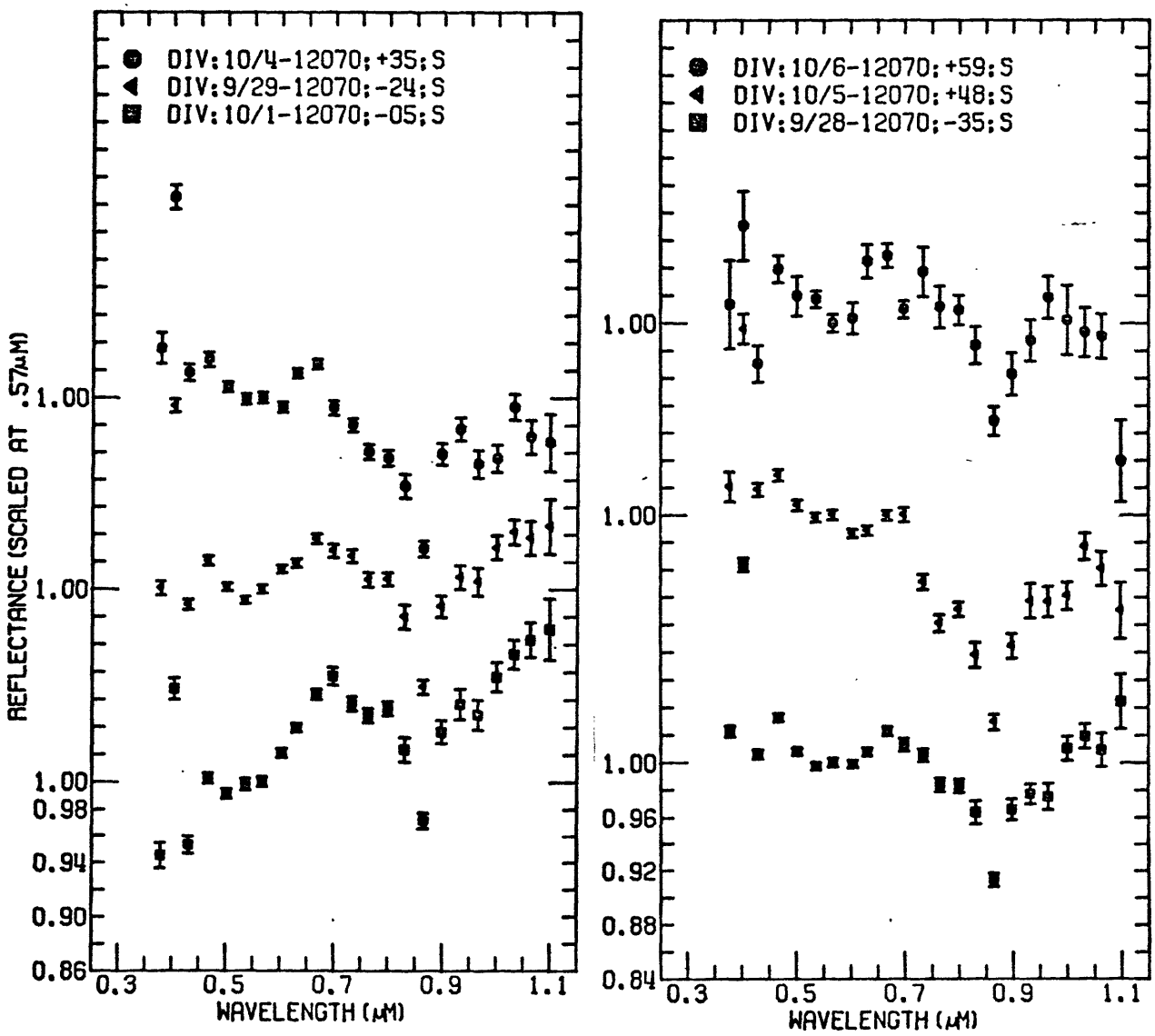
DIV:10/4-12070;+35;S
DIV:9/29-12070;-24;S
DIV:10/1-12070;-05;S
REFLECTANCE (SCALED AT .57μM)
1.00
1.00
1.00
0.98
0.94
0.90
0.86
0.3
0.5
0.7
0.9
1.1
WAVELENGTH (μM)
DIV:10/6-12070;+59;S
DIV:10/5-12070;+48;S
DIV:9/28-12070;-35;S
1.00
1.00
1.00
0.96
0.92
0.88
0.84
0.3
0.5
0.7
0.9
1.1
WAVELENGTH (μM)

Figure II-7,8

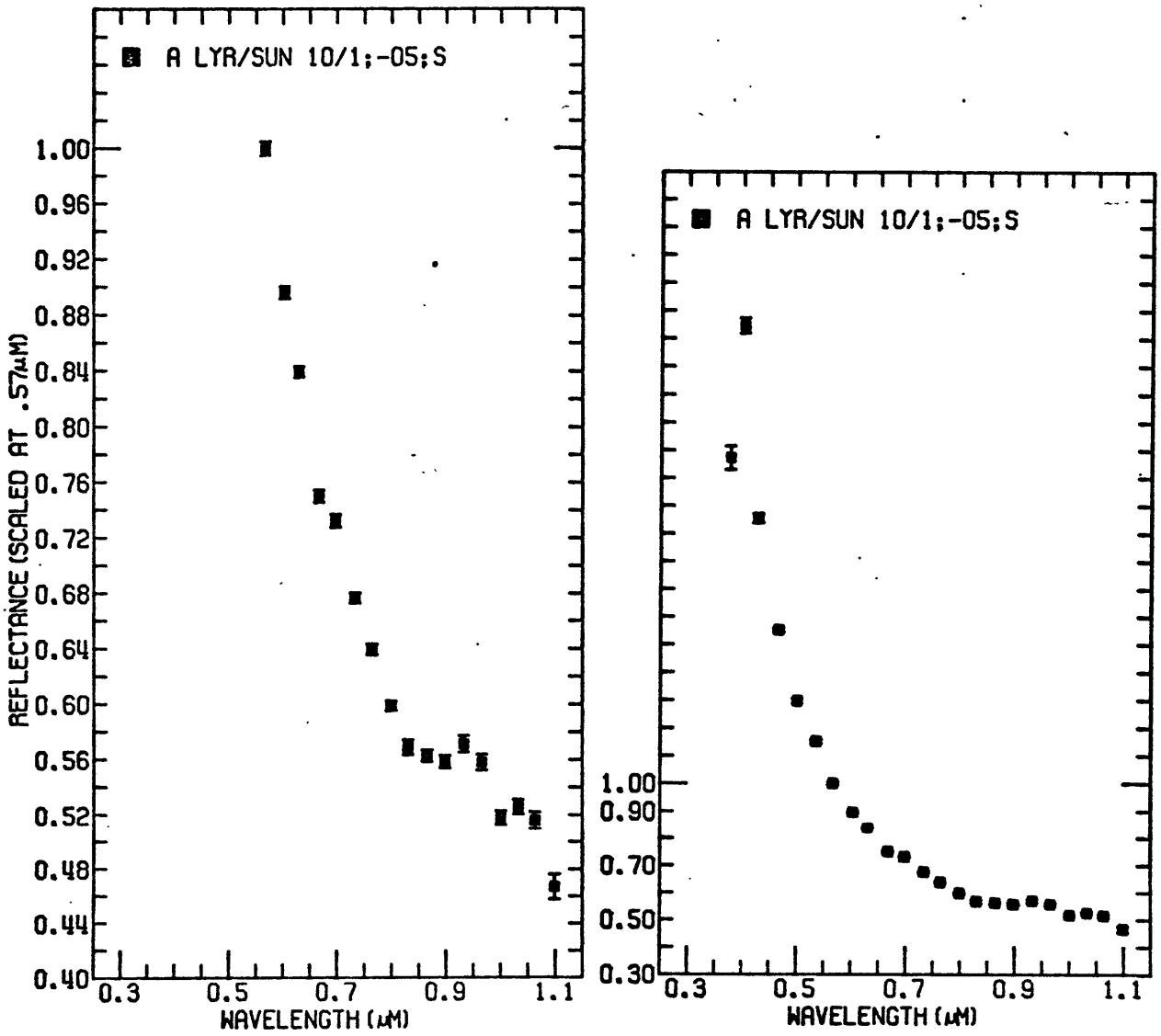
A LYR/SUN 10/1;-05;S
REFLECTANCE (SCALED AT .57μM)
1.00
0.96
0.92
0.88
0.84
0.80
0.76
0.72
0.68
0.64
0.60
0.56
0.52
0.48
0.44
0.40
0.3
0.5
0.7
0.9
1.1
WAVELENGTH (μM)
A LYR/SUN 10/1;-05;S
1.00
0.90
0.70
0.50
0.30
0.3
0.5
0.7
0.9
1.1
WAVELENGTH (μM)

Figure II-9,10

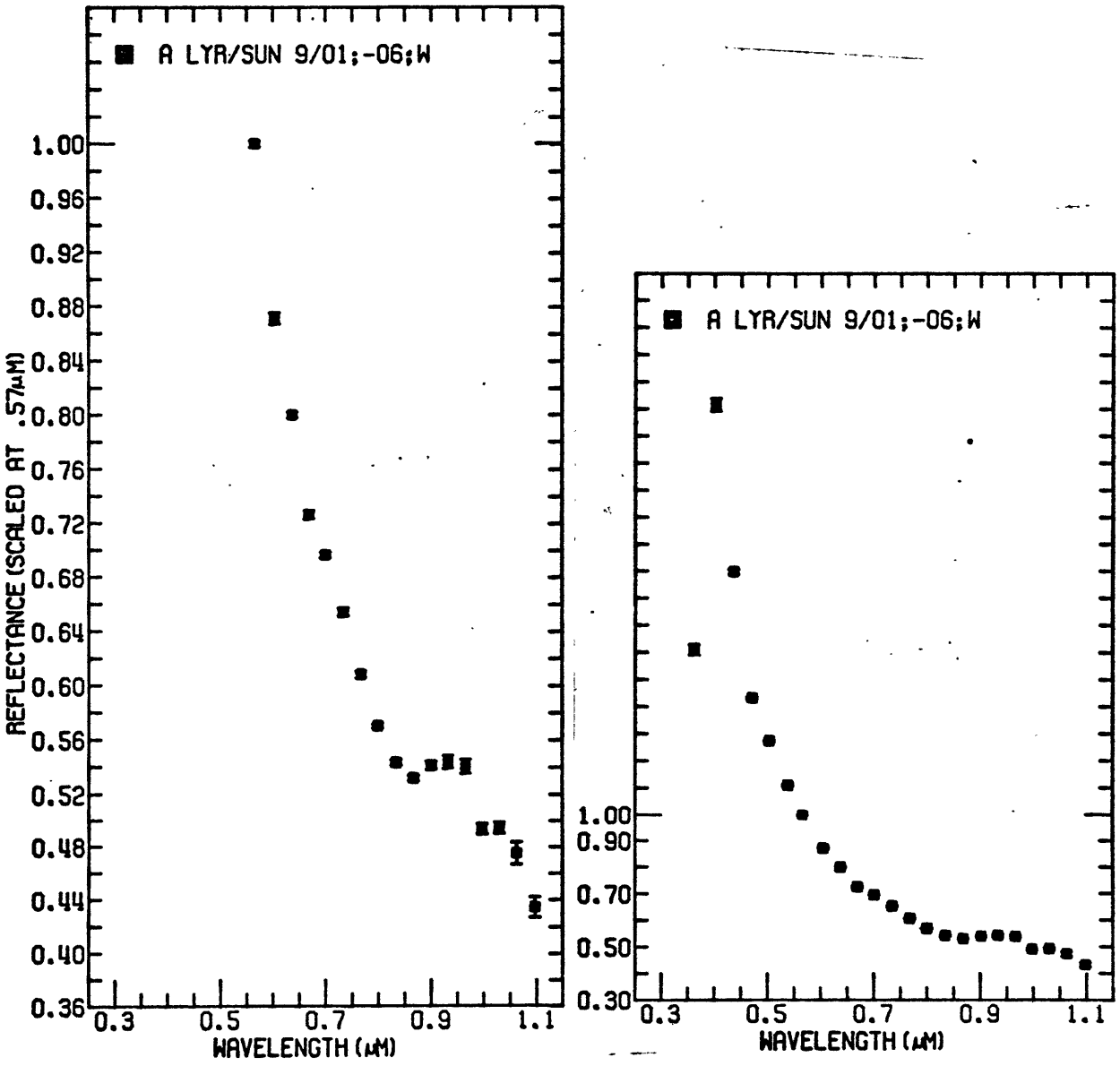

Figure II-11,12

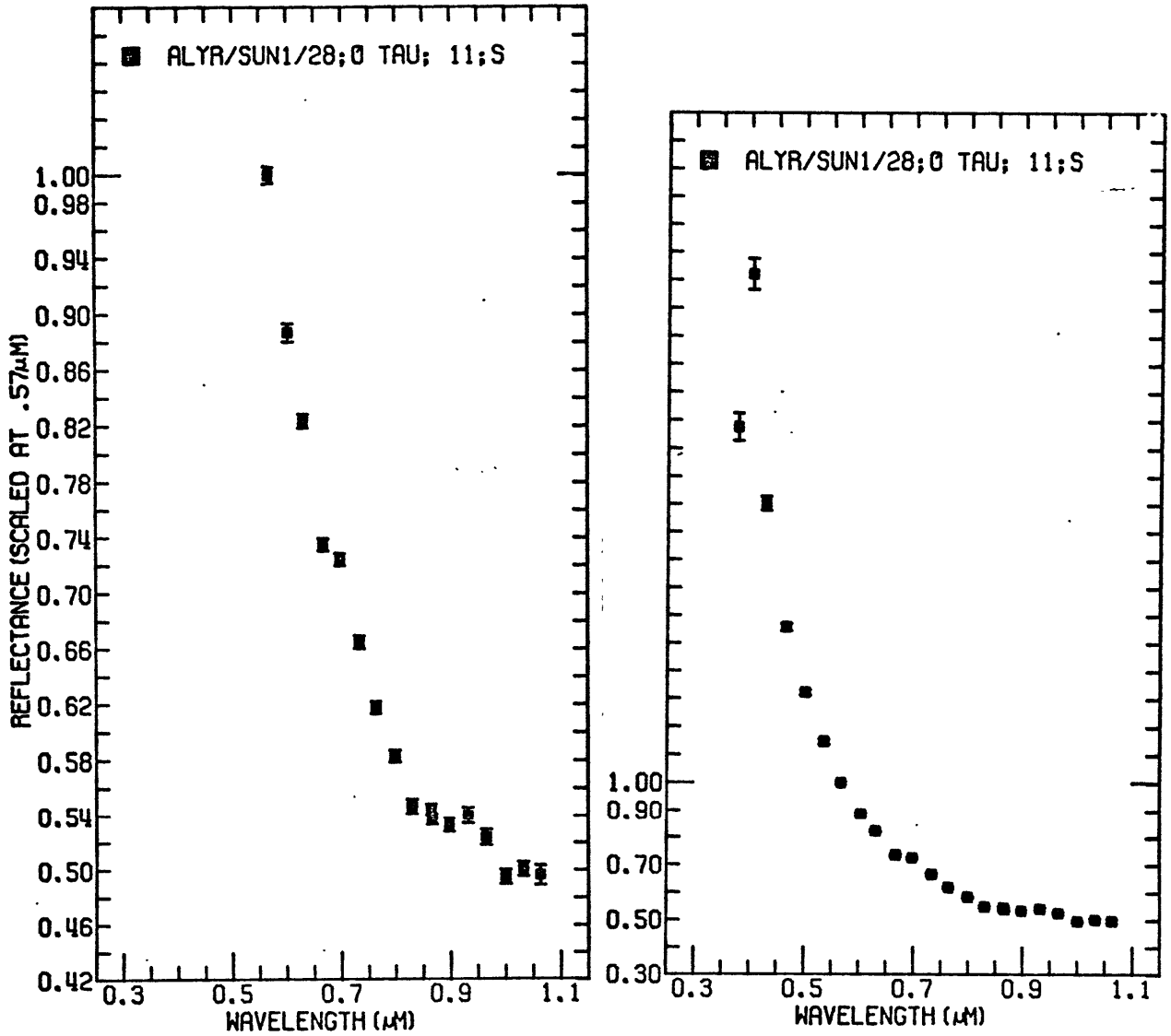

Figure II-13,14

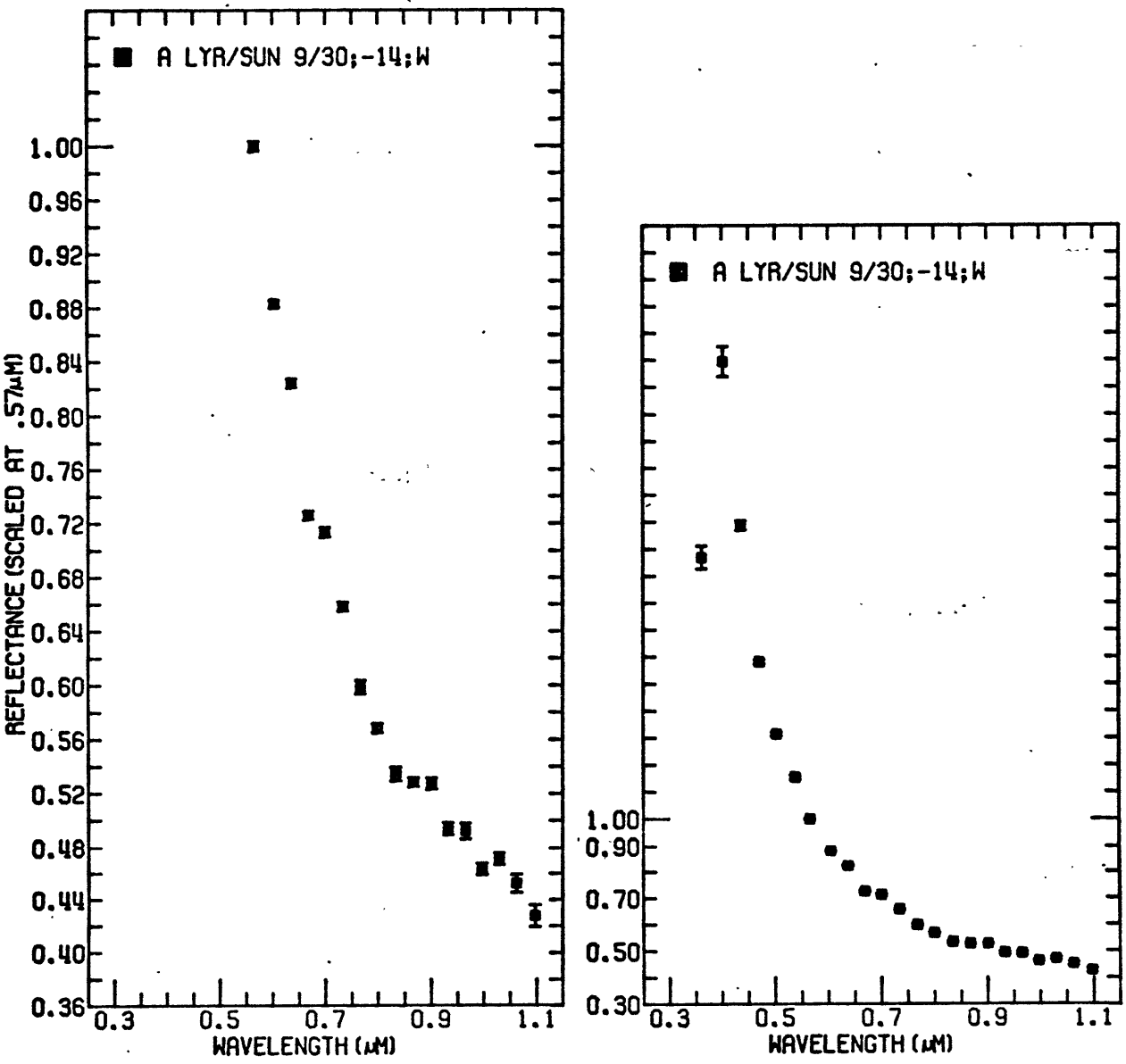

Figure II-15,16

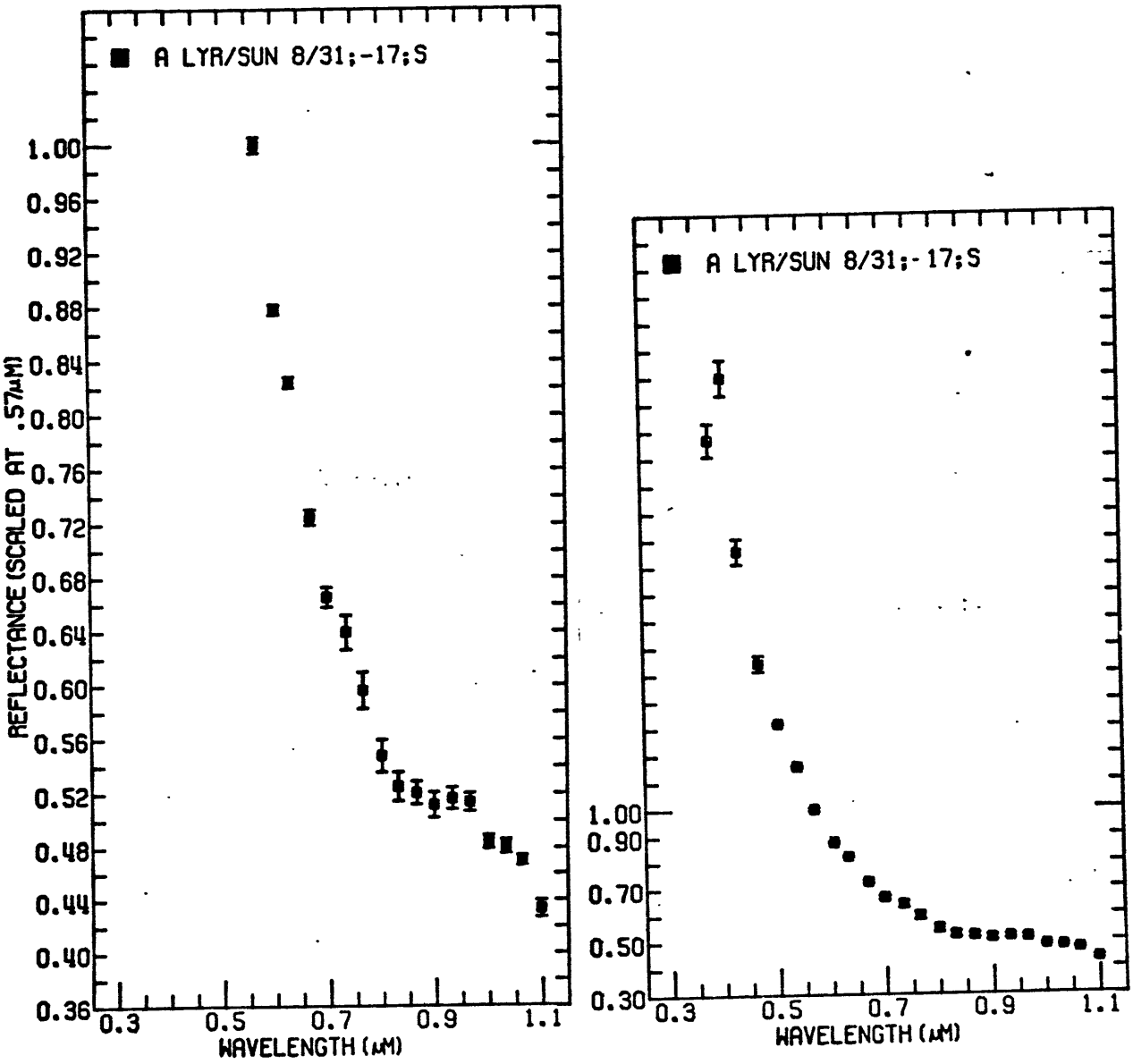

Figure II-17,18

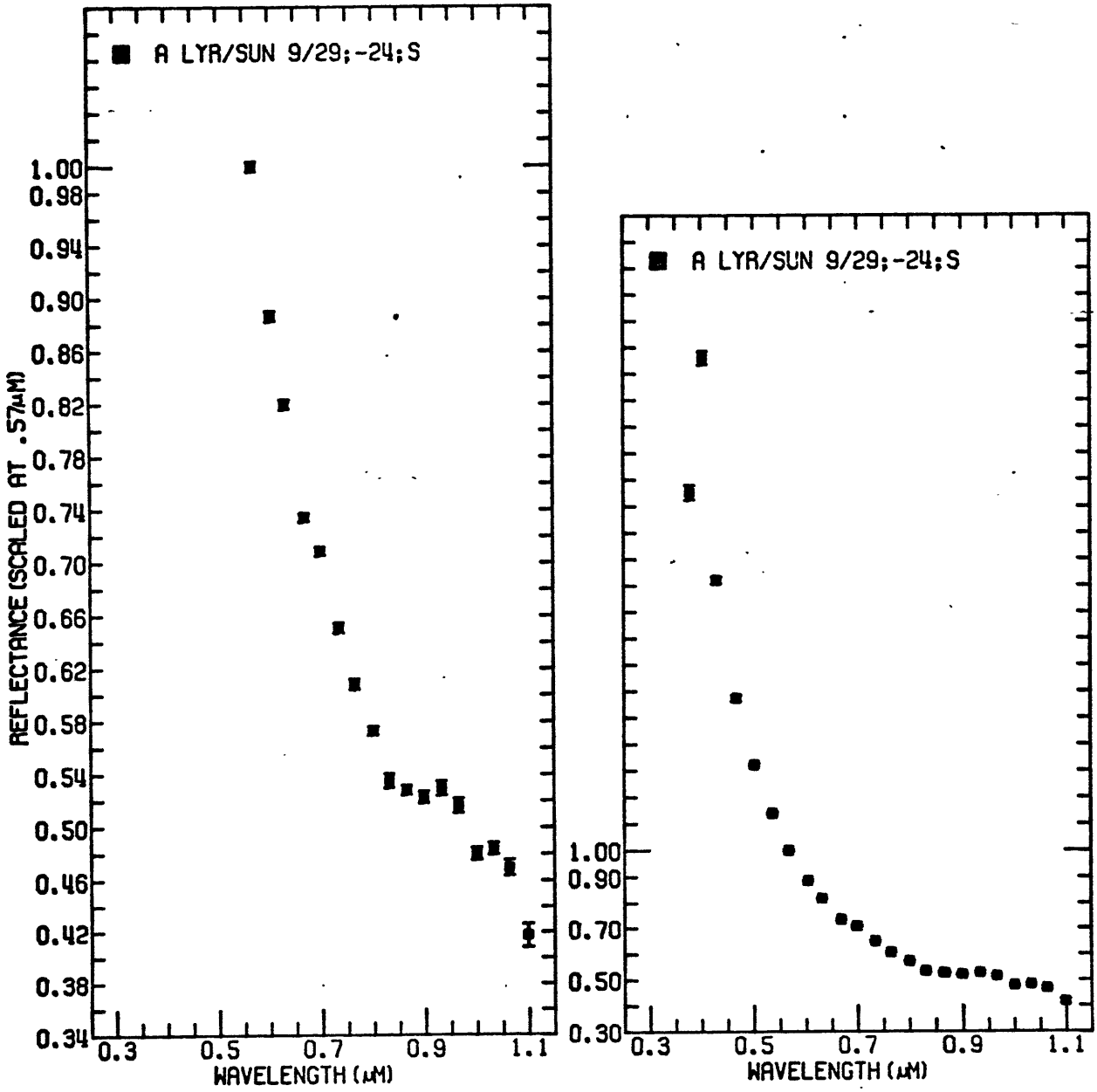

Figure II-19,20

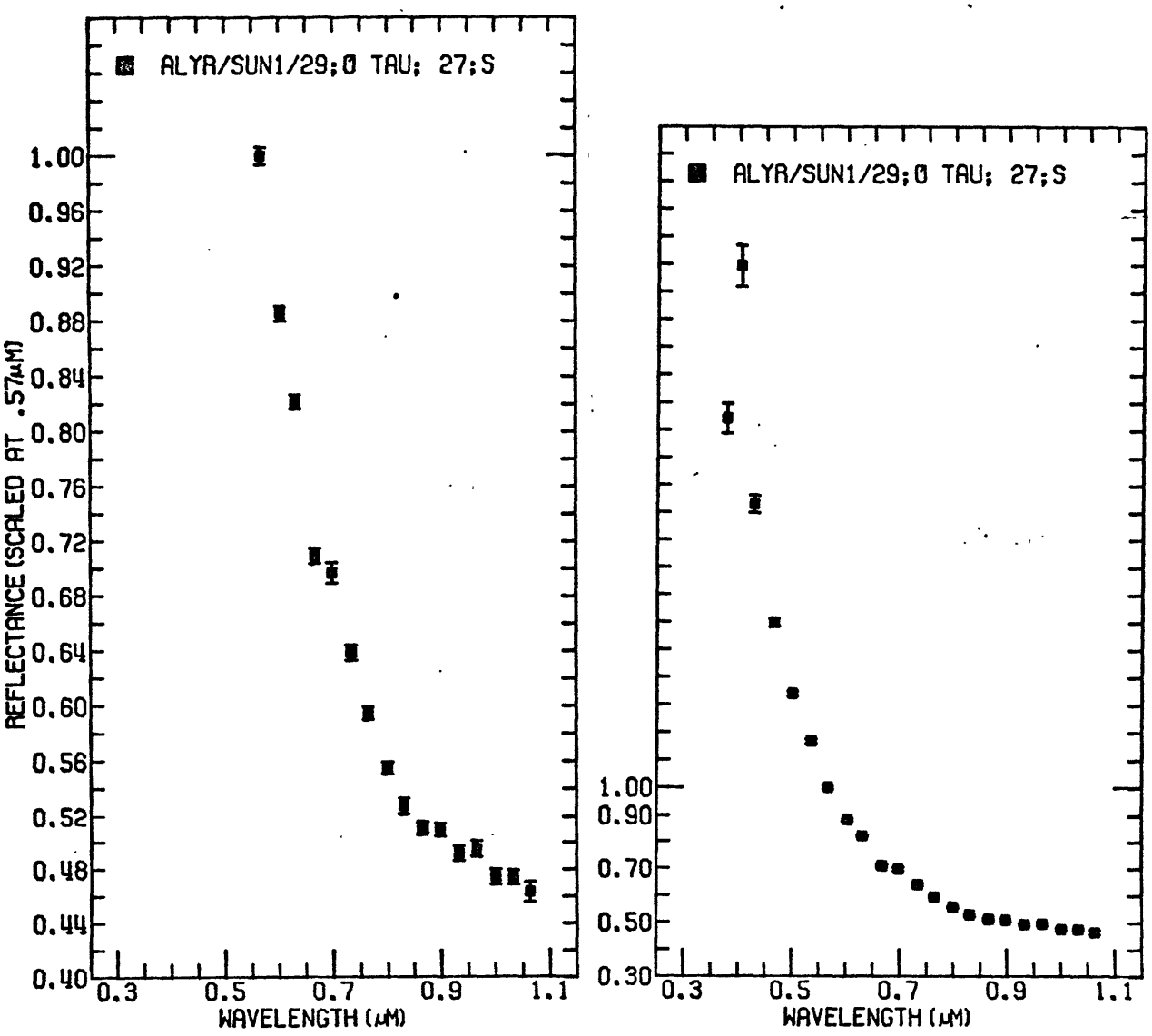

Figure II-21,22

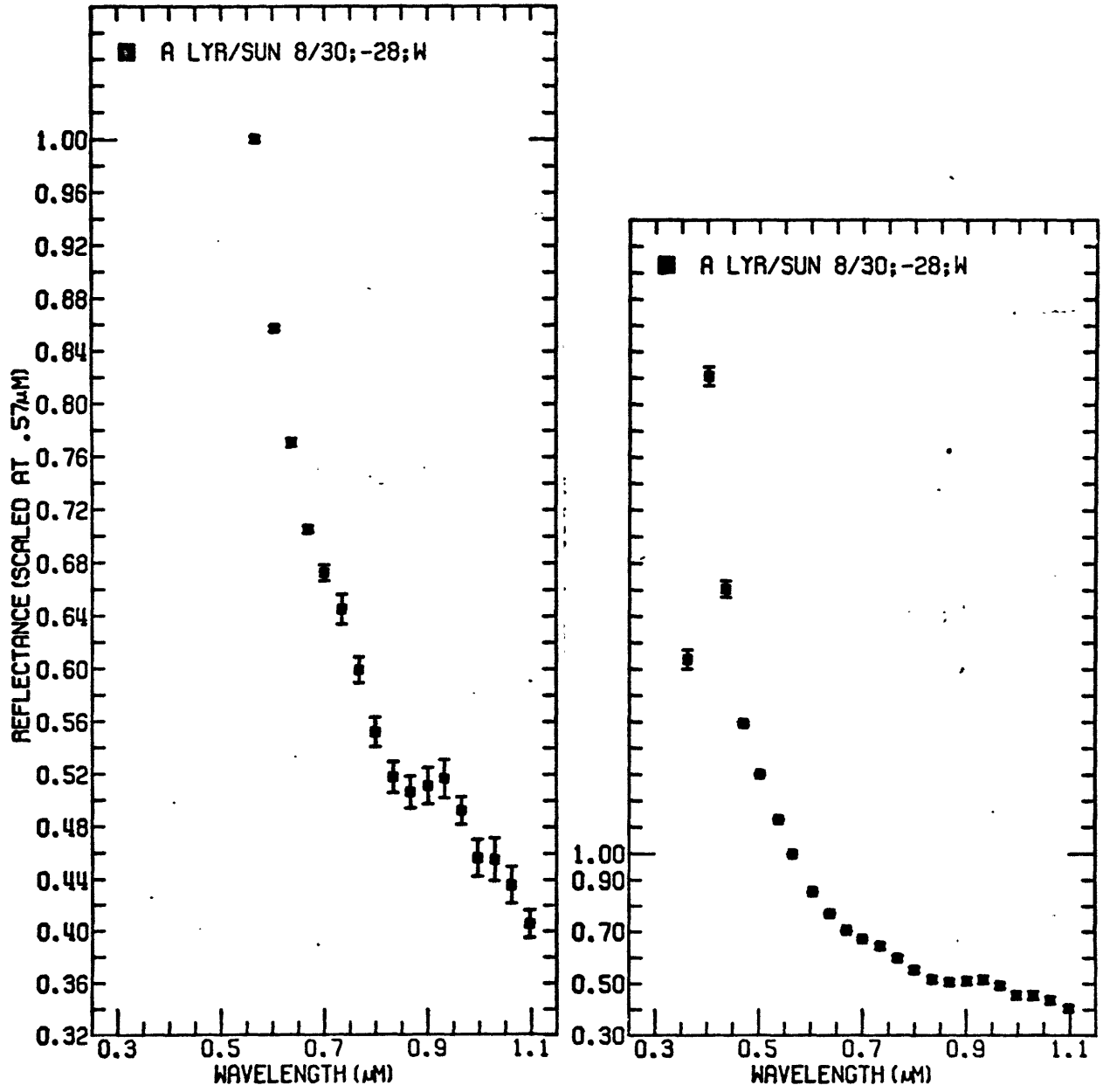

Figure II-23,24

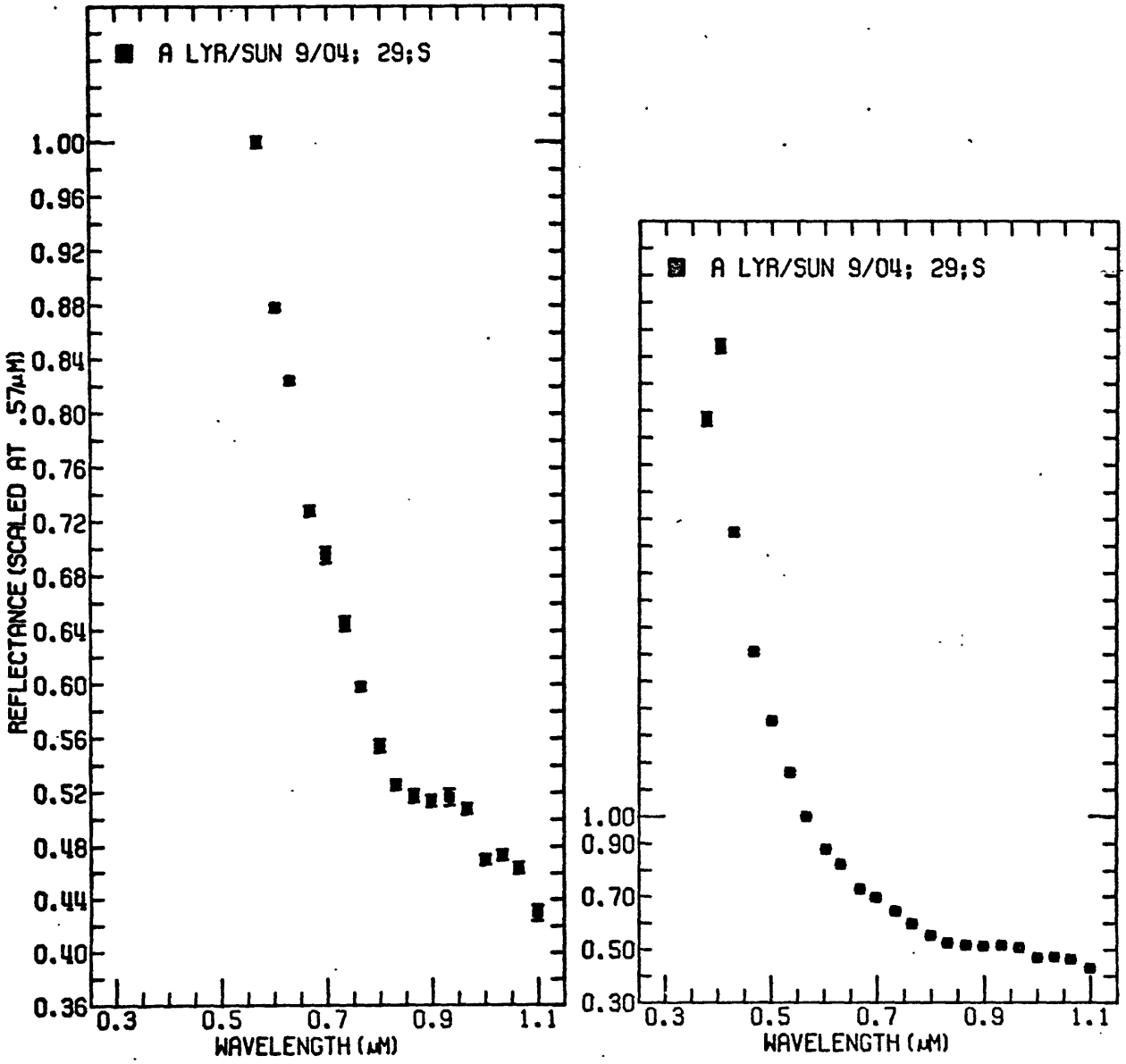

Figure II-25,26

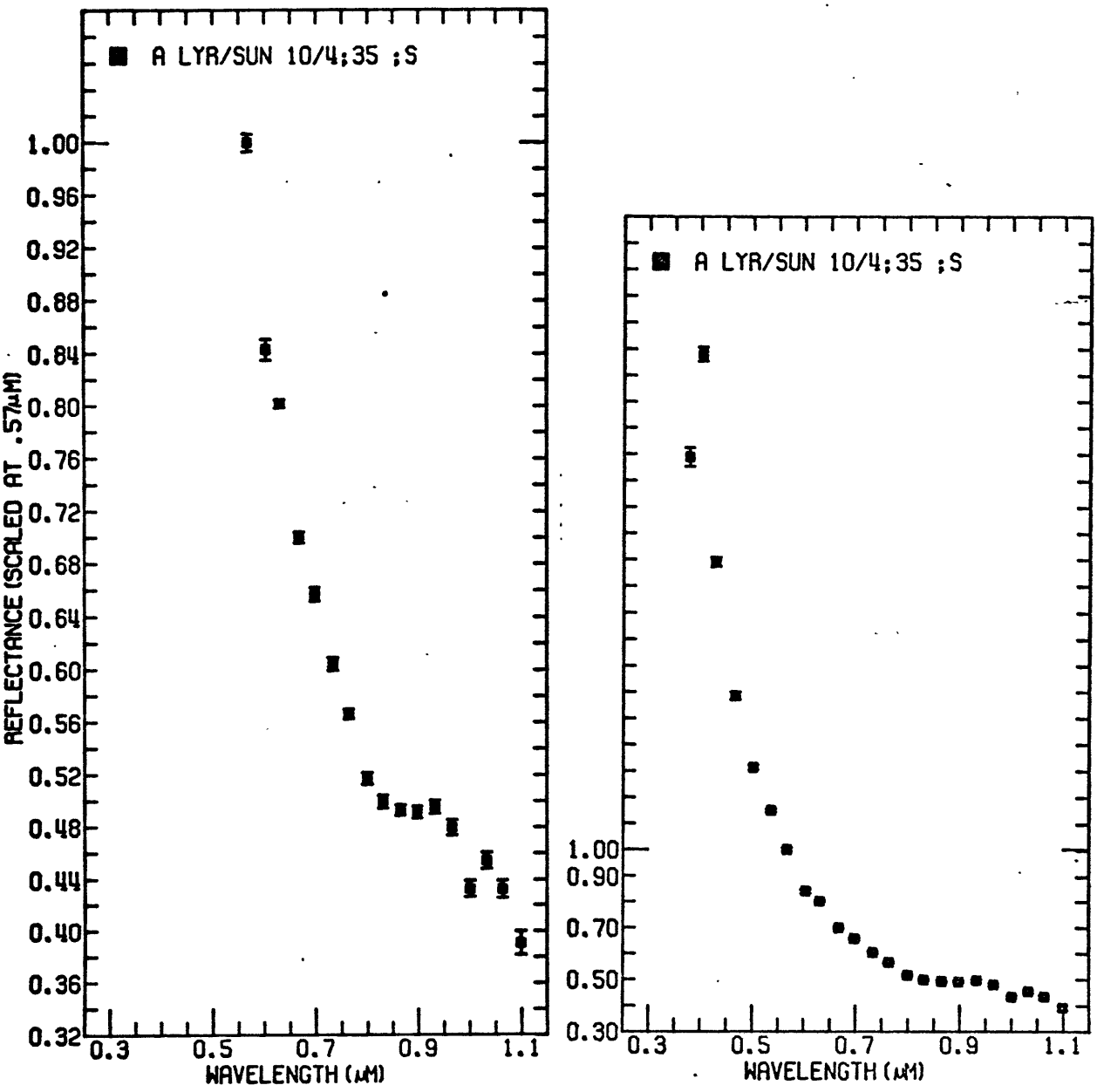

Figure II-27,28

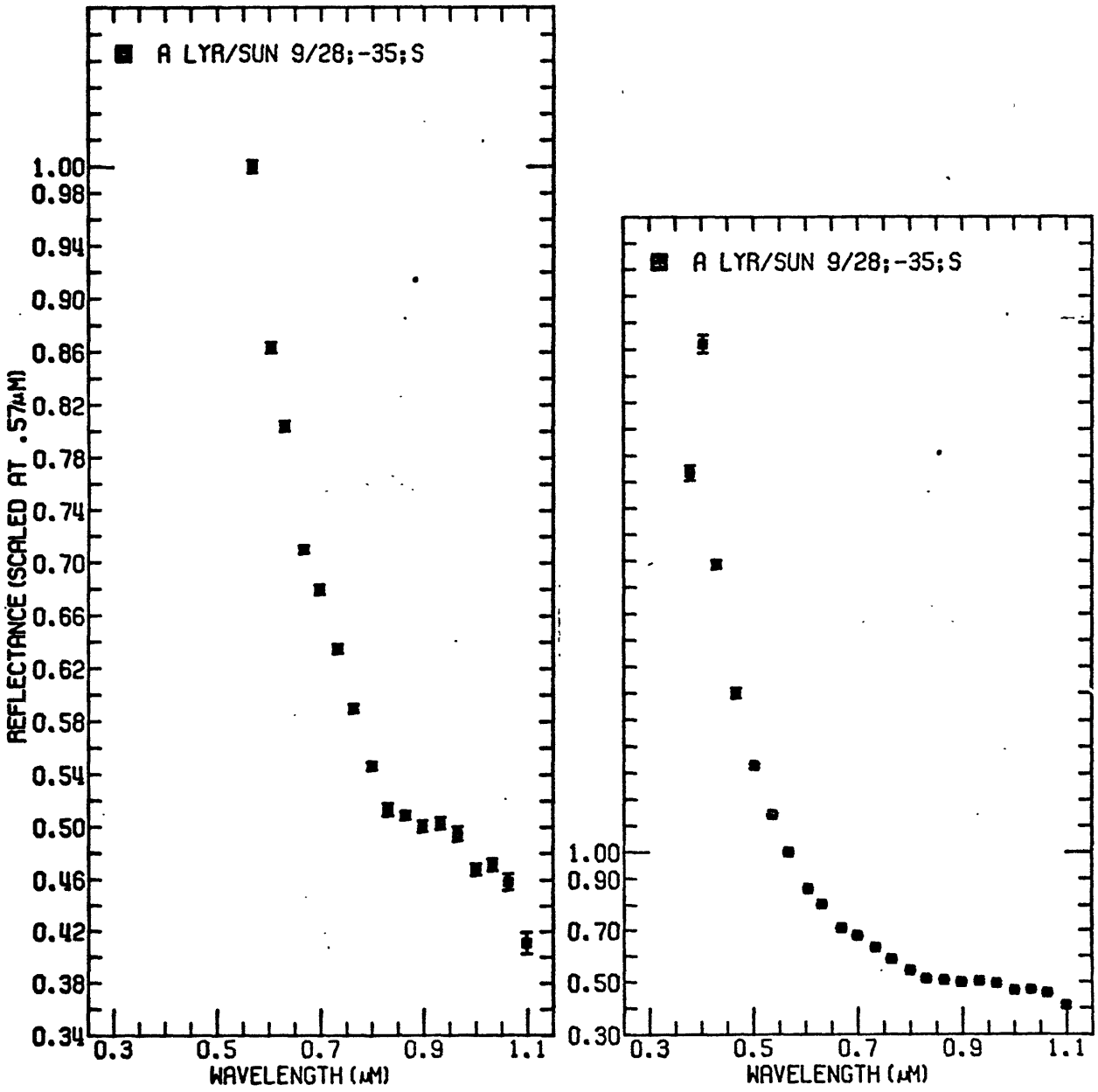

Figure II-29,30

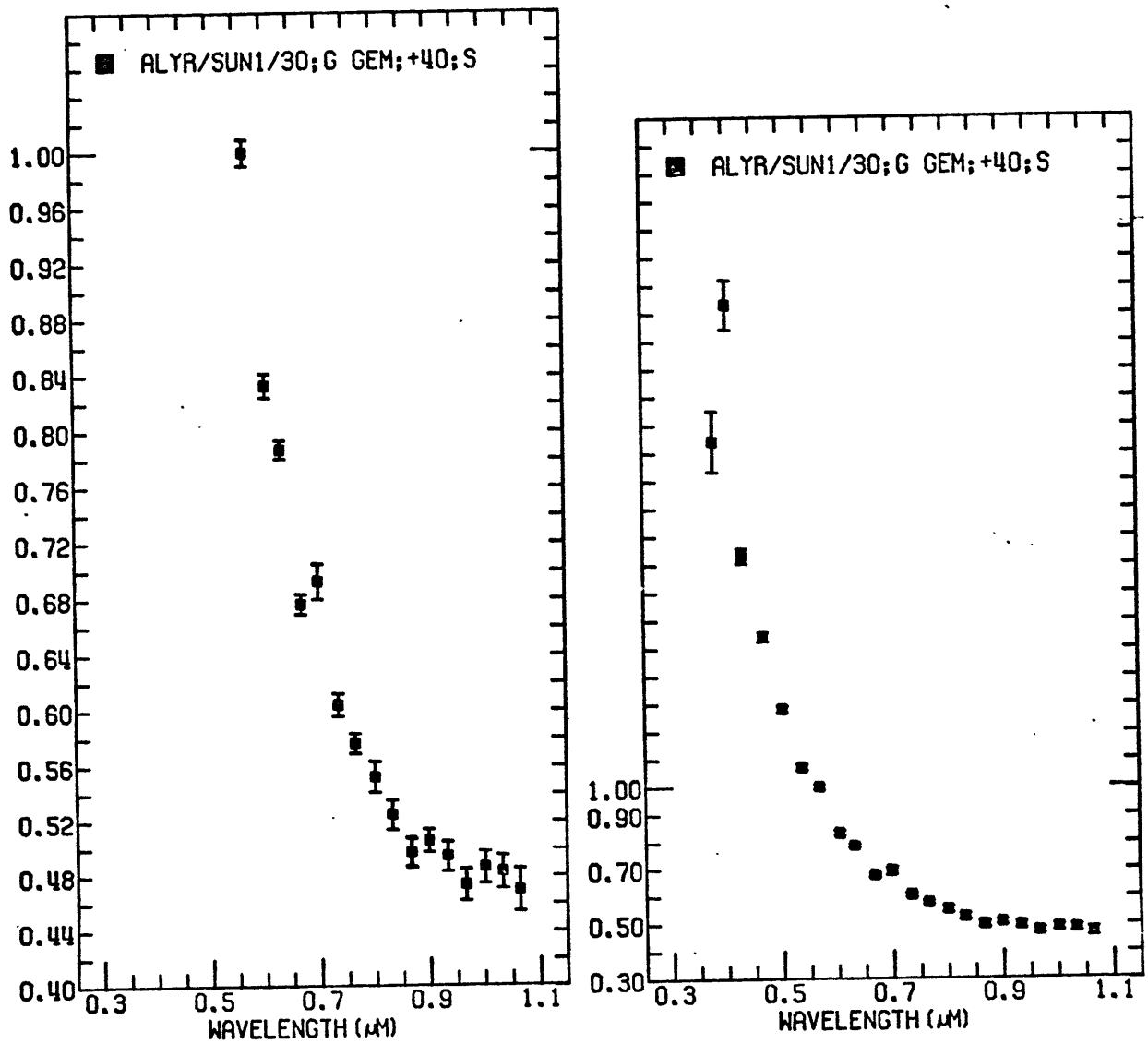

Figure II-31,32

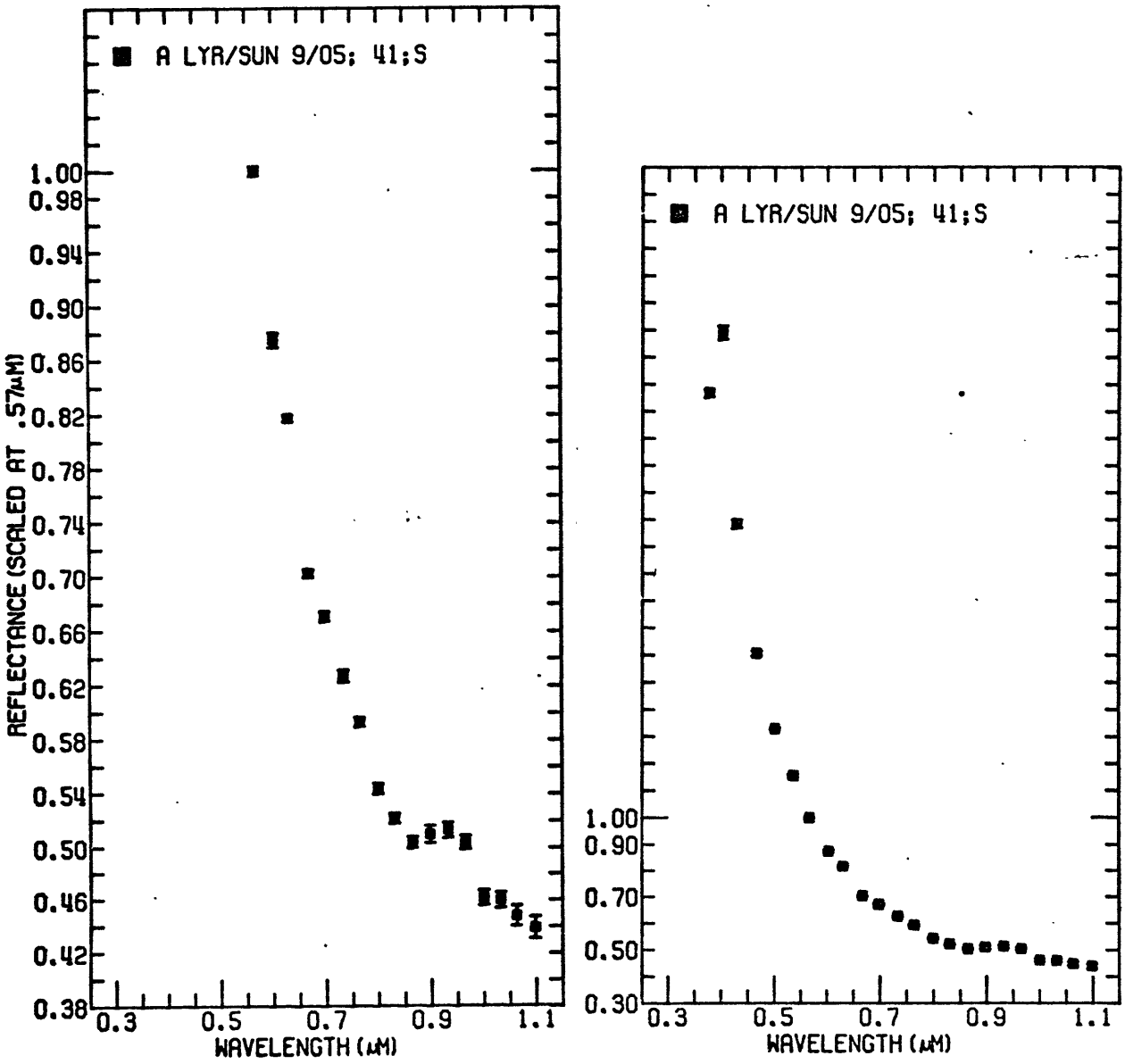

Figure II-33,34

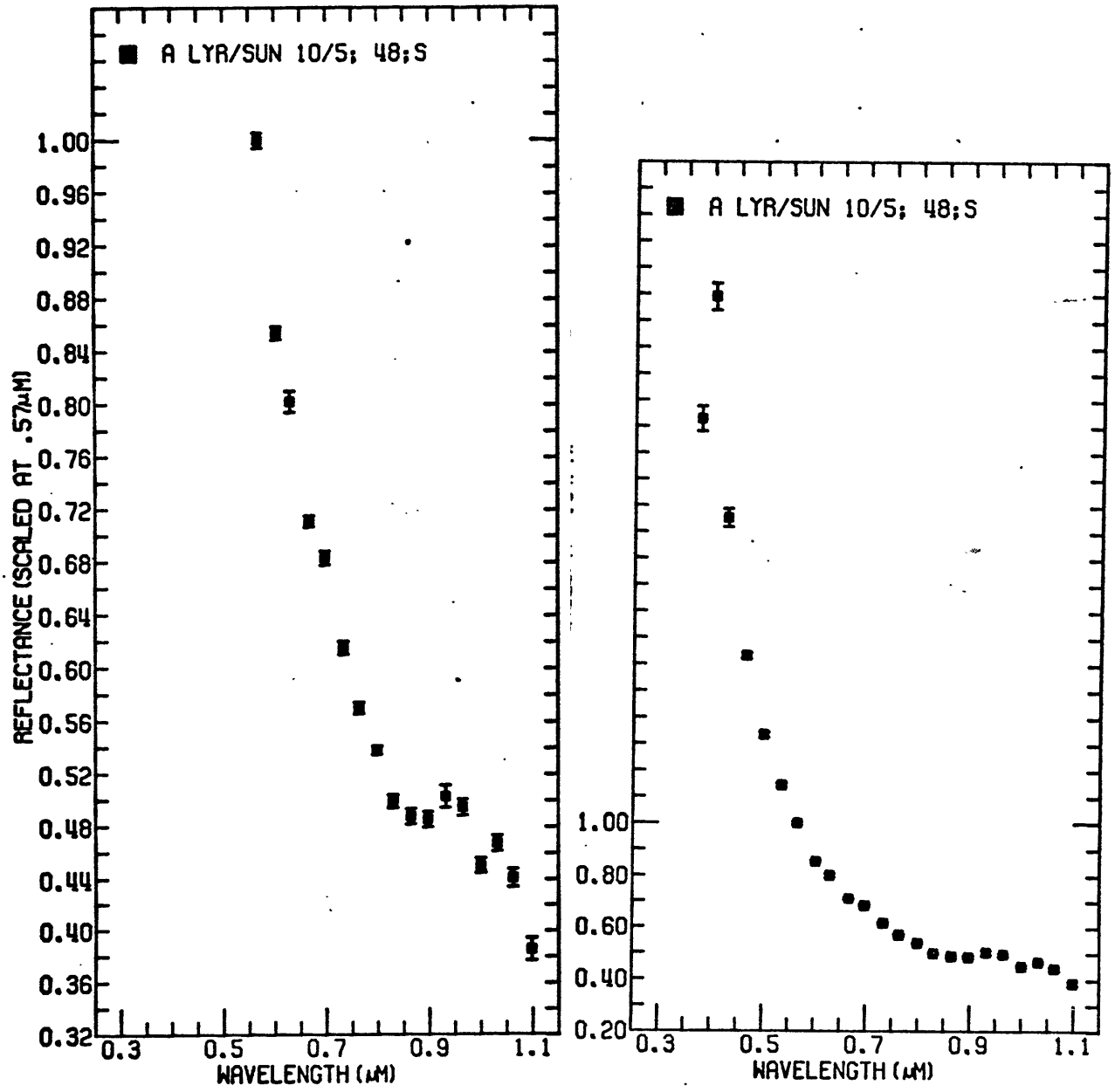

Figure II-35,36

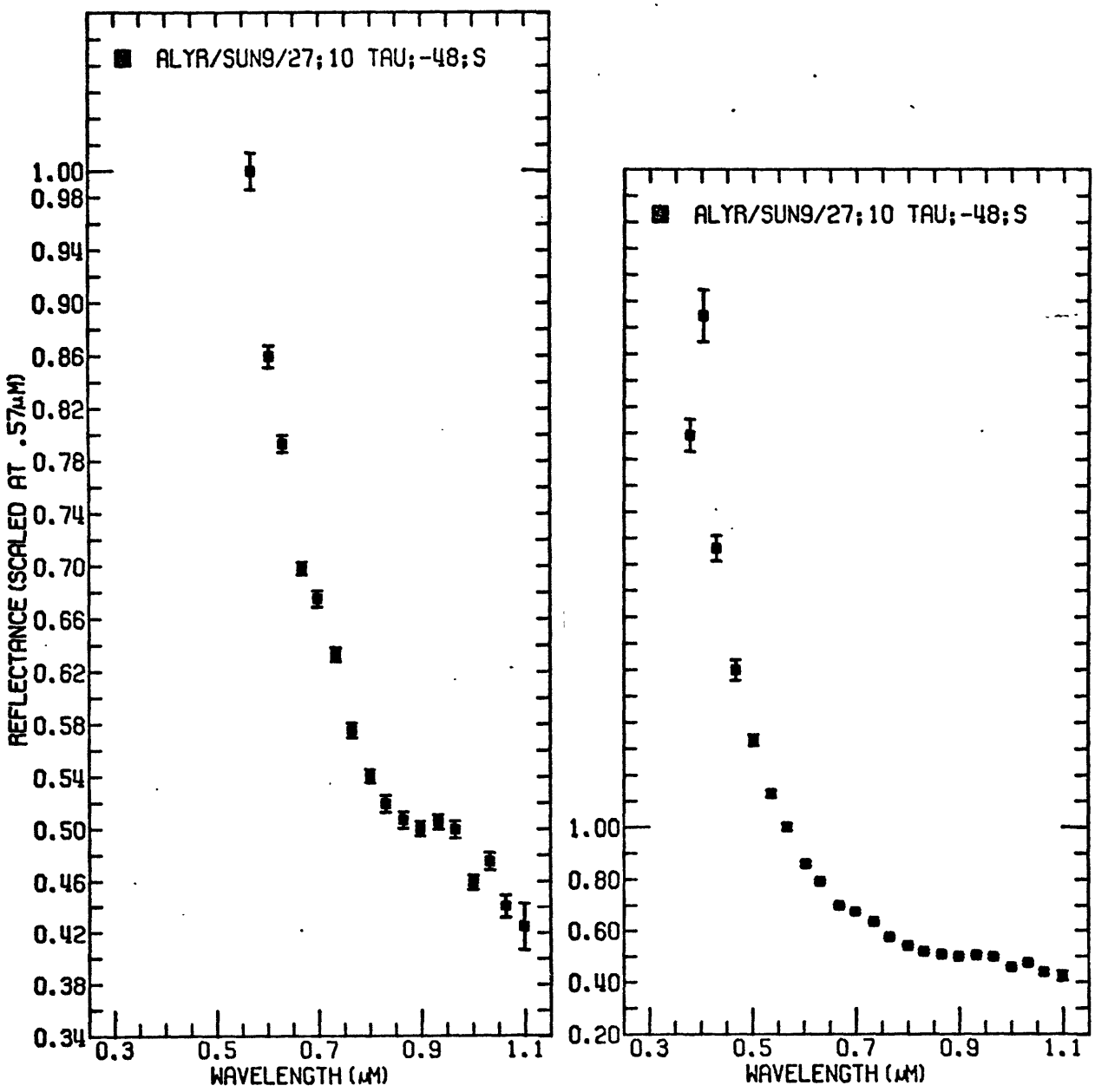

Figure II-37,38

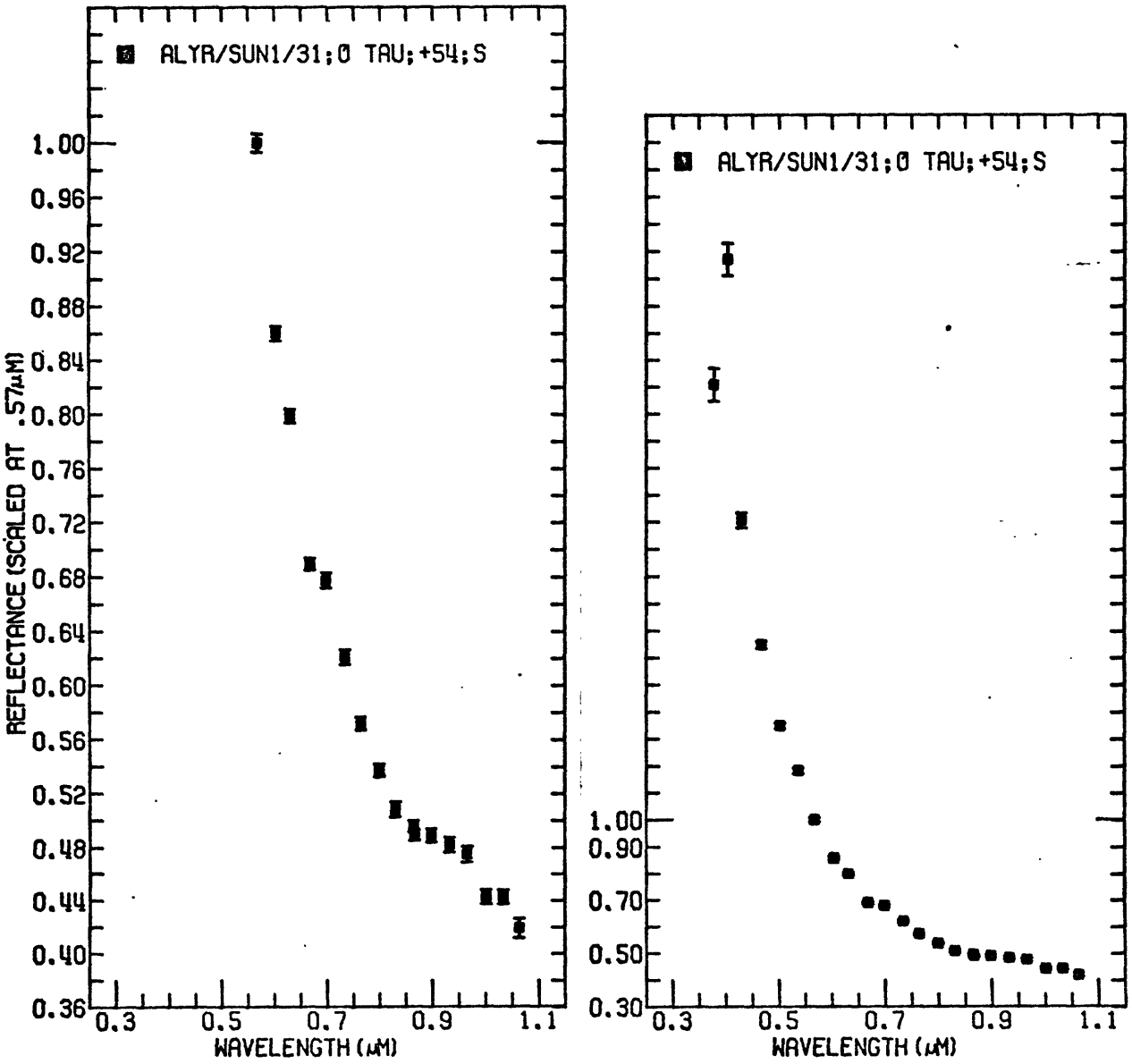

Figure II-39,40

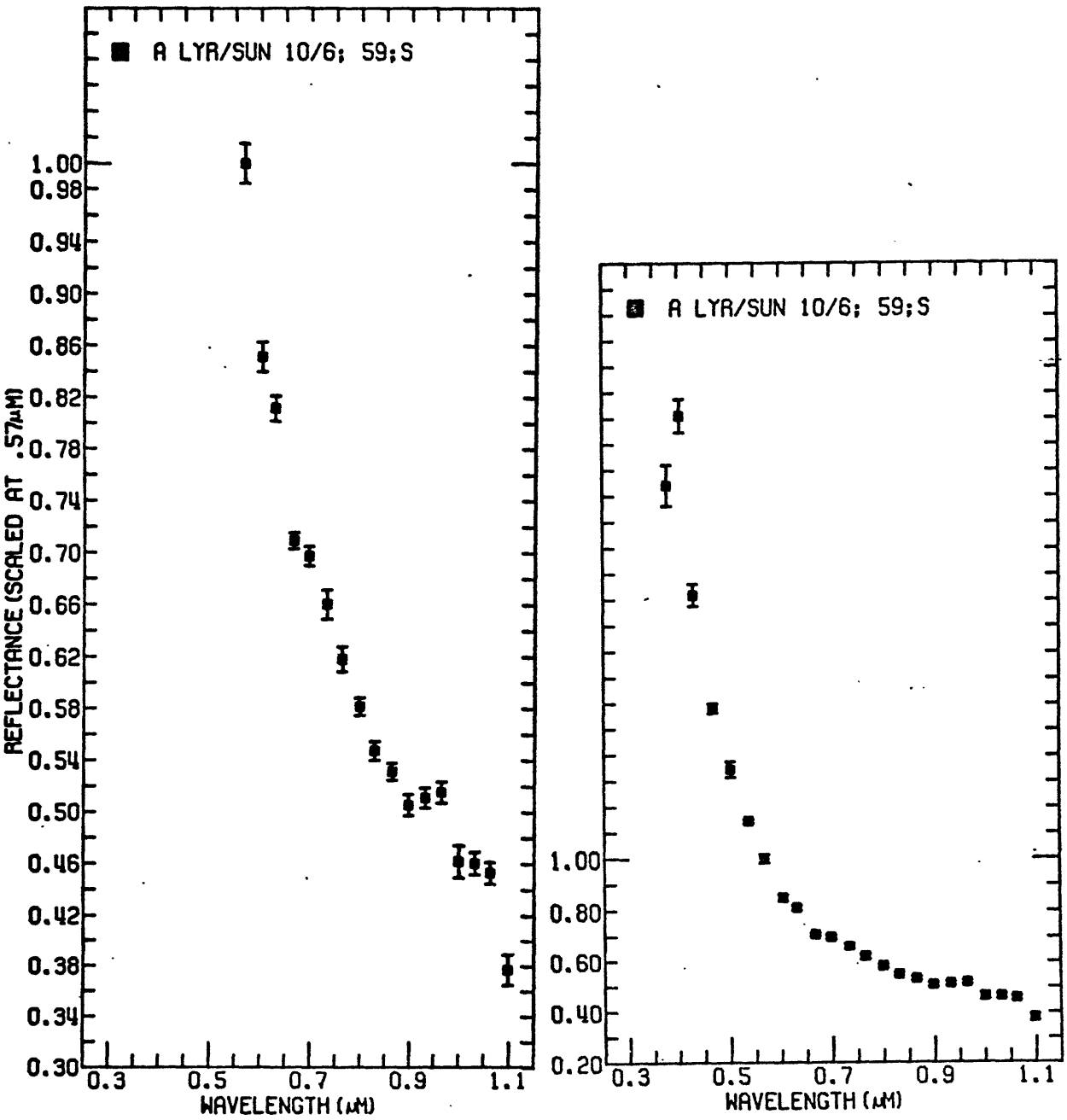

A LYR/SUN 10/1;-05;S

WAVELENGTH	AVE.FLUX	STND.ERROR	PERCENT
0.3784	0.21736E 01	0.42192E-01	1.94
0.4041	0.26486E 01	0.27009E-01	1.02
0.4299	0.19553E 01	0.16572E-01	0.85
0.4677	0.15524E 01	0.63050E-02	0.41
0.5019	0.12978E 01	0.86310E-02	0.67
0.5366	0.11527E 01	0.64380E-02	0.56
0.5674	0.10000E 01	0.47700E-02	0.48
0.6041	0.89600E 00	0.41800E-02	0.47
0.6312	0.83930E 00	0.36880E-02	0.44
0.6679	0.74999E 00	0.44280E-02	0.59
0.6986	0.73210E 00	0.44790E-02	0.61
0.7339	0.67658E 00	0.36360E-02	0.54
0.7645	0.63921E 00	0.37700E-02	0.59
0.7999	0.59870E 00	0.33210E-02	0.55
0.8310	0.56866E 00	0.52800E-02	0.93
0.8653	0.56269E 00	0.40490E-02	0.72
0.8987	0.55826E 00	0.45420E-02	0.81
0.9329	0.57129E 00	0.59350E-02	1.04
0.9660	0.55785E 00	0.57040E-02	1.02
1.0008	0.51798E 00	0.50750E-02	0.98
1.0330	0.52554E 00	0.51820E-02	0.99
1.0637	0.51582E 00	0.61740E-02	1.20
1.0991	0.46657E 00	0.91800E-02	1.97

A LYR/SUN 9/01;-06;W

WAVELENGTH	AVE.FLUX	STND.ERROR	PERCENT
0.3626	0.16117E 01	0.17807E-01	1.10
0.4037	0.25170E 01	0.23799E-01	0.95
0.4370	0.18985E 01	0.86410E-02	0.46
0.4716	0.14324E 01	0.39050E-02	0.27
0.5033	0.12736E 01	0.37430E-02	0.29
0.5383	0.11101E 01	0.38160E-02	0.34
0.5659	0.10000E 01	0.23490E-02	0.23
0.6050	0.87115E 00	0.40970E-02	0.47
0.6376	0.80006E 00	0.20990E-02	0.26
0.6696	0.72618E 00	0.28940E-02	0.40
0.7010	0.69613E 00	0.18970E-02	0.27
0.7348	0.65381E 00	0.27110E-02	0.41
0.7685	0.60808E 00	0.23670E-02	0.39
0.8006	0.56997E 00	0.13100E-02	0.23
0.8348	0.54310E 00	0.18550E-02	0.34
0.8679	0.53163E 00	0.19890E-02	0.37
0.9020	0.54107E 00	0.27500E-02	0.51
0.9336	0.54357E 00	0.45340E-02	0.83
0.9667	0.54031E 00	0.50520E-02	0.94
0.9980	0.49337E 00	0.40170E-02	0.81
1.0305	0.49418E 00	0.42670E-02	0.86
1.0631	0.47481E 00	0.84760E-02	1.79
1.0981	0.43414E 00	0.75660E-02	1.74

Table II-5

ALYR/SUN1/28;0 TAU; 11;S

WAVELENGTH	AVE.FLUX	STND.ERROR	PERCENT
0.3784	0.22773E 01	0.48961E-01	2.15
0.4041	0.28224E 01	0.56152E-01	1.99
0.4299	0.20035E 01	0.25361E-01	1.27
0.4677	0.15579E 01	0.12854E-01	0.83
0.5019	0.13222E 01	0.88720E-02	0.67
0.5366	0.11468E 01	0.92770E-02	0.81
0.5674	0.10000E 01	0.60250E-02	0.60
0.6041	0.88681E 00	0.65790E-02	0.74
0.6312	0.82349E 00	0.48990E-02	0.59
0.6679	0.73481E 00	0.44550E-02	0.61
0.6986	0.72420E 00	0.43740E-02	0.60
0.7339	0.66478E 00	0.45140E-02	0.68
0.7645	0.61759E 00	0.42710E-02	0.69
0.7999	0.58288E 00	0.40990E-02	0.70
0.8310	0.54698E 00	0.52990E-02	0.97
0.8653	0.54436E 00	0.42590E-02	0.78
0.8987	0.53279E 00	0.49470E-02	0.93
0.9329	0.54000E 00	0.59280E-02	1.10
0.9660	0.52364E 00	0.56800E-02	1.08
1.0008	0.49502E 00	0.52710E-02	1.06
1.0330	0.50039E 00	0.51480E-02	1.03
1.0637	0.49612E 00	0.71360E-02	1.44
0.8670	0.53767E 00	0.41970E-02	0.78

A LYR/SUN 9/30;-14;W

WAVELENGTH	AVE.FLUX	STND.ERROR	PERCENT
0.3626	0.19701E 01	0.42460E-01	2.16
0.4037	0.26955E 01	0.55721E-01	2.07
0.4370	0.20894E 01	0.16903E-01	0.81
0.4716	0.15822E 01	0.75560E-02	0.48
0.5033	0.13148E 01	0.67060E-02	0.51
0.5383	0.11552E 01	0.67310E-02	0.58
0.5659	0.10000E 01	0.33600E-02	0.34
0.6050	0.88292E 00	0.25550E-02	0.29
0.6376	0.82401E 00	0.32170E-02	0.39
0.6696	0.72592E 00	0.29630E-02	0.41
0.7010	0.71346E 00	0.35180E-02	0.49
0.7348	0.65815E 00	0.32030E-02	0.49
0.7685	0.59839E 00	0.48910E-02	0.82
0.8006	0.56812E 00	0.33200E-02	0.58
0.8348	0.53412E 00	0.50580E-02	0.95
0.8679	0.52826E 00	0.32390E-02	0.61
0.9020	0.52693E 00	0.42230E-02	0.80
0.9336	0.49352E 00	0.44210E-02	0.90
0.9667	0.49197E 00	0.56970E-02	1.16
0.9980	0.46301E 00	0.44520E-02	0.96
1.0305	0.47091E 00	0.46310E-02	0.98
1.0631	0.45195E 00	0.68850E-02	1.52
1.0981	0.42731E 00	0.82920E-02	1.94

Table II-6

A LYR/SUN 8/31;-17;S

WAVELENGTH	AVE.FLUX	STND.ERROR	PERCENT
0.3784	0.23714E 01	0.61693E-01	2.60
0.4041	0.26015E 01	0.65976E-01	2.54
0.4299	0.19587E 01	0.46851E-01	2.39
0.4677	0.15420E 01	0.29992E-01	1.95
0.5019	0.13173E 01	0.43510E-02	0.33
0.5366	0.11581E 01	0.49590E-02	0.43
0.5674	0.10000E 01	0.58600E-02	0.59
0.6041	0.87803E 00	0.36050E-02	0.41
0.6312	0.82426E 00	0.38780E-02	0.47
0.6679	0.72494E 00	0.56190E-02	0.78
0.6986	0.66582E 00	0.74800E-02	1.12
0.7339	0.63957E 00	0.12925E-01	2.02
0.7645	0.59625E 00	0.13672E-01	2.29
0.7999	0.54757E 00	0.12101E-01	2.21
0.8310	0.52491E 00	0.10687E-01	2.04
0.8653	0.52029E 00	0.84940E-02	1.63
0.8987	0.51147E 00	0.94070E-02	1.84
0.9329	0.51623E 00	0.79540E-02	1.54
0.9660	0.51333E 00	0.67460E-02	1.31
1.0008	0.48392E 00	0.48150E-02	1.00
1.0330	0.48063E 00	0.49530E-02	1.03
1.0637	0.47004E 00	0.39610E-02	0.84
1.0991	0.43292E 00	0.62940E-02	1.45

A LYR/SUN 9/29;-24;S

WAVELENGTH	AVE.FLUX	STND.ERROR	PERCENT
0.3784	0.23529E 01	0.26784E-01	1.14
0.4041	0.28607E 01	0.24936E-01	0.87
0.4299	0.20208E 01	0.13115E-01	0.65
0.4677	0.15740E 01	0.12110E-01	0.77
0.5019	0.13218E 01	0.56360E-02	0.43
0.5366	0.11399E 01	0.49920E-02	0.44
0.5674	0.10000E 01	0.36090E-02	0.36
0.6041	0.88694E 00	0.36490E-02	0.41
0.6312	0.81982E 00	0.35980E-02	0.44
0.6679	0.73436E 00	0.28580E-02	0.39
0.6986	0.70874E 00	0.32340E-02	0.46
0.7339	0.65079E 00	0.35450E-02	0.54
0.7645	0.60810E 00	0.39940E-02	0.66
0.7999	0.57280E 00	0.32530E-02	0.57
0.8310	0.53494E 00	0.52100E-02	0.97
0.8653	0.52810E 00	0.32680E-02	0.62
0.8987	0.52273E 00	0.43360E-02	0.83
0.9329	0.52939E 00	0.53150E-02	1.00
0.9660	0.51622E 00	0.53510E-02	1.04
1.0008	0.48001E 00	0.46120E-02	0.96
1.0330	0.48380E 00	0.44190E-02	0.91
1.0637	0.46942E 00	0.58670E-02	1.25
1.0991	0.41672E 00	0.89320E-02	2.14

Table II-7

ALYR/SUN1/29;0 TAU; 27;S

WAVELENGTH	AVE.FLUX	STND.ERROR	PERCENT
0.3784	0.23436E 01	0.54789E-01	2.34
0.4041	0.28958E 01	0.76186E-01	2.63
0.4299	0.20306E 01	0.31797E-01	1.57
0.4677	0.15984E 01	0.12136E-01	0.76
0.5019	0.13391E 01	0.92450E-02	0.69
0.5366	0.11675E 01	0.83600E-02	0.72
0.5674	0.10000E 01	0.63300E-02	0.63
0.6041	0.88518E 00	0.51530E-02	0.58
0.6312	0.82133E 00	0.50030E-02	0.61
0.6679	0.70908E 00	0.55800E-02	0.79
0.6986	0.69660E 00	0.76100E-02	1.09
0.7339	0.63835E 00	0.54560E-02	0.85
0.7645	0.59444E 00	0.45970E-02	0.77
0.7999	0.55480E 00	0.41810E-02	0.75
0.8310	0.52755E 00	0.54900E-02	1.04
0.8653	0.51036E 00	0.47230E-02	0.93
0.8987	0.50936E 00	0.51310E-02	1.01
0.9329	0.49151E 00	0.54000E-02	1.10
0.9660	0.49504E 00	0.58380E-02	1.18
1.0008	0.47425E 00	0.55520E-02	1.17
1.0330	0.47387E 00	0.53090E-02	1.12
1.0637	0.46315E 00	0.74170E-02	1.60
0.8670	0.51180E 00	0.46630E-02	0.91

A LYR/SUN 8/30;-28;W

WAVELENGTH	AVE.FLUX	STND.ERROR	PERCENT
0.3626	0.17380E 01	0.36262E-01	2.09
0.4037	0.28075E 01	0.35404E-01	1.26
0.4370	0.20053E 01	0.30698E-01	1.53
0.4716	0.14965E 01	0.60250E-02	0.40
0.5033	0.13017E 01	0.39350E-02	0.30
0.5383	0.11280E 01	0.27640E-02	0.25
0.5659	0.10000E 01	0.21730E-02	0.22
0.6050	0.85729E 00	0.19830E-02	0.23
0.6376	0.77062E 00	0.30260E-02	0.39
0.6696	0.70483E 00	0.25190E-02	0.36
0.7010	0.67248E 00	0.58900E-02	0.88
0.7348	0.64495E 00	0.11367E-01	1.76
0.7685	0.59905E 00	0.98150E-02	1.64
0.8006	0.55188E 00	0.11303E-01	2.05
0.8348	0.51743E 00	0.11918E-01	2.30
0.8679	0.50623E 00	0.12228E-01	2.42
0.9020	0.51108E 00	0.13981E-01	2.74
0.9336	0.51632E 00	0.14718E-01	2.85
0.9667	0.49212E 00	0.10508E-01	2.14
0.9980	0.45626E 00	0.14022E-01	3.07
1.0305	0.45501E 00	0.16308E-01	3.58
1.0631	0.43578E 00	0.14153E-01	3.25
1.0981	0.40515E 00	0.10713E-01	2.64

Table II-8

A LYR/SUN 9/04; 29;S

WAVELENGTH	AVE.FLUX	STND.ERROR	PERCENT
0.3784	0.24696E 01	0.24261E-01	0.98
0.4041	0.27402E 01	0.24886E-01	0.91
0.4299	0.20525E 01	0.10471E-01	0.51
0.4677	0.16089E 01	0.85140E-02	0.53
0.5019	0.13533E 01	0.59130E-02	0.44
0.5366	0.11631E 01	0.70430E-02	0.61
0.5674	0.10000E 01	0.38110E-02	0.38
0.6041	0.87811E 00	0.23330E-02	0.27
0.6312	0.82392E 00	0.23280E-02	0.28
0.6679	0.72792E 00	0.35660E-02	0.49
0.6986	0.69536E 00	0.56980E-02	0.82
0.7339	0.64473E 00	0.50960E-02	0.79
0.7645	0.59768E 00	0.29790E-02	0.50
0.7999	0.55398E 00	0.45480E-02	0.82
0.8310	0.52534E 00	0.34990E-02	0.67
0.8653	0.51698E 00	0.45370E-02	0.88
0.8987	0.51358E 00	0.41070E-02	0.80
0.9329	0.51624E 00	0.59630E-02	1.16
0.9660	0.50742E 00	0.37240E-02	0.73
1.0008	0.47004E 00	0.38440E-02	0.82
1.0330	0.47350E 00	0.34580E-02	0.73
1.0637	0.46370E 00	0.42990E-02	0.93
1.0991	0.42957E 00	0.57270E-02	1.33

A LYR/SUN 10/4;35 ;S

WAVELENGTH	AVE.FLUX	STND.ERROR	PERCENT
0.3784	0.24895E 01	0.35832E-01	1.44
0.4041	0.28811E 01	0.26443E-01	0.92
0.4299	0.20921E 01	0.17384E-01	0.83
0.4677	0.15863E 01	0.14271E-01	0.90
0.5019	0.13143E 01	0.96390E-02	0.73
0.5366	0.11496E 01	0.59240E-02	0.52
0.5674	0.10000E 01	0.67590E-02	0.68
0.6041	0.84285E 00	0.78020E-02	0.93
0.6312	0.80167E 00	0.29130E-02	0.36
0.6679	0.69988E 00	0.41740E-02	0.60
0.6986	0.65683E 00	0.50760E-02	0.77
0.7339	0.60440E 00	0.47210E-02	0.78
0.7645	0.56623E 00	0.35370E-02	0.62
0.7999	0.51725E 00	0.42660E-02	0.82
0.8310	0.49943E 00	0.48720E-02	0.98
0.8653	0.49303E 00	0.40480E-02	0.82
0.8987	0.49141E 00	0.45950E-02	0.94
0.9329	0.49552E 00	0.51030E-02	1.03
0.9660	0.47963E 00	0.58610E-02	1.22
1.0008	0.43284E 00	0.60860E-02	1.41
1.0330	0.45428E 00	0.60940E-02	1.34
1.0637	0.43251E 00	0.67820E-02	1.57
1.0991	0.39069E 00	0.90630E-02	2.32

Table II-9

A LYR/SUN 9/28;-35;S

WAVELENGTH	AVE.FLUX	STND.ERROR	PERCENT
0.3784	0.24360E 01	0.28121E-01	1.15
0.4041	0.29235E 01	0.33121E-01	1.13
0.4299	0.20865E 01	0.15104E-01	0.72
0.4677	0.16003E 01	0.18456E-01	1.15
0.5019	0.13290E 01	0.78120E-02	0.59
0.5366	0.11434E 01	0.46240E-02	0.40
0.5674	0.10000E 01	0.45450E-02	0.45
0.6041	0.86327E 00	0.39410E-02	0.46
0.6312	0.80388E 00	0.37990E-02	0.47
0.6679	0.71013E 00	0.26600E-02	0.37
0.6986	0.67957E 00	0.36640E-02	0.54
0.7339	0.63489E 00	0.32920E-02	0.52
0.7645	0.58946E 00	0.30810E-02	0.52
0.7999	0.54607E 00	0.28670E-02	0.53
0.8310	0.51305E 00	0.46660E-02	0.91
0.8653	0.50862E 00	0.29350E-02	0.58
0.8987	0.50043E 00	0.40910E-02	0.82
0.9329	0.50267E 00	0.43000E-02	0.86
0.9660	0.49466E 00	0.52910E-02	1.07
1.0008	0.46750E 00	0.43350E-02	0.93
1.0330	0.47124E 00	0.44770E-02	0.95
1.0637	0.45823E 00	0.60760E-02	1.33
1.0991	0.41059E 00	0.84110E-02	2.05

ALYR/SUN1/30;G GEM;+40;S

WAVELENGTH	AVE.FLUX	STND.ERROR	PERCENT
0.3784	0.22424E 01	0.10951E 00	4.88
0.4041	0.27331E 01	0.90051E-01	3.29
0.4299	0.18311E 01	0.25911E-01	1.42
0.4677	0.15427E 01	0.15201E-01	0.99
0.5019	0.12816E 01	0.11406E-01	0.89
0.5366	0.10712E 01	0.10600E-01	0.99
0.5674	0.10000E 01	0.96450E-02	0.96
0.6041	0.83293E 00	0.87690E-02	1.05
0.6312	0.78710E 00	0.66590E-02	0.85
0.6679	0.67650E 00	0.72220E-02	1.07
0.6986	0.69275E 00	0.12729E-01	1.84
0.7339	0.60402E 00	0.81830E-02	1.35
0.7645	0.57626E 00	0.72190E-02	1.25
0.7999	0.55208E 00	0.11252E-01	2.04
0.8310	0.52472E 00	0.10916E-01	2.08
0.8653	0.49747E 00	0.10878E-01	2.19
0.8987	0.50572E 00	0.85940E-02	1.70
0.9329	0.49430E 00	0.11217E-01	2.27
0.9660	0.47322E 00	0.11532E-01	2.44
1.0008	0.48614E 00	0.11854E-01	2.44
1.0330	0.48279E 00	0.12373E-01	2.56
1.0637	0.46948E 00	0.15684E-01	3.34
0.8670	0.49690E 00	0.10974E-01	2.21

Table II-10

A LYR/SUN 9/05; 41;S

WAVELENGTH	AVE.FLUX	STND.ERROR	PERCENT
0.3784	0.25695E 01	0.14904E-01	0.58
0.4041	0.27913E 01	0.24618E-01	0.88
0.4299	0.20856E 01	0.14609E-01	0.70
0.4677	0.16071E 01	0.93220E-02	0.58
0.5019	0.13290E 01	0.42960E-02	0.32
0.5366	0.11547E 01	0.49390E-02	0.43
0.5674	0.10000E 01	0.34530E-02	0.35
0.6041	0.87520E 00	0.54480E-02	0.62
0.6312	0.81749E 00	0.23090E-02	0.28
0.6679	0.70253E 00	0.27800E-02	0.40
0.6986	0.67082E 00	0.34990E-02	0.52
0.7339	0.62698E 00	0.44330E-02	0.71
0.7645	0.59303E 00	0.32850E-02	0.55
0.7999	0.54342E 00	0.37030E-02	0.68
0.8310	0.52156E 00	0.34840E-02	0.67
0.8653	0.50366E 00	0.40810E-02	0.81
0.8987	0.50964E 00	0.64160E-02	1.26
0.9329	0.51276E 00	0.56240E-02	1.10
0.9660	0.50368E 00	0.49980E-02	0.99
1.0008	0.46129E 00	0.54740E-02	1.19
1.0330	0.45956E 00	0.56720E-02	1.23
1.0637	0.44761E 00	0.76260E-02	1.70
1.0991	0.43860E 00	0.81900E-02	1.87

A LYR/SUN 10/5; 48;S

WAVELENGTH	AVE.FLUX	STND.ERROR	PERCENT
0.4041	0.29928E 01	0.51580E-01	1.72
0.4299	0.21542E 01	0.35330E-01	1.64
0.4677	0.16332E 01	0.12115E-01	0.74
0.5019	0.13365E 01	0.98380E-02	0.74
0.5366	0.11442E 01	0.76510E-02	0.67
0.5674	0.10000E 01	0.58060E-02	0.58
0.6041	0.85403E 00	0.48350E-02	0.57
0.6312	0.80198E 00	0.80520E-02	1.00
0.6679	0.71109E 00	0.41220E-02	0.58
0.6986	0.68311E 00	0.51620E-02	0.76
0.7339	0.61504E 00	0.48040E-02	0.78
0.7645	0.56976E 00	0.41360E-02	0.73
0.7999	0.53785E 00	0.30340E-02	0.56
0.8310	0.49908E 00	0.49690E-02	1.00
0.8653	0.48762E 00	0.58150E-02	1.19
0.8987	0.48526E 00	0.57080E-02	1.18
0.9329	0.50286E 00	0.85900E-02	1.71
0.9660	0.49455E 00	0.61300E-02	1.24
1.0008	0.45028E 00	0.55090E-02	1.22
1.0330	0.46726E 00	0.58350E-02	1.25
1.0637	0.44095E 00	0.65640E-02	1.49
1.0991	0.38541E 00	0.85370E-02	2.22

Table II-11

ALYR/SUN9/27;10 TAU;-48;S

WAVELENGTH	AVE.FLUX	STND.ERROR	PERCENT
0.3784	0.25306E 01	0.47952E-01	1.89
0.3784	0.24916E 01	0.61114E-01	2.45
0.4041	0.29454E 01	0.99863E-01	3.39
0.4299	0.20604E 01	0.48246E-01	2.34
0.4677	0.15985E 01	0.39094E-01	2.45
0.5019	0.13318E 01	0.20627E-01	1.55
0.5366	0.11280E 01	0.13200E-01	1.17
0.5674	0.10000E 01	0.14225E-01	1.42
0.6041	0.85936E 00	0.82950E-02	0.97
0.6312	0.79309E 00	0.64170E-02	0.81
0.6679	0.69803E 00	0.48380E-02	0.69
0.6986	0.67493E 00	0.60910E-02	0.90
0.7339	0.63277E 00	0.51850E-02	0.82
0.7645	0.57516E 00	0.56250E-02	0.98
0.7999	0.54040E 00	0.50410E-02	0.93
0.8310	0.51914E 00	0.64710E-02	1.25
0.8653	0.50680E 00	0.62890E-02	1.24
0.8987	0.50012E 00	0.54820E-02	1.10
0.9329	0.50533E 00	0.55570E-02	1.10
0.9660	0.49935E 00	0.65630E-02	1.31
1.0008	0.45915E 00	0.55030E-02	1.20
1.0330	0.47505E 00	0.67380E-02	1.42
1.0637	0.44044E 00	0.87550E-02	1.99
1.0991	0.42439E 00	0.18312E-01	4.31

ALYR/SUN1/31;0 TAU;+54;S

WAVELENGTH	AVE.FLUX	STND.ERROR	PERCENT
0.3784	0.26094E 01	0.61762E-01	2.37
0.4041	0.30718E 01	0.59356E-01	1.93
0.4299	0.21057E 01	0.28116E-01	1.34
0.4677	0.16487E 01	0.12995E-01	0.79
0.5019	0.13484E 01	0.10443E-01	0.77
0.5366	0.11831E 01	0.10198E-01	0.86
0.5674	0.10000E 01	0.68030E-02	0.68
0.6041	0.86009E 00	0.54640E-02	0.64
0.6312	0.79892E 00	0.51600E-02	0.65
0.6679	0.68955E 00	0.43410E-02	0.63
0.6986	0.67769E 00	0.55660E-02	0.82
0.7339	0.62087E 00	0.53940E-02	0.87
0.7645	0.57193E 00	0.47210E-02	0.83
0.7999	0.53715E 00	0.45870E-02	0.85
0.8310	0.50827E 00	0.55370E-02	1.09
0.8653	0.49567E 00	0.42070E-02	0.85
0.8987	0.48885E 00	0.48540E-02	0.99
0.9329	0.48201E 00	0.54720E-02	1.14
0.9660	0.47517E 00	0.56710E-02	1.19
1.0008	0.44240E 00	0.51840E-02	1.17
1.0330	0.44234E 00	0.51710E-02	1.17
1.0637	0.41893E 00	0.72520E-02	1.73
0.8670	0.48993E 00	0.41360E-02	0.84

Table II-12

A LYR/SUN 10/6; 59;S

WAVELENGTH	AVE.FLUX	STND.ERROR	PERCENT
0.3784	0.24424E 01	0.79282E-01	3.25
0.4041	0.27120E 01	0.65234E-01	2.41
0.4299	0.20194E 01	0.42291E-01	2.09
0.4677	0.15828E 01	0.18625E-01	1.18
0.5019	0.13462E 01	0.30162E-01	2.24
0.5366	0.11445E 01	0.70440E-02	0.62
0.5674	0.10000E 01	0.15823E-01	1.58
0.6041	0.85105E 00	0.11644E-01	1.37
0.6312	0.81138E 00	0.10080E-01	1.24
0.6679	0.70923E 00	0.61590E-02	0.87
0.6986	0.69730E 00	0.75710E-02	1.09
0.7339	0.65992E 00	0.11246E-01	1.70
0.7645	0.61808E 00	0.97730E-02	1.58
0.7999	0.58141E 00	0.70680E-02	1.22
0.8310	0.54718E 00	0.72030E-02	1.32
0.8653	0.53094E 00	0.66040E-02	1.24
0.8987	0.50540E 00	0.81750E-02	1.62
0.9329	0.51075E 00	0.78460E-02	1.54
0.9660	0.51520E 00	0.81320E-02	1.58
1.0008	0.46133E 00	0.12513E-01	2.71
1.0330	0.46019E 00	0.87020E-02	1.89
1.0637	0.45262E 00	0.83440E-02	1.84
1.0991	0.37668E 00	0.12305E-01	3.27

Table II-13

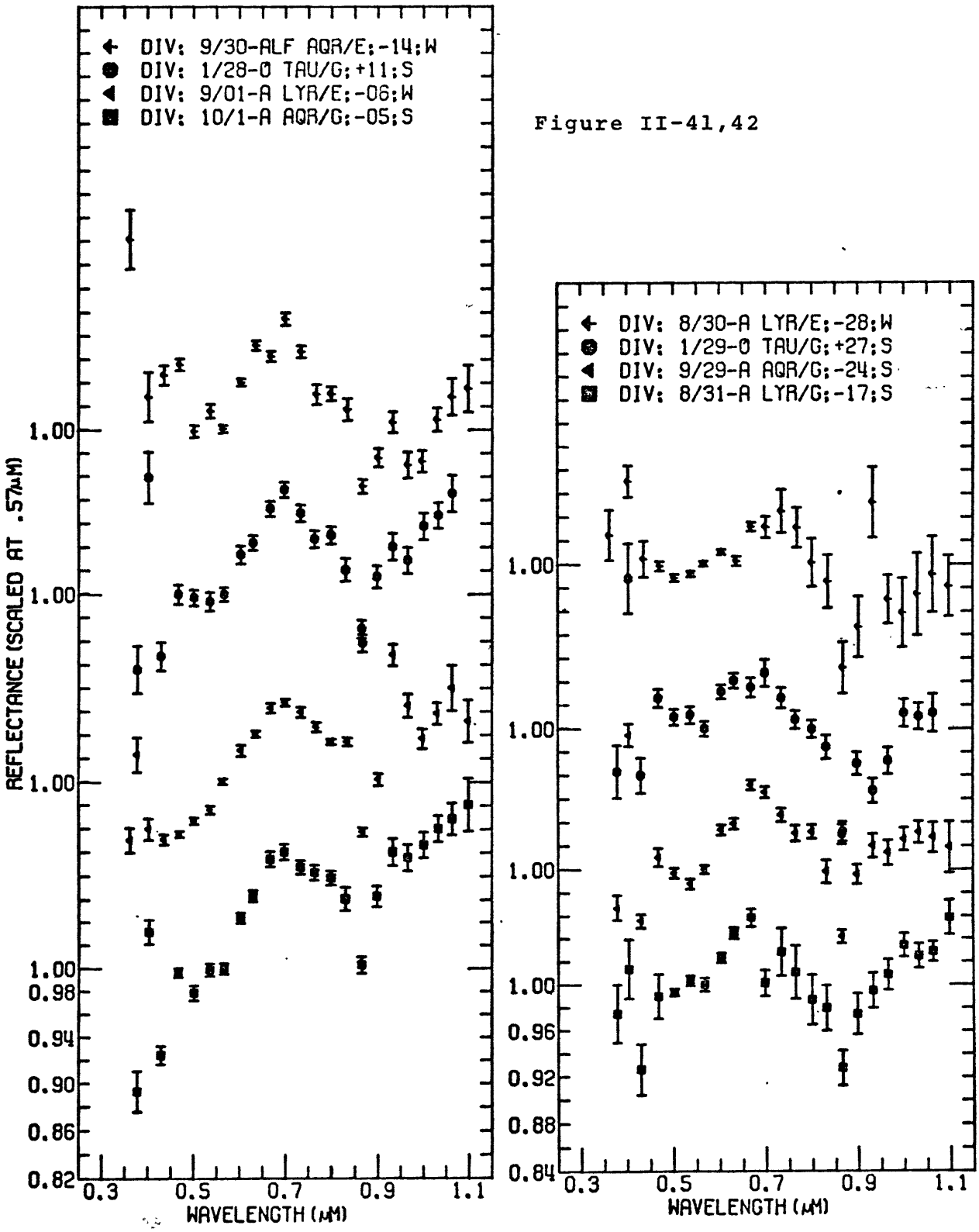

Figure II-41,42

Figure II-43,44

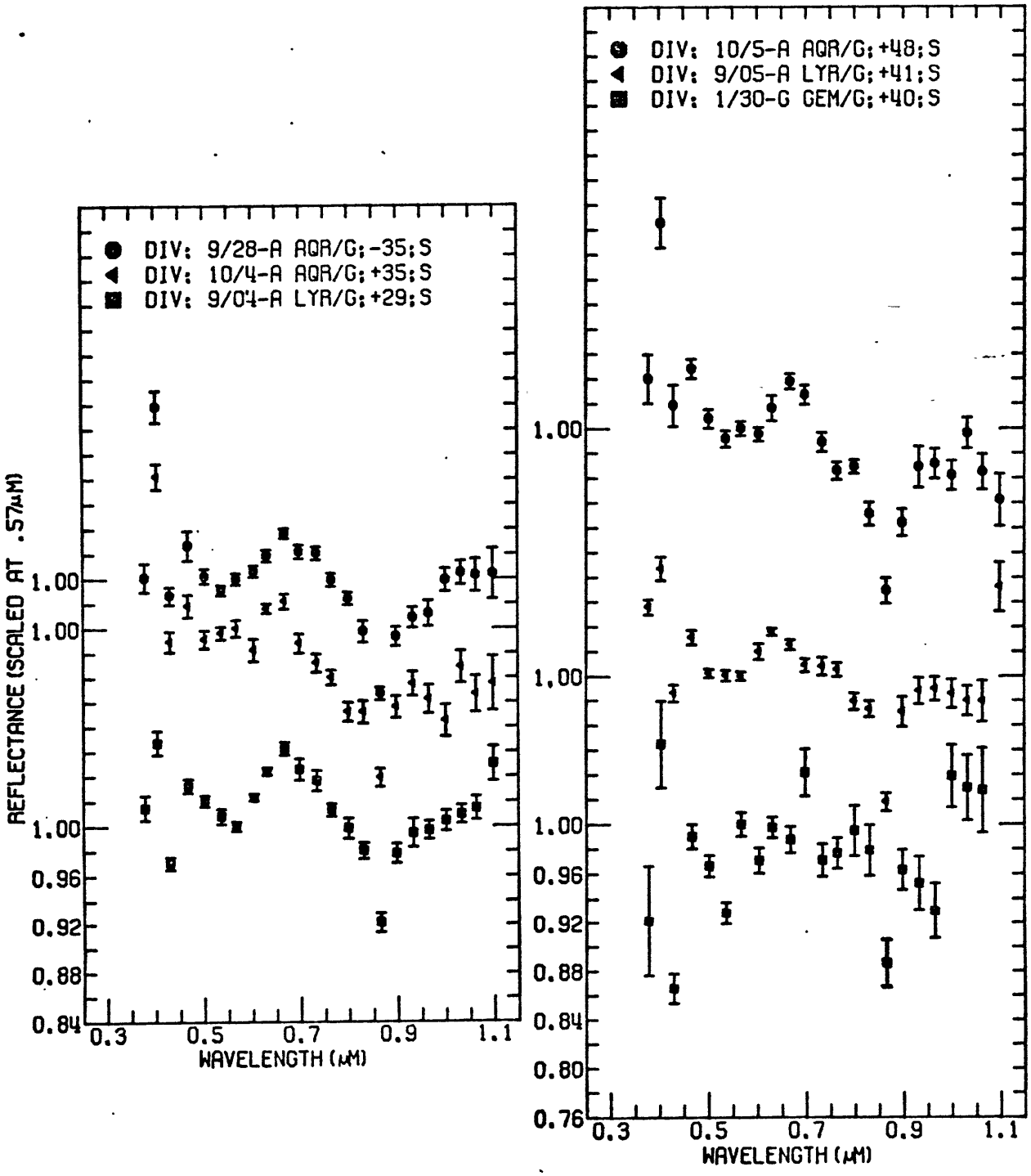

Figure II-45

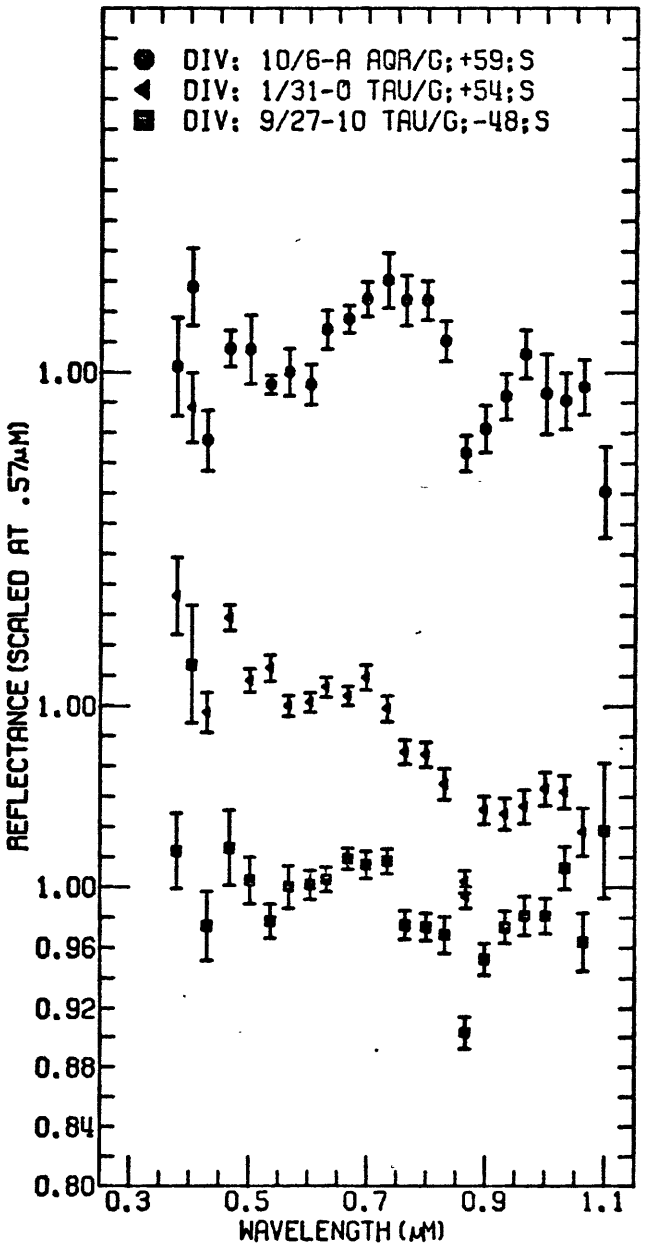
DIV: 10/6-A AQR/G;+59;S
DIV: 1/31-0 TAU/G;+54;S
DIV: 9/27-10 TAU/G;-48;S
REFLECTANCE (SCALED AT .57μM)
1.00
1.00
1.00
0.96
0.92
0.88
0.84
0.80
0.3
0.5
0.7
0.9
1.1
WAVELENGTH (μM)

Figure II-46

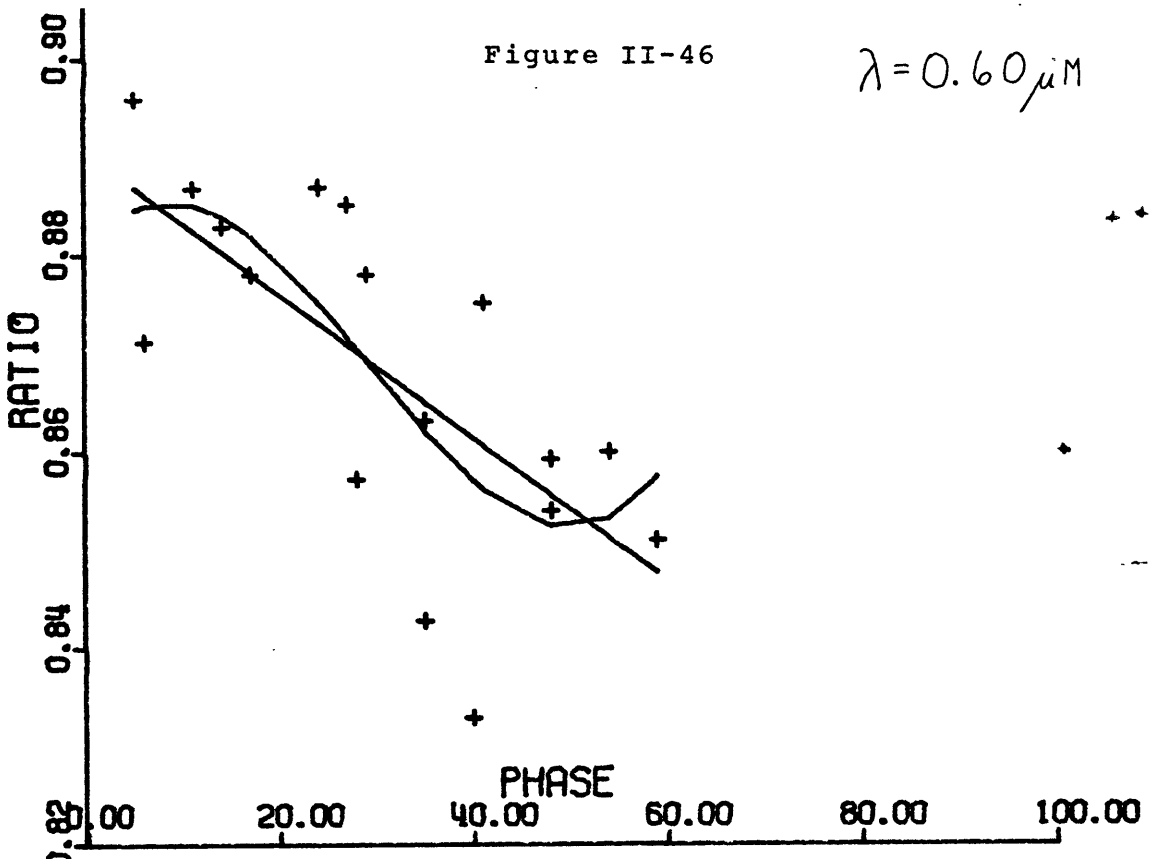
λ = 0.60 μM
RATIO
0.90
0.88
0.86
0.84
0.82
PHASE
0.00
20.00
40.00
60.00
80.00
100.00

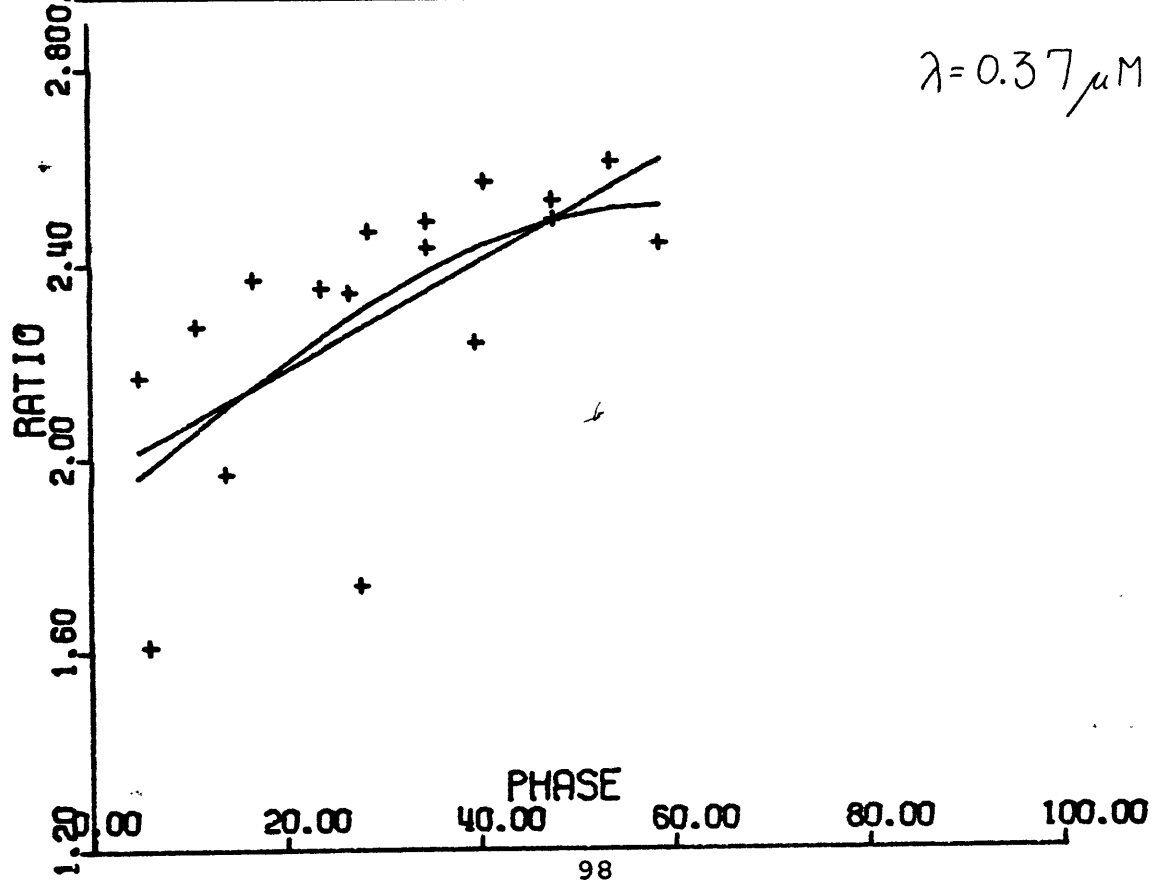
λ = 0.37 μM
RATIO
2.800
2.40
2.00
1.60
1.20
PHASE
0.00
20.00
40.00
60.00
80.00
100.00

Figure II-47

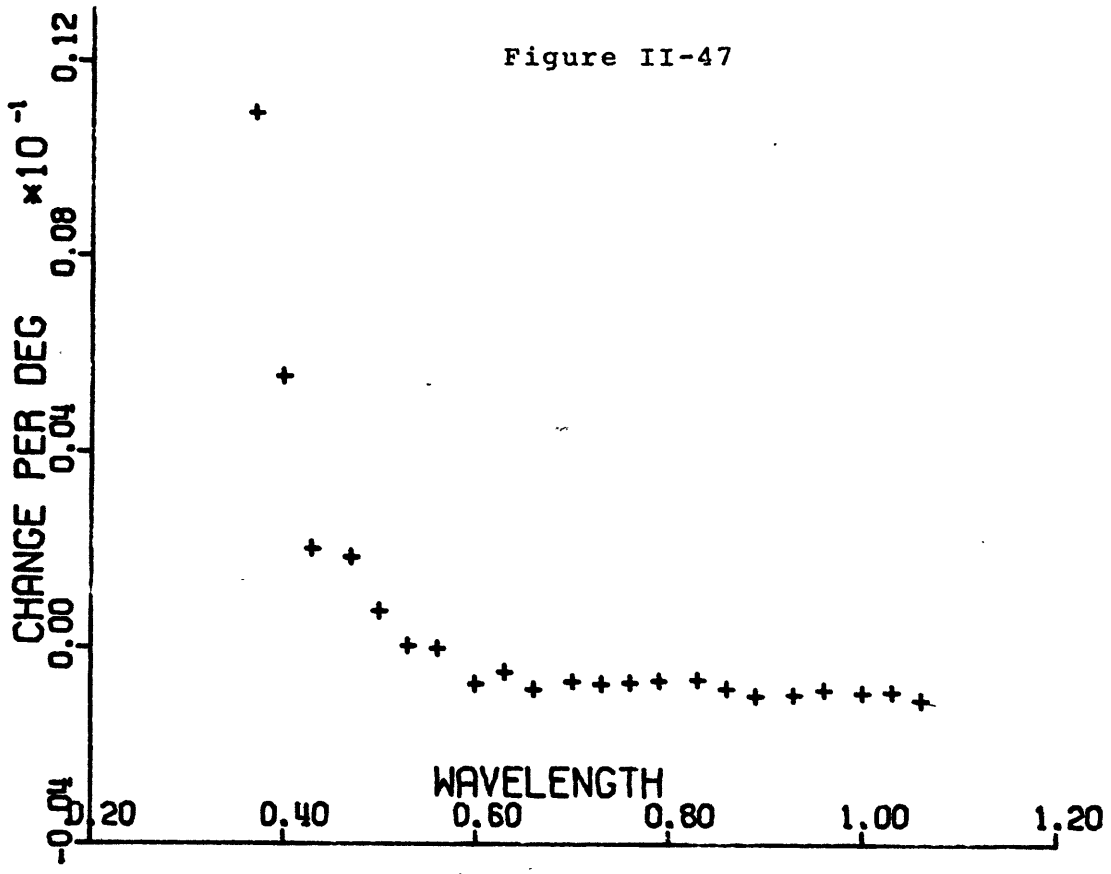

Table II-14

Wavelength	Coeff.	Wavelength	Coeff.
0.37	0.010925	0.73	-0.000722
0.40	0.005555	0.76	-0.000685
0.43	0.002037	0.79	-0.000648
0.47	0.001870	0.83	-0.000629
0.50	0.000759	0.86	-0.000814
0.53	0.000055	0.89	-0.000962
0.56	0.0	0.93	-0.000925
0.60	-0.000722	0.96	-0.000833
0.63	-0.000481	1.00	-0.000888
0.66	-0.000833	1.03	-0.000870
0.70	-0.000666	1.06	-0.001037

Figure II-48,49

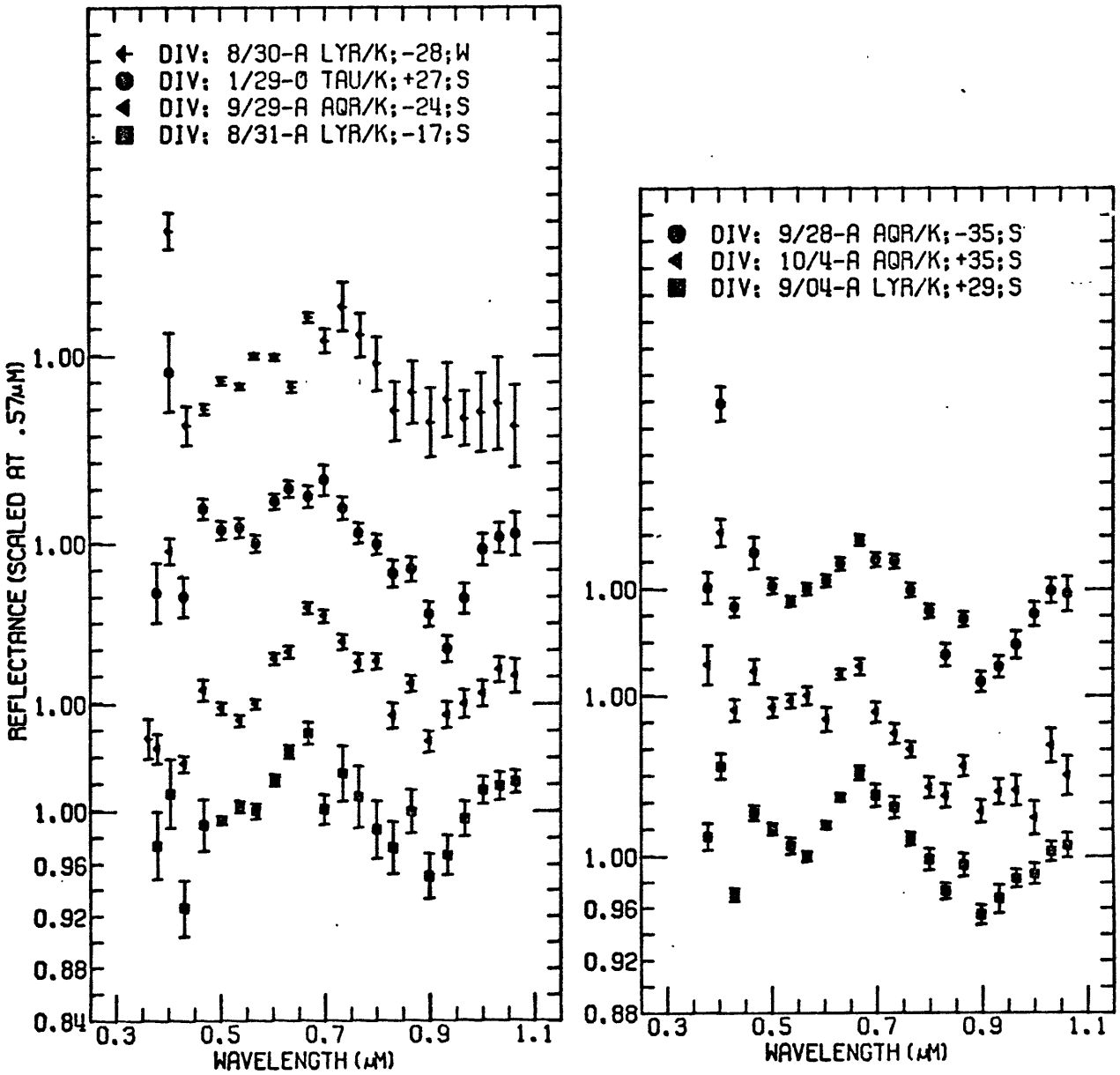

Figure II-50,51

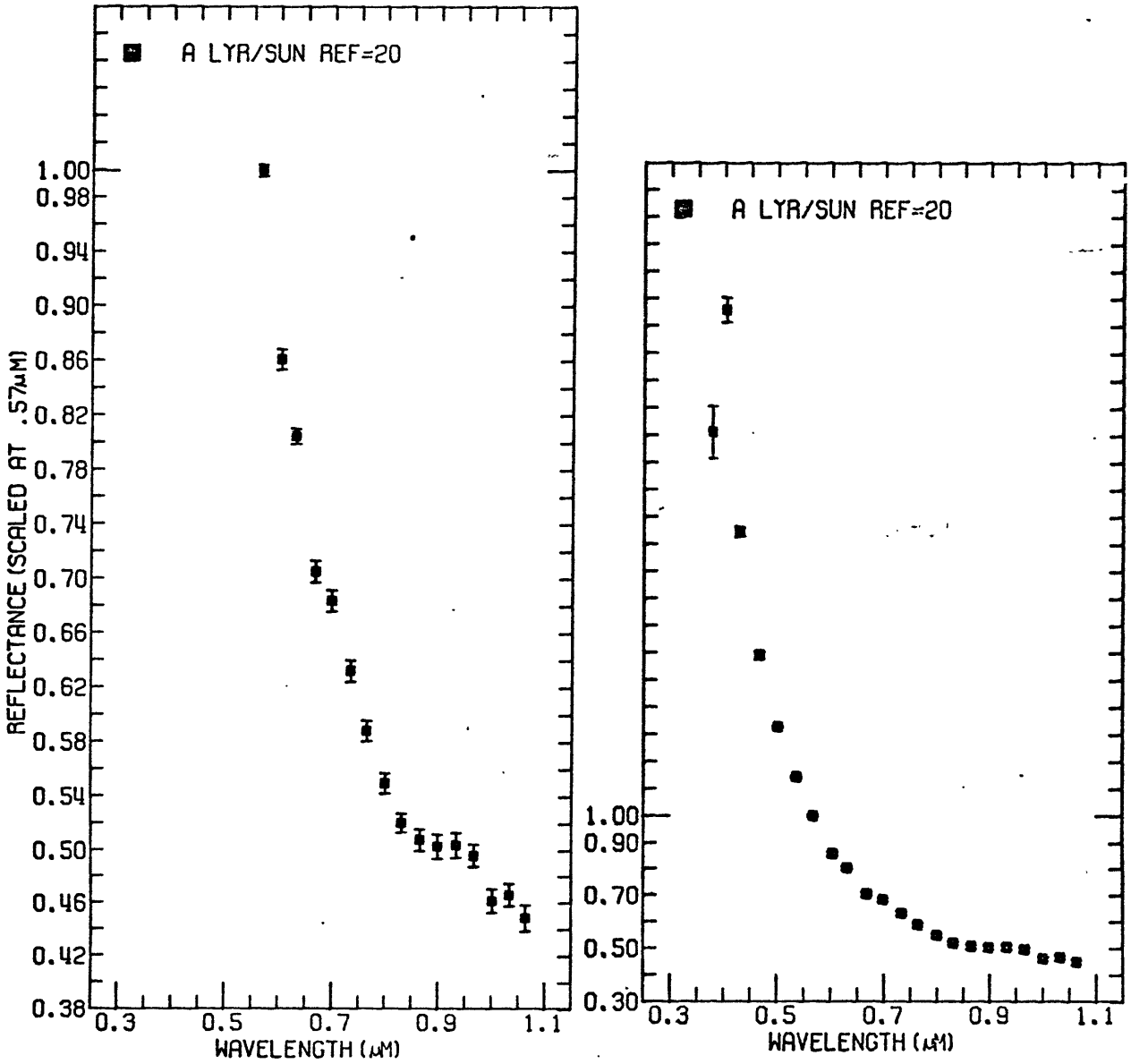

Figure II-52,53

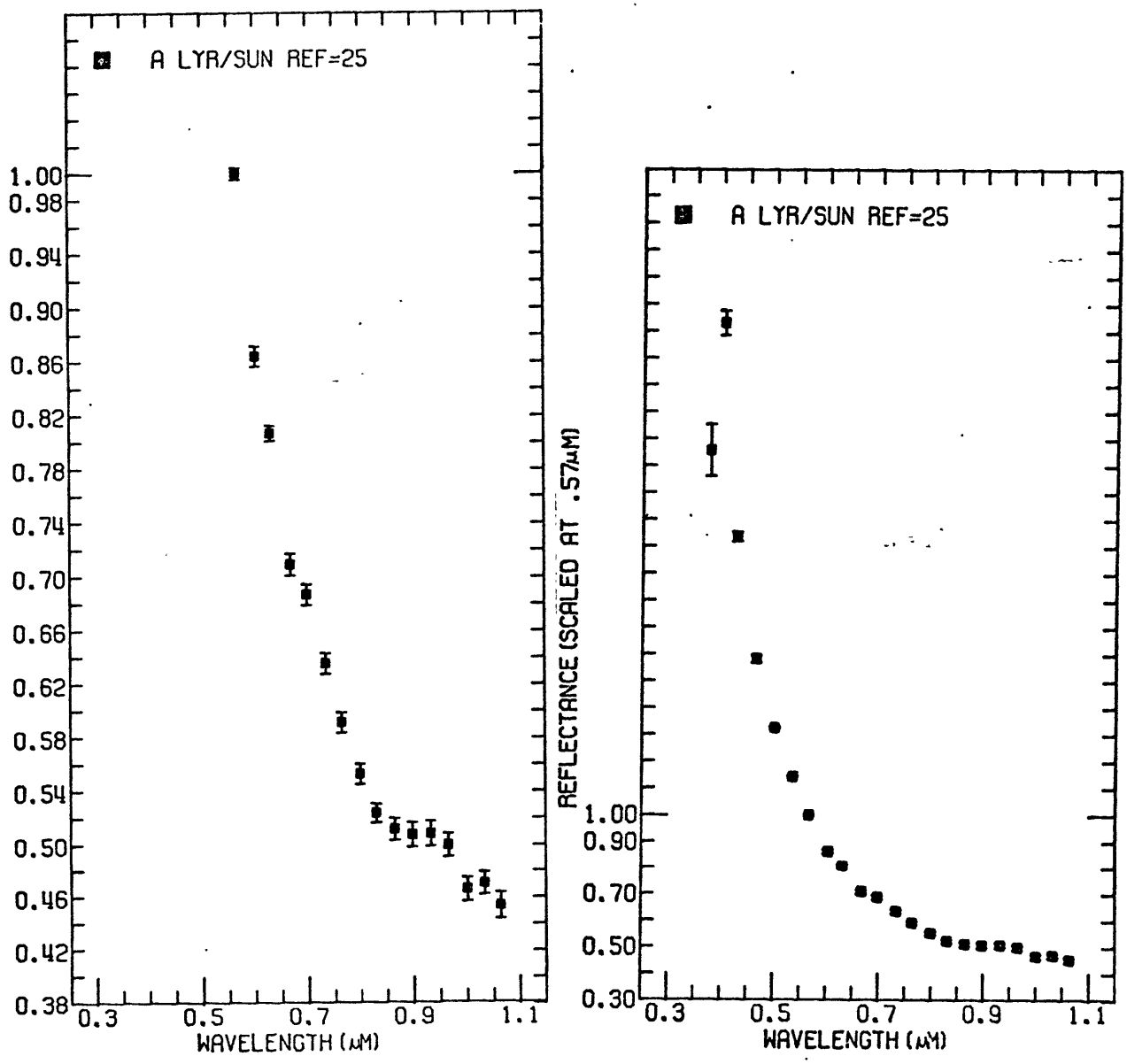

Figure II-54,55

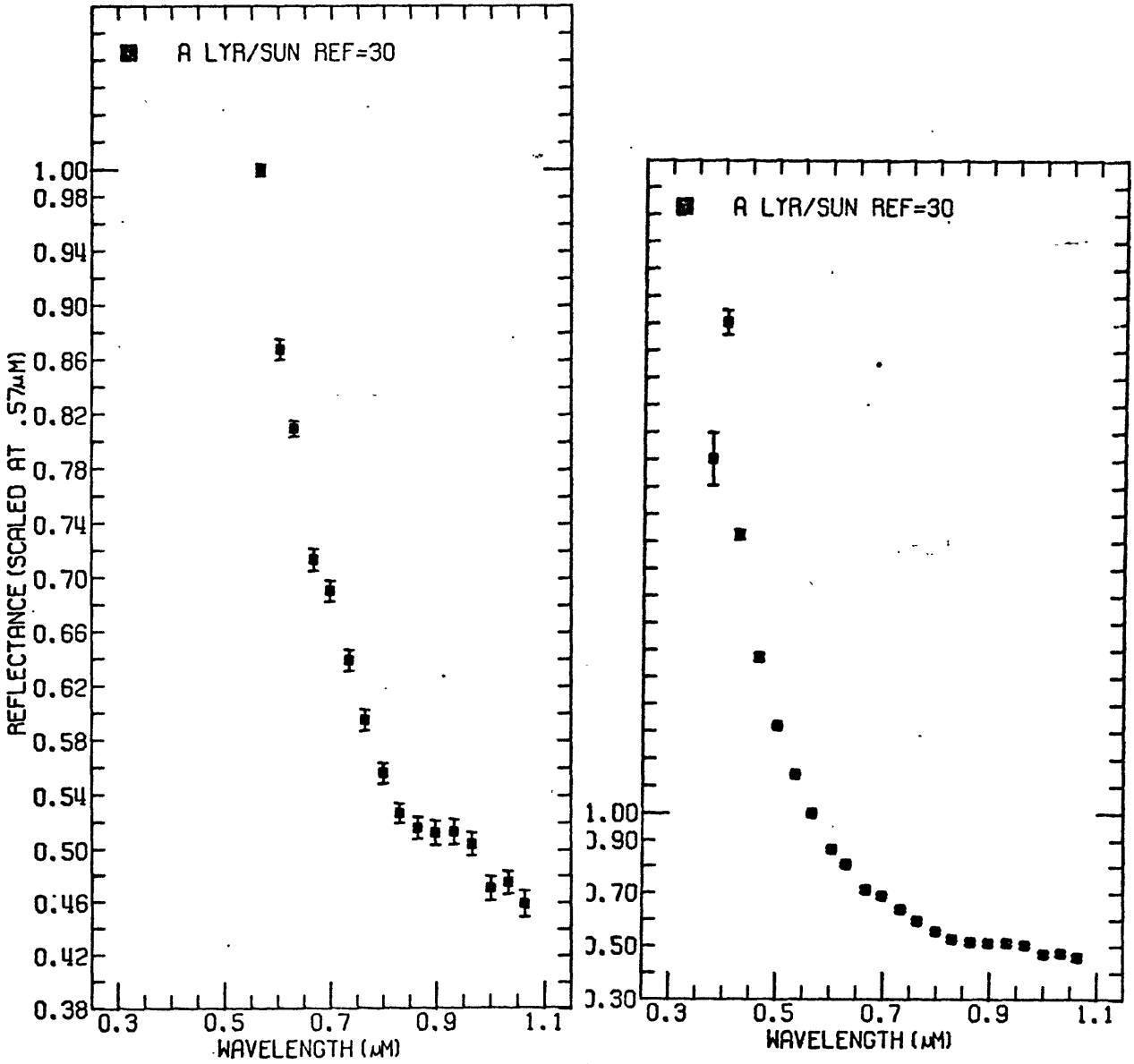

Figure II-56,57

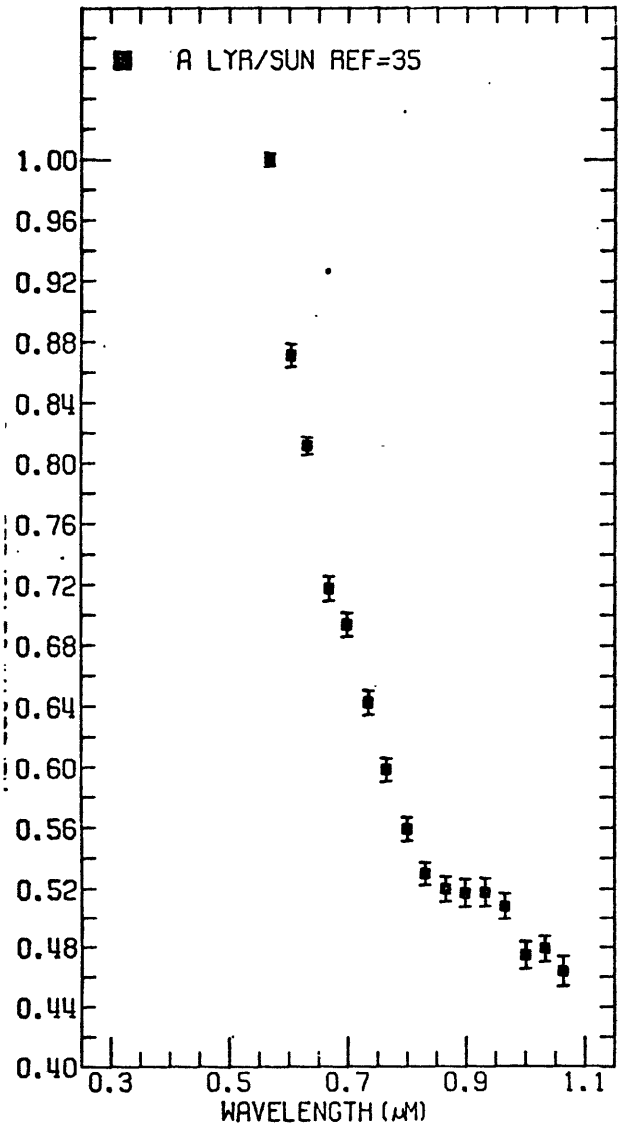

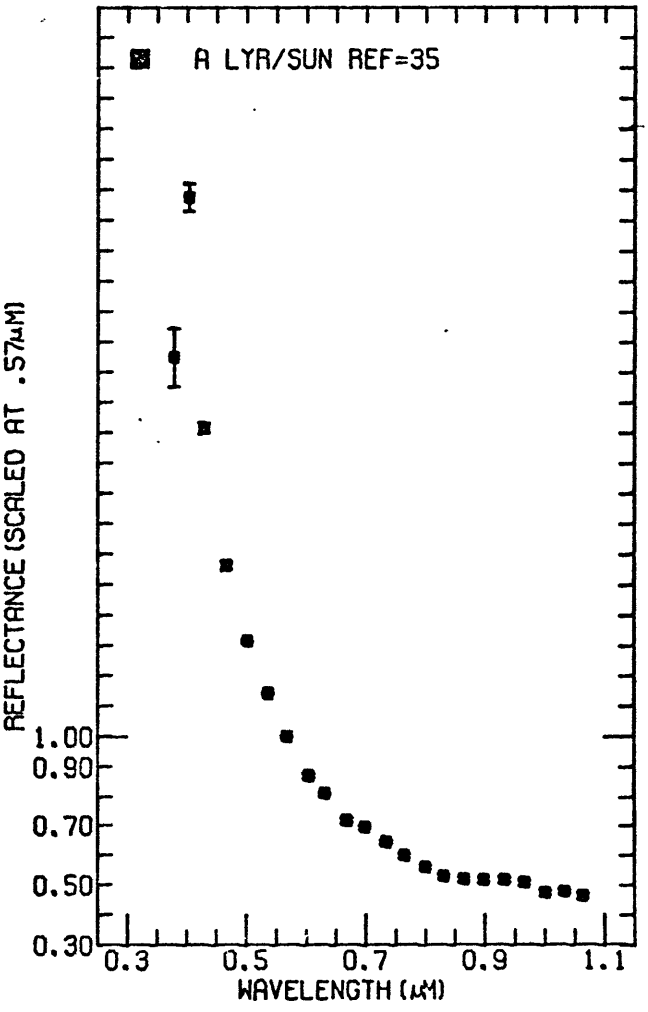

Figure II-58,59

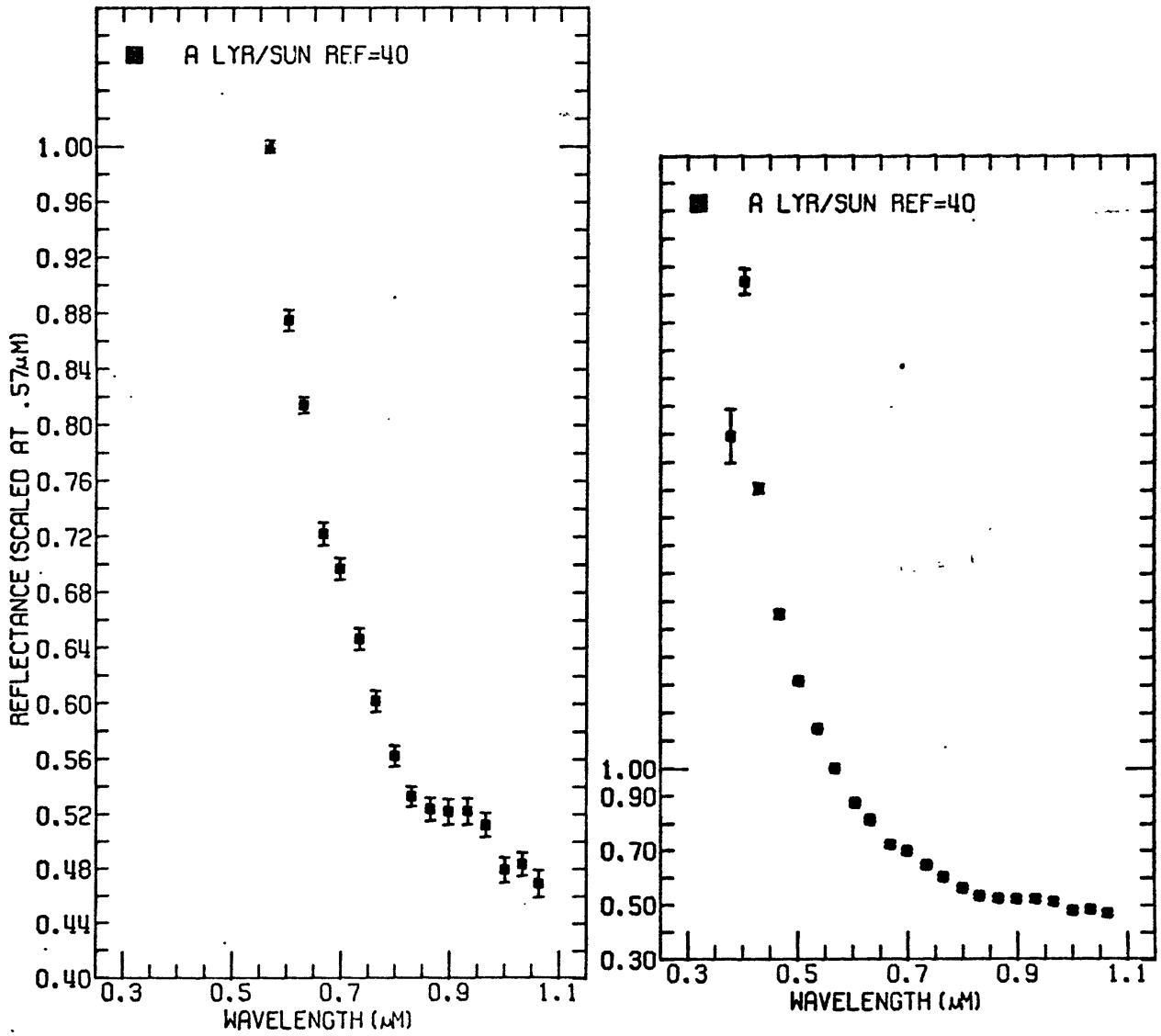

A LYR/SUN REF=20

WAVELENGTH	AVE.FLUX	STND.ERROR	PERCENT
0.3784	0.24129E 01	0.97214E-01	4.03
0.4041	0.28594E 01	0.46259E-01	1.62
0.4299	0.20467E 01	0.17524E-01	0.86
0.4677	0.15921E 01	0.13725E-01	0.86
0.5019	0.13287E 01	0.46880E-02	0.35
0.5366	0.11438E 01	0.33790E-02	0.30
0.5674	0.10000E 01	0.44720E-02	0.45
0.6041	0.86061E 00	0.75510E-02	0.88
0.6312	0.80435E 00	0.57970E-02	0.72
0.6679	0.70500E 00	0.82550E-02	1.17
0.6986	0.68344E 00	0.78680E-02	1.15
0.7339	0.63183E 00	0.80120E-02	1.27
0.7645	0.58804E 00	0.78070E-02	1.33
0.7999	0.54948E 00	0.76850E-02	1.40
0.8310	0.52024E 00	0.72550E-02	1.39
0.8653	0.50750E 00	0.82630E-02	1.63
0.8987	0.50257E 00	0.92180E-02	1.83
0.9329	0.50355E 00	0.94300E-02	1.87
0.9660	0.49559E 00	0.88030E-02	1.78
1.0008	0.46108E 00	0.91410E-02	1.98
1.0330	0.46568E 00	0.86940E-02	1.87
1.0637	0.44811E 00	0.10083E-01	2.25

A LYR/SUN REF=25

WAVELENGTH	AVE.FLUX	STND.ERROR	PERCENT
0.3784	0.23583E 01	0.97345E-01	4.13
0.4041	0.28316E 01	0.46300E-01	1.64
0.4299	0.20365E 01	0.17549E-01	0.86
0.4677	0.15828E 01	0.13742E-01	0.87
0.5019	0.13249E 01	0.46880E-02	0.35
0.5366	0.11435E 01	0.33790E-02	0.30
0.5674	0.10000E 01	0.44760E-02	0.45
0.6041	0.86422E 00	0.75610E-02	0.87
0.6312	0.80676E 00	0.58030E-02	0.72
0.6679	0.70916E 00	0.82650E-02	1.17
0.6986	0.68677E 00	0.78770E-02	1.15
0.7339	0.63544E 00	0.80210E-02	1.26
0.7645	0.59147E 00	0.78160E-02	1.32
0.7999	0.55272E 00	0.76940E-02	1.39
0.8310	0.52338E 00	0.72640E-02	1.39
0.8653	0.51157E 00	0.82730E-02	1.62
0.8987	0.50738E 00	0.92310E-02	1.82
0.9329	0.50818E 00	0.94430E-02	1.86
0.9660	0.49976E 00	0.88130E-02	1.76
1.0008	0.46552E 00	0.91550E-02	1.97
1.0330	0.47003E 00	0.87060E-02	1.85
1.0637	0.45329E 00	0.10096E-01	2.23

Table II-15

A LYR/SUN REF=30

WAVELENGTH	AVE.FLUX	STND.ERROR	PERCENT
0.3784	0.23036E 01	0.97476E-01	4.23
0.4041	0.28039E 01	0.46341E-01	1.65
0.4299	0.20263E 01	0.17573E-01	0.87
0.4677	0.15734E 01	0.13759E-01	0.87
0.5019	0.13211E 01	0.46880E-02	0.35
0.5366	0.11432E 01	0.33790E-02	0.30
0.5674	0.10000E 01	0.44810E-02	0.45
0.6041	0.86783E 00	0.75710E-02	0.87
0.6312	0.80916E 00	0.58100E-02	0.72
0.6679	0.71333E 00	0.82750E-02	1.16
0.6986	0.69010E 00	0.78860E-02	1.14
0.7339	0.63905E 00	0.80300E-02	1.26
0.7645	0.59489E 00	0.78260E-02	1.32
0.7999	0.55596E 00	0.77040E-02	1.39
0.8310	0.52653E 00	0.72740E-02	1.38
0.8653	0.51564E 00	0.82830E-02	1.61
0.8987	0.51219E 00	0.92450E-02	1.81
0.9329	0.51280E 00	0.94560E-02	1.84
0.9660	0.50392E 00	0.88230E-02	1.75
1.0008	0.46996E 00	0.91680E-02	1.95
1.0330	0.47438E 00	0.87190E-02	1.84
1.0637	0.45848E 00	0.10109E-01	2.20

A LYR/SUN REF=35

WAVELENGTH	AVE.FLUX	STND.ERROR	PERCENT
0.3784	0.22490E 01	0.97608E-01	4.34
0.4041	0.27761E 01	0.46382E-01	1.67
0.4299	0.20161E 01	0.17597E-01	0.87
0.4677	0.15641E 01	0.13777E-01	0.88
0.5019	0.13173E 01	0.46890E-02	0.36
0.5366	0.11429E 01	0.33790E-02	0.30
0.5674	0.10000E 01	0.44850E-02	0.45
0.6041	0.87144E 00	0.75810E-02	0.87
0.6312	0.81157E 00	0.58160E-02	0.72
0.6679	0.71749E 00	0.82850E-02	1.15
0.6986	0.69343E 00	0.78960E-02	1.14
0.7339	0.64266E 00	0.80390E-02	1.25
0.7645	0.59832E 00	0.78360E-02	1.31
0.7999	0.55920E 00	0.77130E-02	1.38
0.8310	0.52967E 00	0.72840E-02	1.38
0.8653	0.51971E 00	0.82930E-02	1.60
0.8987	0.51700E 00	0.92590E-02	1.79
0.9329	0.51743E 00	0.94680E-02	1.83
0.9660	0.50809E 00	0.88340E-02	1.74
1.0008	0.47440E 00	0.91820E-02	1.94
1.0330	0.47873E 00	0.87320E-02	1.82
1.0637	0.46366E 00	0.10123E-01	2.18

Table II-16

A LYR/SUN REF=40

WAVELENGTH	AVE.FLUX	STND.ERROR	PERCENT
0.3784	0.21944E 01	0.97740E-01	4.45
0.4041	0.27483E 01	0.46424E-01	1.69
0.4299	0.20059E 01	0.17622E-01	0.88
0.4677	0.15547E 01	0.13794E-01	0.89
0.5019	0.13135E 01	0.46890E-02	0.36
0.5366	0.11426E 01	0.33790E-02	0.30
0.5674	0.10000E 01	0.44900E-02	0.45
0.6041	0.87505E 00	0.75910E-02	0.87
0.6312	0.81397E 00	0.58220E-02	0.72
0.6679	0.72166E 00	0.82950E-02	1.15
0.6986	0.69676E 00	0.79050E-02	1.13
0.7339	0.64627E 00	0.80480E-02	1.25
0.7645	0.60174E 00	0.78460E-02	1.30
0.7999	0.56244E 00	0.77230E-02	1.37
0.8310	0.53282E 00	0.72940E-02	1.37
0.8653	0.52378E 00	0.83030E-02	1.59
0.8987	0.52181E 00	0.92730E-02	1.78
0.9329	0.52205E 00	0.94810E-02	1.82
0.9660	0.51225E 00	0.88440E-02	1.73
1.0008	0.47884E 00	0.91960E-02	1.92
1.0330	0.48308E 00	0.87440E-02	1.81
1.0637	0.46885E 00	0.10136E-01	2.16

Table II-17

III. Relative Calibration via Absolute Calibrations

A second method attempted by the author to calculate Alf Lyr/Sun flux ratios was to ratio absolute calibrations of Alpha Lyrae and the sun. This was first done by Elias (5) at the MIT Remote Sensing Laboratory in 1972. Elias used the Alpha Lyrae model spectrum of Schild, Peterson, and Oke (25) and the observational solar spectrum of Arvesen, Griffin, and Pearson (3).

Oke and Schild conducted an observing program at the Lickand Palomar observatories in 1969 to determine the absolute spectral-energy distribution of Alpha Lyrae (Vega) over the wavelength region 0.33-1.08μM. Their results agreed well with Hayes (7) in the Paschen continuum between 4000-8000Å. However, the two calibrations disagreed by 7 percent across the Paschen discontinuity. They then derived a theoretical model spectrum for Vega with parameters $T_{eff}=9650^{o}K$ and log g=4.05. This model had maximum differences of the order of 2% in the Balmer and Paschen continua, although the calculations began to diverge appreciably from the observations beyond 1μM. This was the Alpha Lyrae model used by Elias in 1972.

Hayes, Latham, and Hayes carried out an observing program at Mount Hopkins Observatory in 1971-1972 to measure the monochromatic flux from Alpha Lyrae at several wavelengths in the near infrared, primarily 10,400, 8090, and 6800Å. They found some major flaws in the previous calibra-

tions of Oke and Schild, derived corrections for the Lick and Palomar calibrations, and then combined selected portions of these calibrations with their own Mount Hopkins calibration to produce a new absolute spectral-energy distribution for Alpha Lyrae for the region 0.33-1.08μM (9).

One of the problems with the Oke and Schild calibration was the incorrect calculation of extinction coefficients. A stellar-flux calibration is made by comparing stars against a nearby terrestrial standard. Errors in extinction coefficients are multiplied by the mean air mass itself instead of by the difference in mean air mass at which the stars were observed as for relative stellar photometry. Thus, stellar-flux calibrations are much more sensitive to extinction errors.

The three main sources of extinction in the Earth's atmosphere are (1) Rayleigh scattering by molecules, (2) aerosol scattering, and (3) molecular absorption--water and ozone. Each has its own characteristic wavelength dependence, distribution with height, and variation with time. For the Palomar calibration Oke and Schild modified the Palomar standard extinction coefficients for use with wavelengths in the region 3200-6400Å. However, their correction did not take into consideration the fact that both aerosol scattering and ozone absorption have different distributions with altitude and different wavelength dependences than Rayleigh

scattering. Thus, the mean vertical extinction coefficients adopted for the data reductions were systematically too large, especially in the ultraviolet (0.02-0.07 mag(air mass)$^{-1}$). Oke and Schild also calculated the horizontal extinction as a fraction of the vertical extinction for the Lick and Palomar calibrations. This too was not valid. Hayes and Latham corrected the Lick and Palomar calibrations for the extinction errors (8).

In combining the Oke and Schild calibrations with their own Mount Hopkins calibration, Hayes, Latham, and Hayes rejected all of the Palomar platinum blackbody data. Oke and Schild adopted a temperature for their platinum blackbody that was 6°K below the standard freezing point of platinum in order to obtain agreement with their other sources. They also quoted an uncertainty of two to three times worse for this blackbody than for the lamp and copper blackbody results. The data at three extreme wavelengths in the Lick calibration and two in the Palomar calibration were also deleted (9).

Hayes, Latham, and Hayes have listed the various wavelength regions of their adopted calibration in order of decreasing accuracy as follows: (1) Paschen discontinuity--The color of the adopted calibration between 8090 and 10,400Å is 0.157±0.01 mag. (2) Paschen continuum--Most colors in the region 4036 to 8090Å should be more accurate than ±0.02 mag. (3) Balmer discontinuity--The color of the adopted

calibration between 3636 and 4036Å is -1.358±0.03 mag. (4) Balmer and Brackett continua--The colors in the regions 3300-3636Å and 9700-10,800Å may have errors larger than ±0.02 mag. (5) Flux calibration at 5556Å--0±0.02 mag. (8).

Kurucz (12) is presently developing stellar models to better fit the new adopted Alpha Lyrae calibration of Hayes, Latham, and Hayes. His best model uses the parameters T_{eff}=9400°K and log g=3.95. A slightly different earlier model for T_{eff}=9400°K and log g=4.00 can be seen in Figure (III-1). The model fits the observations very well showing only ±2-±3% disagreement with the observation at a few wavelengths.

The Alpha Lyrae model of Kurucz was used for the analysis presented here. Kurucz very kindly provided the author with magnitudes in frequency space, m_ν, for the wavelength region 0.8197μM and far into the infrared. (The ultraviolet and visible regions are not yet available.) It was necessary to convert these values into fluxes in wavelength space, F_λ, to be consistent with the already existing F_λ values for the region 0.27-0.82μM using the model of Schild, Peterson, and Oke (see Appendix B). Thus, a new Alpha Lyrae spectrum was pieced together for the region 0.27-2.00μM.

Many solar calibrations have been made. The most recent ones are those done by Labs and Neckel (15), Arvesen,

Griffin, and Pearson (3), and Thekaekara, Kruger, and Duncan (26). The results of Labs and Neckel were obtained at the Jungfraujoch Scientific Station, Switzerland (altitude 3.6km). Those of Arvesen, Griffin, and Pearson (Ames Research Center) were obtained during eleven research flights on board a NASA CV-900 aircraft at altitudes between 11.6km and 12.5km. Thoseof Thekaekara, Kruger, and Duncan of Goddard Space Flight Center (GSFC) were also made from this aircraft.

The solar spectral irradiance of Arvesen et al. agreed with the Labs and Neckel data very well except in the region 0.20-0.50μM where the Labs and Neckel results averaged about 5% lower than those of Arvesen et al. The GSFC data, on the other hand, showed considerable discrepancies with both the Labs and Neckel data and the Ames data. It was also noted that the deviations between the three individual high-altitude experiments of GSFC were of the same order as the deviations between their final weighted average and that of Ames and of Labs and Neckel.

The main argument for performing solar radiation measurements at high altitudes is that at an altitude of 11.5km the remaining atmospheric pressure above the observation platform is only 20 percent of its value at sea level and the correction for extinction no longer imposes serious problems. Labs and Neckel have disputed this point (14).

The issues are many, and it seems to be at least an open question whether the ground-based or aircraft measurements gave the higher reliability.

Kurucz feels that the Labs and Neckel data are the most accurate (13). He is currently working on solar models to match the observational data. Figure (III-2) shows his model for $T_{eff}=5770^{\circ}K$ and log g=4.44. Molecular lines are not included, thus the G band at 0.43μM is too weak, the calculated intensity is too high at 0.34μM, and the intensity is too low in the red. He eventually plans to add molecular opacity to his models (12). Although this model is not suitable for use as an absolute solar calibration to date, it shouldbe noted that in the future solar models by Kurucz, Peytremann, or others could provide a suitable absolute calibration.

Elias used the Arvesen et al. spectrum because of its higher spectral resolution (1Å over most of the visible spectrum to 50Å beyond 1.0μM). The resolution of Labs and Neckel is about 20Å in the visible and near infrared. He also felt that the Arvesen et al. spectrum was probably more accurate below 0.50μM where the measurements diverge. In light of more recent discussions of the observations, the author notes that it may be the Arvesen, not the Labs and Neckel, measurements which are off an average of 5% below 0.50μM. It might be best, therefore, to use the Labs and

Neckel measurements below 0.50μM and the higher spectral resolution measurements of Arvesen et al. for the rest of the desired wavelength region. Time, however, did not permit the keypunching of the Labs and Neckel solar spectrum, and the Arvesen et al. spectrum was again used.

Thus, the Alpha Lyrae model spectrum of Schild, Peterson, and Oke from 0.27-0.82μM, the Alpha Lyrae model spectrum of Kurucz from 0.82-2.00μM, and the observational solar spectrum of Arvesen, Griffin, and Pearson were used for the relative Alf Lyr/Sun calibration. A computer program (6) was used to calculate the flux ratios for the S-1 detector tube for each of the Spectrum filters from 0.33-1.10μM. This program used as input the solar spectrum, Alpha Lyrae spectrum, atmospheric transmission data, detector response, and filter responses. The atmospheric transmission data were calculated by Elias (5) and applied unmodified. Corrections for Rayleigh scattering, dust, ozone, oxygen, 1cm precipitable water, and carbon dioxide were made. The detector response for the S-1 was also taken from Elias. The filter responses were measured with a Cary 17 transmission spectrometer. The resulting flux ratios are given in Table (III-1) along with the previous values for the Wallace and Spectrum filter sets. Graphs of flux ratio versus wavelength are shown in Figures (III-3-8).

Hayes and Latham rated the Paschen discontinuity (8090-

10,400Å) as the most accurate spectral area. From Figure (III-1) it can be seen that the Kurucz model matches the observed points in this region very well. There is, however, approximately a 3-4% discrepancy between the observation and the model at 0.87μM; the model giving the lower intensity. In the previous model of Schild et al. the Paschen lines were not included which led to an Alf Lyr/Sun flux ratio that was too high. In this case, there is a possibility that the flux ratio is too low. Perhaps a value between the two is the best approximation at the present time. The Labs and Neckel and Arvesen et al. data also agree very well in the 8090-10,400Å wavelength region. Thus, the Alf Lyr/Sun flux ratios for the 0.82-1.10μM region covered by the Spectrum filters should be improved, but by how much is uncertain. The errors in this calibration are due primarily to our imperfect knowledge of the stellar and solar fluxes. These results are compared to those of the other sections in section V.

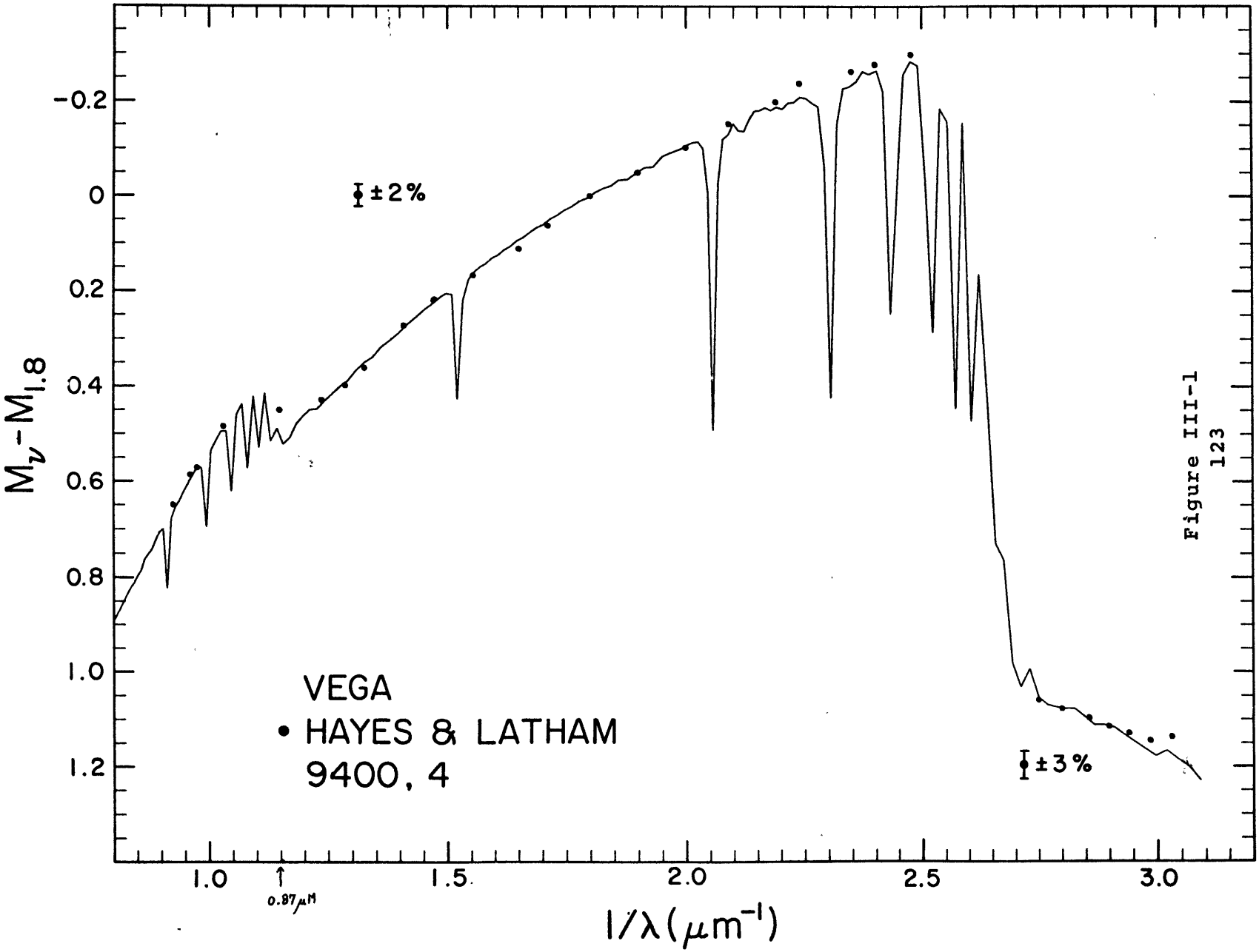

Figure III-1
123

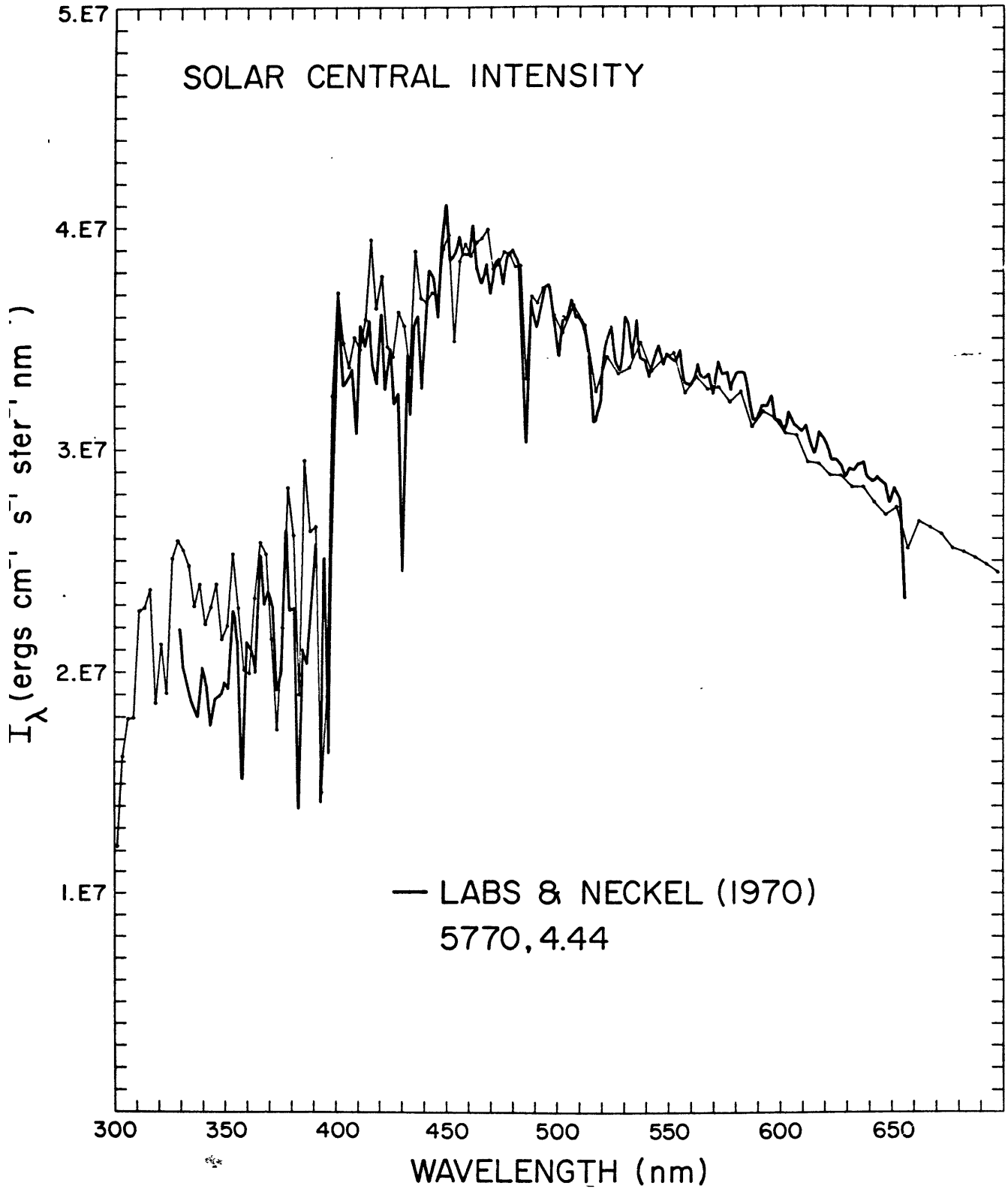
SOLAR CENTRAL INTENSITY
5.E7
4.E7
3.E7
2.E7
1.E7
I_λ (ergs cm^{-1} s^{-1} ster^{-1} nm^{-1})
— LABS & NECKEL (1970)
5770, 4.44
300
350
400
450
500
550
600
650
WAVELENGTH (nm)

Figure III-2

Figure III-3,4

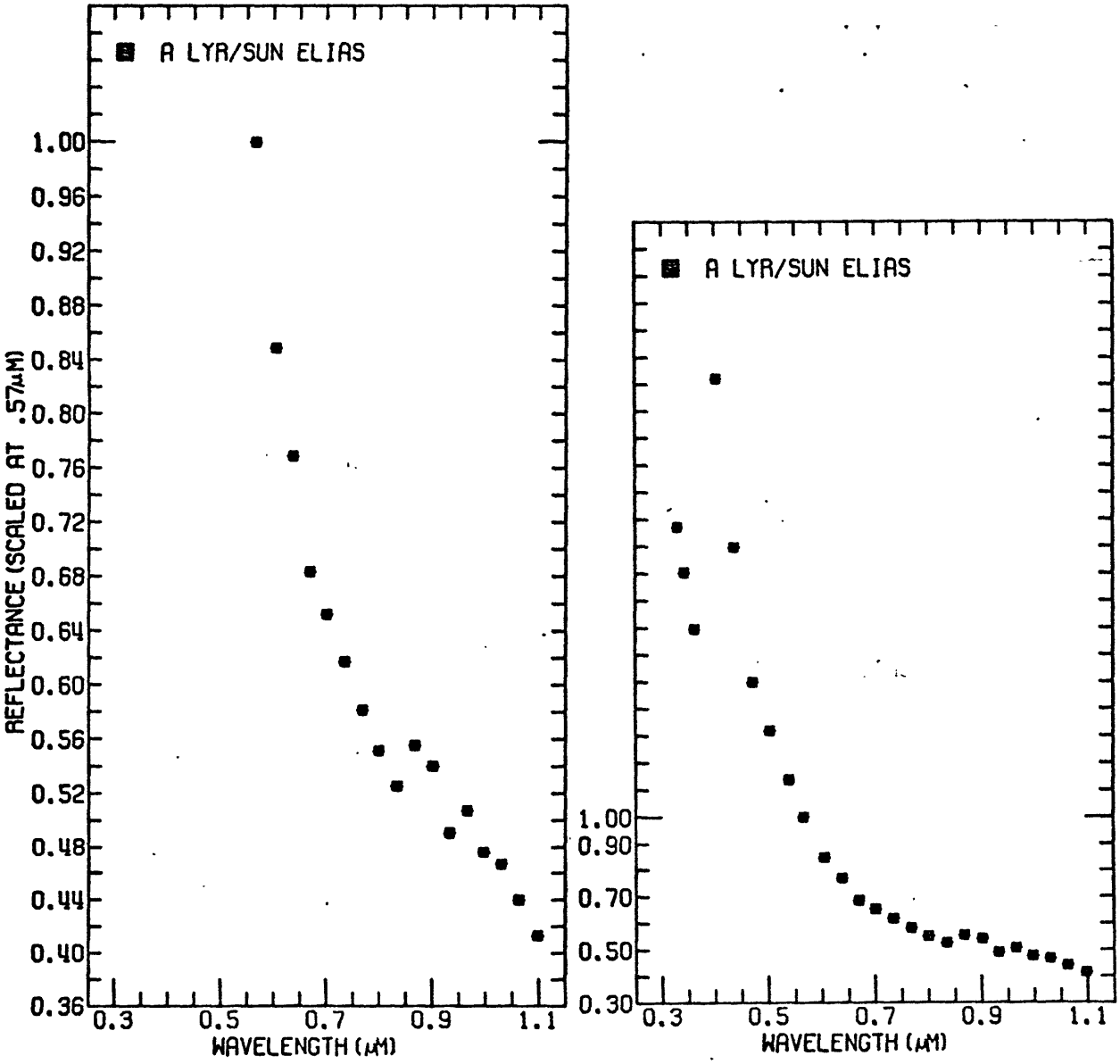

Figure III-5,6

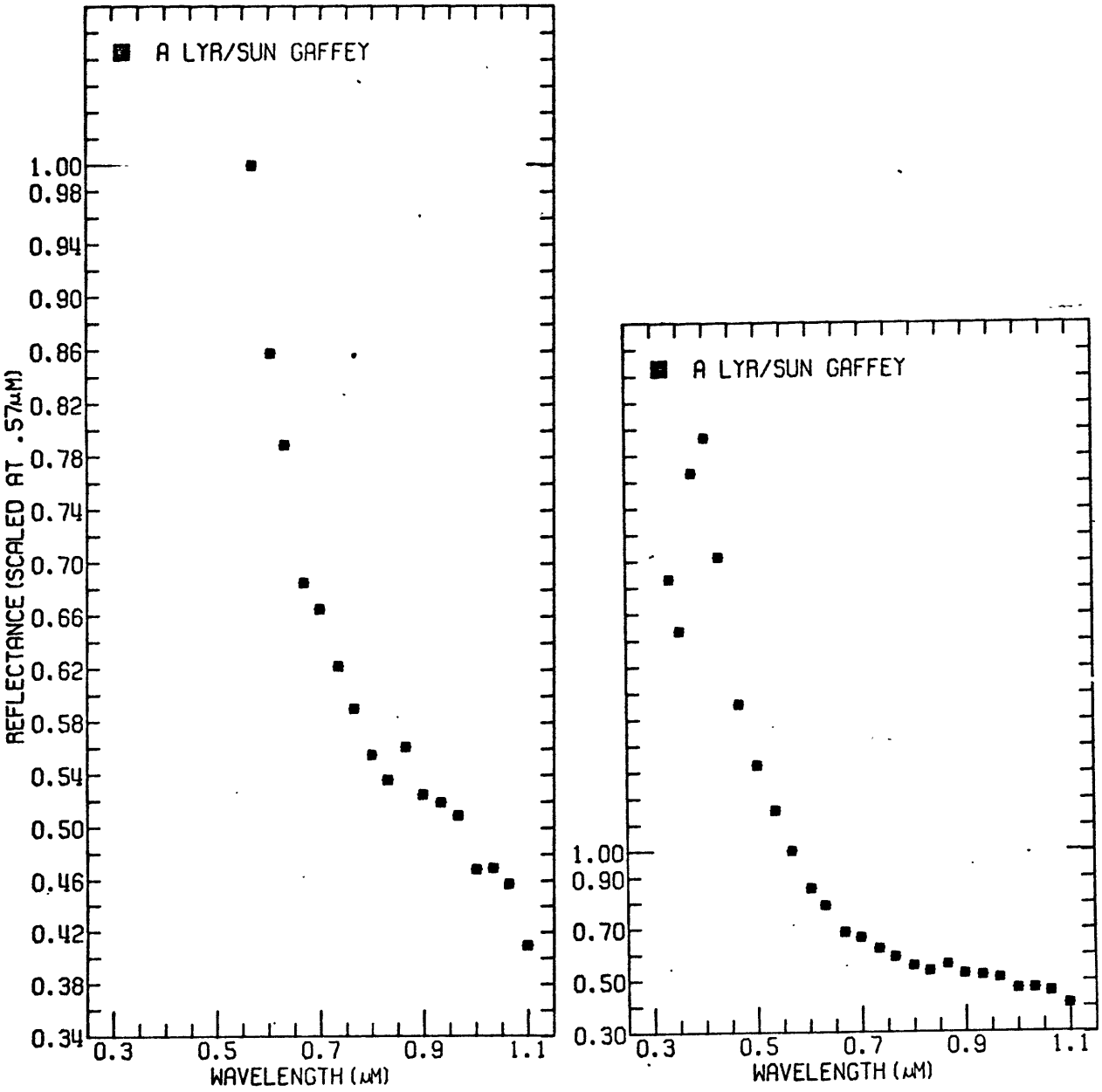

Figure III-7,8

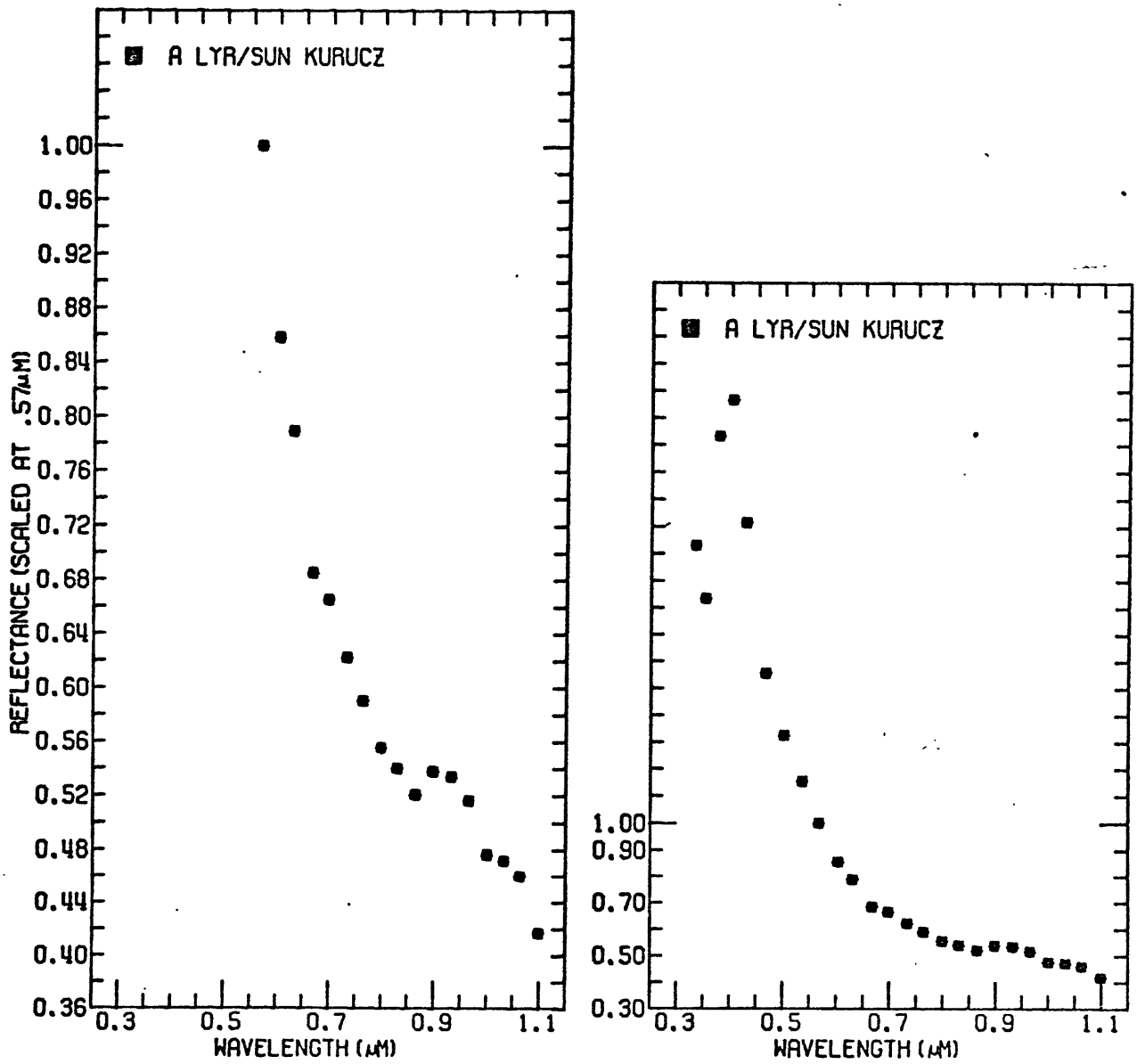

Wavelength	Elias Flux	Wavelength	Gaffey Flux	Kurucz Flux
0.330600	2.072743	0.334700	2.030999	2.0309
0.342800	1.905042	0.353400	1.834999	1.8349
0.362600	1.696817	0.378400	2.433000	2.4330
0.403700	2.623673	0.404100	2.566999	2.5669
0.437000	1.997297	0.429900	2.115000	2.1150
0.471600	1.499498	0.467700	1.558000	1.5580
0.503300	1.317590	0.501900	1.325999	1.3259
0.538300	1.137681	0.536600	1.153999	1.1539
0.565900	1.000000	0.567400	1.000000	1.0000
0.605000	0.848400	0.604100	0.858000	0.8580
0.637600	0.768500	0.631200	0.789000	0.7890
0.669600	0.683000	0.667900	0.685000	0.6850
0.701000	0.651800	0.698600	0.665000	0.6650
0.734800	0.617000	0.733900	0.622000	0.6220
0.768500	0.580900	0.764500	0.590000	0.5900
0.800600	0.551100	0.799900	0.555000	0.5553
0.834800	0.525100	0.831000	0.536000	0.5398
0.867900	0.555200	0.865300	0.561000	0.5204
0.902000	0.539900	0.898700	0.525000	0.5379
0.933600	0.490400	0.932900	0.519000	0.5338
0.966700	0.507300	0.966000	0.509000	0.5162
0.998000	0.475900	1.000796	0.468000	0.4764
1.030499	0.466900	1.033000	0.469000	0.4718
1.063100	0.439600	1.063700	0.457000	0.4599
1.098100	0.412800	1.099098	0.409000	0.4166

Table III-1

IV. Relative Calibration via Solar-type Stars

The third method to determine Alf Lyr/Sun flux ratios was to calculate Alf Lyr/Star ratios for those stars judged to be most similar to the sun and to average the results. The observational data used weregathered during Runs II,III, IV, and V.

There are seven main spectral classes, O,B,A,F,G,K,M, and three minor classes, R,N,S, which are related to the K and M classes. Each of these classes are subdivided into ten subgroups (eg. G0, G1,...G9). The spectral classes form a color sequence from blue-white to yellow to red and a temperature sequence from hottest (50,000°K or hotter) to coolest (3500°K). These classes are not sharply differentiated but rather represent a continuum of varying spectral characteristics. There is also a system to distinguish between different luminosities within the same spectral class. Roman numerals are used to designate luminosity classes as follows:

Ia--bright supergiants
Ib--faint supergiants
II--bright giants
III--normal giants
IV--subgiants
V--normal dwarfs or main-sequence stars

This system of assigning a luminosity class to each spectral type is called the MKK system.

Type G stars are yellow stars with a temperature of approximately 6000°K. Compared to the cooler K stars (4500°K), the lines of ionized calcium and the Balmer lines are stronger

and the λ-4227 line of neutral calcium and other neutral metal lines are becoming weaker. Type F stars are yellow-white stars with a temperature of about 7500°K. Compared to the G stars, the lines of CaII diminish in strength, the Balmer lines increase in strength, and at F0 the numerous lines of neutral metals have nearly disappeared. The sun is set as the reference spectral type at G2V.

The color index of a star is defined as the difference between the magnitudes determined in two of the standard systems, U, B, or V. The color index for the sun has been measured as B-V=+0.62-+0.64 (14).

Thus, in searching for solar-type stars one should look for $\overset{B-V}{\wedge}$ color indexes in the range of approximately +0.56-+0.71 and for spectral types G0-G5 with luminosity classes III, IV, or V. The spectral types listed in various stellar catalogues vary considerably from source to source. Probably the best sources to check for spectral types and color indexes are the Yale Bright Star Catalogue (10) and the Arizona-Tonantzintla Catalogue (11). It is a good idea to look for stars which meet all three of the above criteria.

The stars for which we presently have data and which meet some of the criteria listed above are Xil Ori, 61 Vir, Bet CrV, Omg2 Sco, and 10 Tau. Omi Tau and Alf Aqr were also examined primarily because the most data existed for them (see Table (IV-1)).

Xi[1] Ori (Xil Ori), of spectral class G0V and B-V color index of +0.60, was observed on January 29 and 31. On January 29 both Gam Gem and Omi Tau were used as standards. As previously mentioned (see section II.B.1.), the Omi Tau/Alf Aqr link was considerably better than the Gam Gem/Alf Aqr flux ratio. Hence, Omi Tau was selected as the standard. Omi Tau was also the standard for January 31. Thus, Xil Ori/Omi Tau flux ratios were averaged for the two nights and an Alf Lyr/Xil Ori flux ratio calculated. Typical standard errors of 2% resulted (see Tables (IV-2-5) for information on all star ratios in this section).

Beta Corvi (Bet CrV) of spectral class G5III and B-V=+0.88 was observed on January 31. 7 runs of Bet CrV/Omi Tau were averaged resulting in typical errors of $\pm$0.8%. The resulting Alf Lyr/Bet CrV flux ratio had errors of approximately 2%.

Omega[2] Scorpii (Omg2 Sco) has a spectral class of gG2 and B-V=+0.85. 12 runs of Omg2 Sco/Gam Gem on March 11 were averaged and then used to compute Alf Lyr/Omg2 Sco flux ratios with a maximum error of 7.9% for the 1.06μM filter and average errors of 3%.

61 Virginis (61 Vir) of spectral class G6V and B-V color indexof +0.71 was observed on March 9 and 11. Gam Gem was the standard for both nights. 9 runs from March 10 and 10 runs from March 11 were used to calculate an average

61 Vir/Gam Gem flux ratio with errors of approximately 2%. The resulting Alf Lyr/61 Vir flux ratios showed errors of 3-3.5% on the average (8.9% for the 1.06μM filter) due primarily to the poor Gam Gem/Alf Aqr link.

10 Tau/Alf Aqr, discussed previously (see section II. B.1.), resulted in an Alf Lyr/10 Tau flux ratio with typical errors of 1%. 10 Tau is type F8V and has B-V=+0.57.

Alf Lyr/Alf Aqr, an average of 47 runs, showed errors of ±0.5%. Alf Aqr, being a faint supergiant (G21b), can differ from the sun by more than 10% in the blue and a few percent at the sodium D lines, H and K lines, etc. (24). This ratio was included here primarily because of the large amount of data which existed for it. Similarly, quite a bit of data existed for Omi Tau (G8III; B-V=+0.89). The Alf Lyr/Omi Tau flux ratios had errors of about 1%.

The above (Alf Lyr/Solar-type star) flux ratios were then compared with one another and with Gaffey's model Alf Lyr/Sun flux ratios. The variation in flux ratios from star to star was so great that averaging of the results was meaningless. The Alf Lyr/Bet CrV, Alf Lyr/Omg2 Sco, Alf Lyr/Alf Aqr, and Alf Lyr/Omi Tau flux ratios were a factor of 2-3 times higher in flux ratio in the 0.33-0.56μM region than Gaffey's model Alf Lyr/Sun. Alf Lyr/Xil Ori, Alf Lyr/61 Vir, and Alf Lyr/10 Tau were better but still had variations of 10-50%. Thus, none of these stars can be considered solar-like in the

0.33-0.56μM region. The flux ratios for Bet CrV, Omg2 Sco, Alf Aqr, and Omi Tau were about 6-8% too low in the 0.7-1.10μM region. Xil Ori was 3-5% too high, and 10 Tau was 4-6% too high in this same region. All of the Gaffey data points for the 0.56-1.10μM region fell within the error bars for those points for 61 Vir (G6V; B-V=+0.71). The Alf Lyr/61 Vir flux ratio, however, had ±2% error bars.

Thus, this method with the present data was not very useful except for an understanding of possible trends of Alf Lyr/Sun in the near infrared. Data for a selection of stars of the same class and color index as 61 Vir, Xil Ori, and 10 Tau might help improve matters in the near infrared, but even for these stars the 0.33-0.56μM region was distinctly not solar-like. These results are compared to the other methods in section V.

Table IV-1*

Star	RA(1900)	Dec.(1900)	Visual Magnitude	B-V	Spectral Class
Omi Tau	$3^h19^m26^s$	$+8°41'$	3.59	+0.90	G8111
10 Tau	$3^h31^m46^s$	$+0°5'$	4.29	+0.57	F8V
Xil Ori	$5^h48^m28^s$	$+20°15'$	4.41	+0.60	GOV
Bet CrV	$12^h29^m8^s$	$-22°51'$	2.66	+0.88	G5111
61 Vir	$13^h13^m10^s$	$-17°45'$	4.75	+0.71	G6V
Omg^2 Sco	$16^h1^m32^s$	$-20°36'$	4.31	+0.85	gG2
Alf Aqr	$22^h0^m39^s$	$-0°48'$	2.93	+0.98	G21b

*Information from Yale Bright Star Catalogue (10) and Arizona-Tonantzintla Catalog (11).

Figure IV-1,2

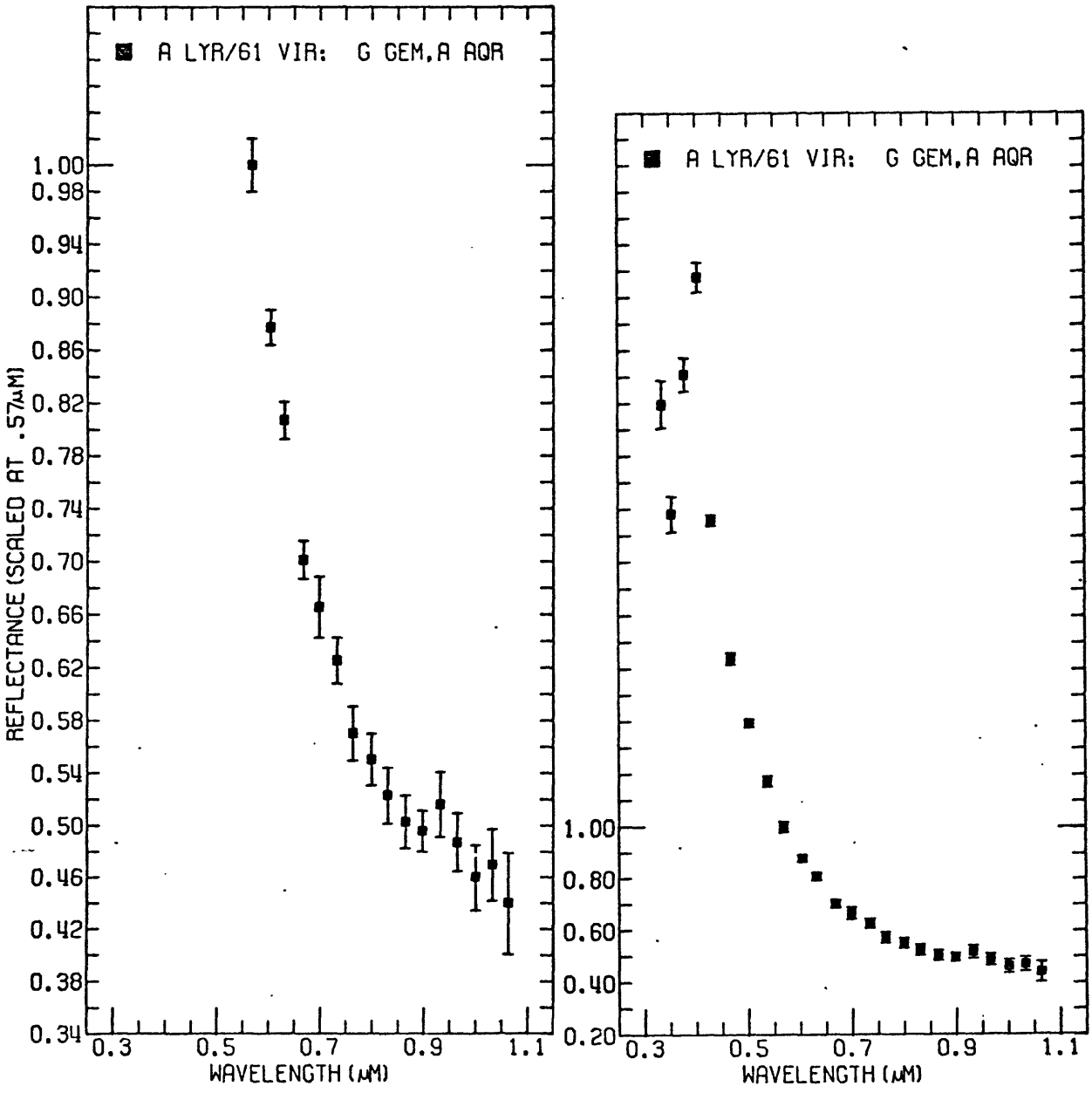
A LYR/61 VIR: G GEM,A AQR
REFLECTANCE (SCALED AT .57μM)
1.00
0.98
0.94
0.90
0.86
0.82
0.78
0.74
0.70
0.66
0.62
0.58
0.54
0.50
0.46
0.42
0.38
0.34
0.3
0.5
0.7
0.9
1.1
WAVELENGTH (μM)
A LYR/61 VIR: G GEM,A AQR
1.00
0.80
0.60
0.40
0.20
0.3
0.5
0.7
0.9
1.1
WAVELENGTH (μM)

Figure IV-3,4

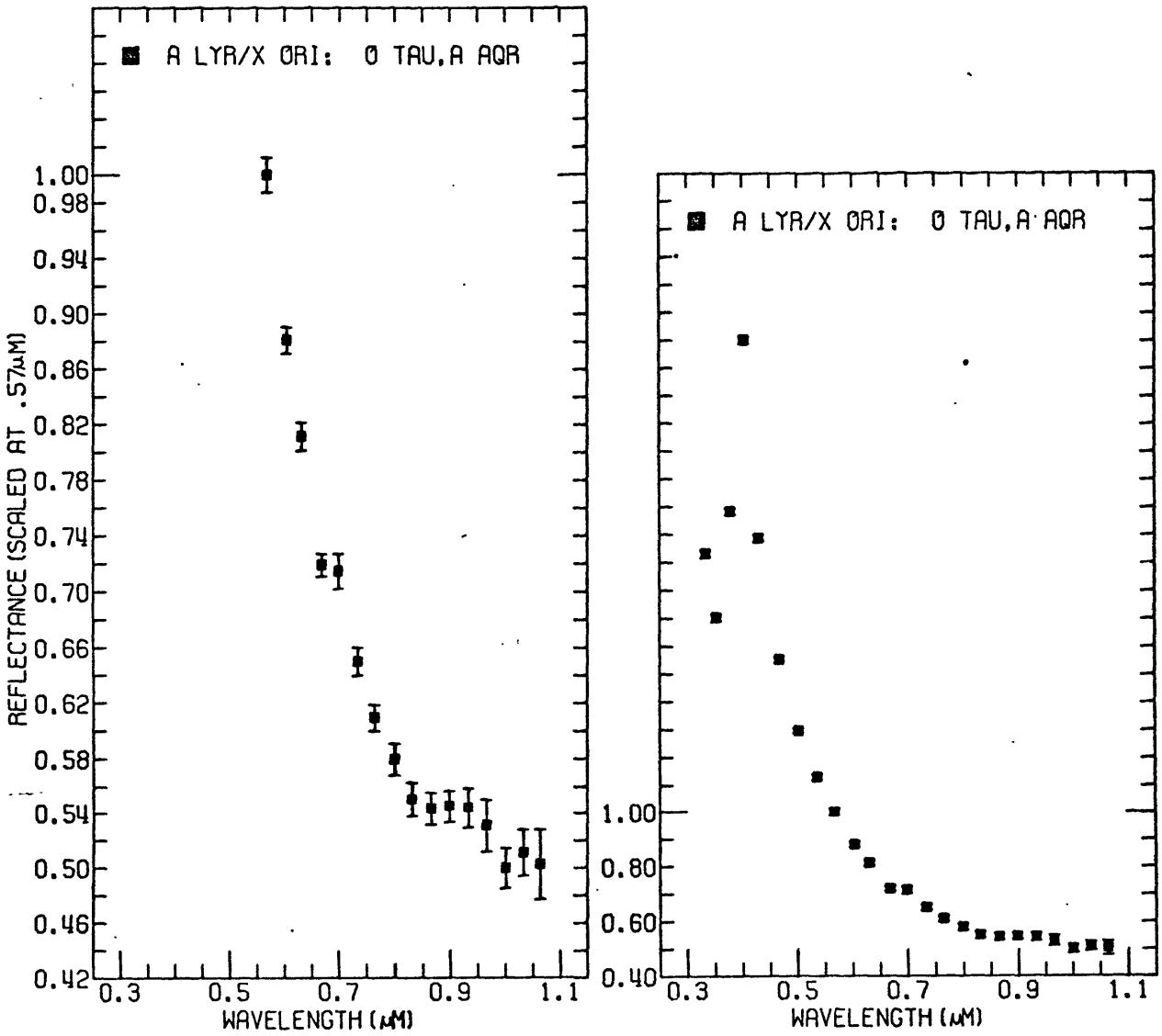
A LYR/X ORI: 0 TAU,A AQR
REFLECTANCE (SCALED AT .57μM)
1.00
0.98
0.94
0.90
0.86
0.82
0.78
0.74
0.70
0.66
0.62
0.58
0.54
0.50
0.46
0.42
0.3
0.5
0.7
0.9
1.1
WAVELENGTH (μM)
A LYR/X ORI: 0 TAU,A AQR
1.00
0.80
0.60
0.40
0.3
0.5
0.7
0.9
1.1
WAVELENGTH (μM)

Figure IV-5,6

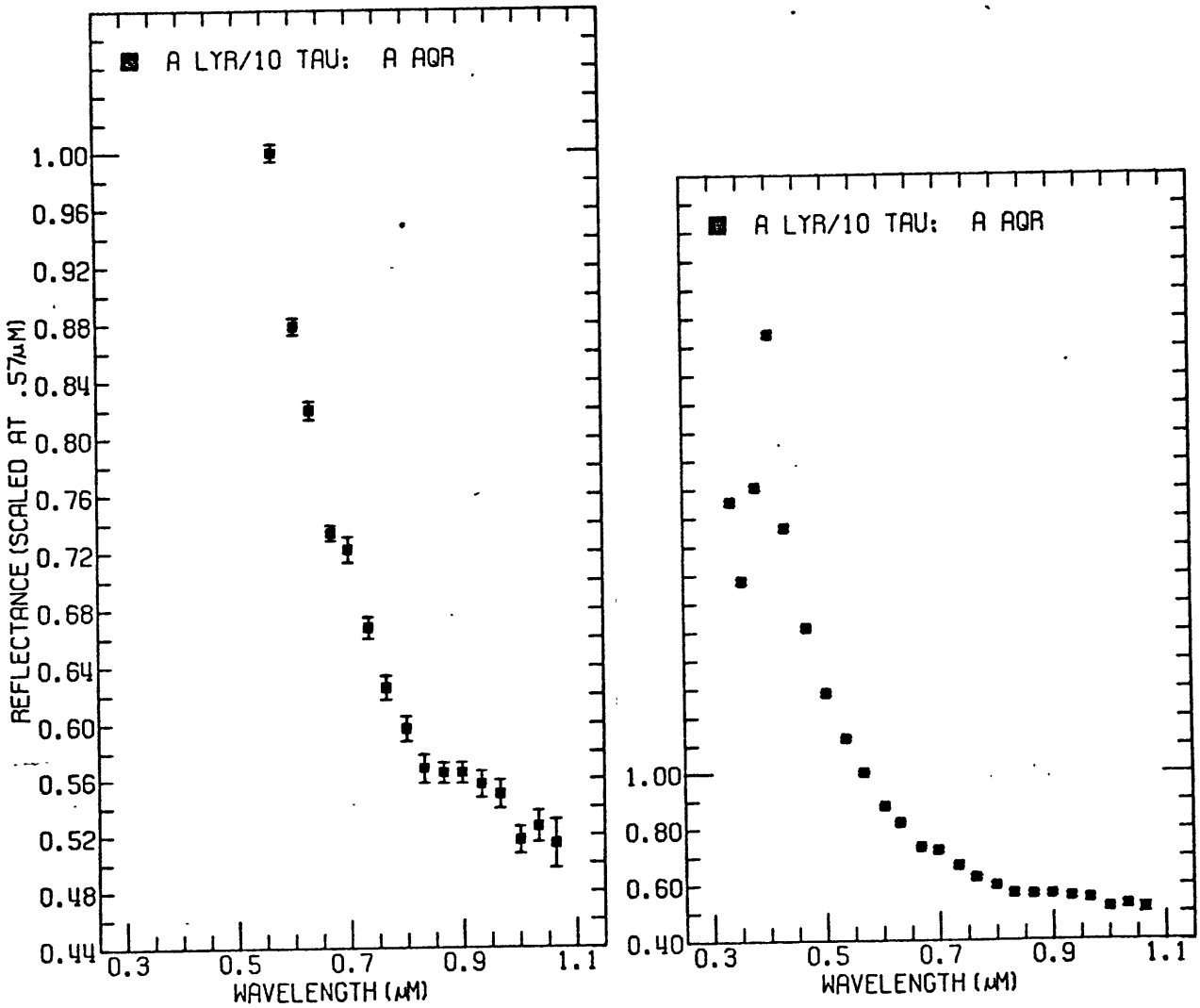
A LYR/10 TAU: A AQR
REFLECTANCE (SCALED AT .57μM)
1.00
0.96
0.92
0.88
0.84
0.80
0.76
0.72
0.68
0.64
0.60
0.56
0.52
0.48
0.44
0.3
0.5
0.7
0.9
1.1
WAVELENGTH (μM)
A LYR/10 TAU: A AQR
1.00
0.80
0.60
0.40
0.3
0.5
0.7
0.9
1.1
WAVELENGTH (μM)

Figure IV-7,8

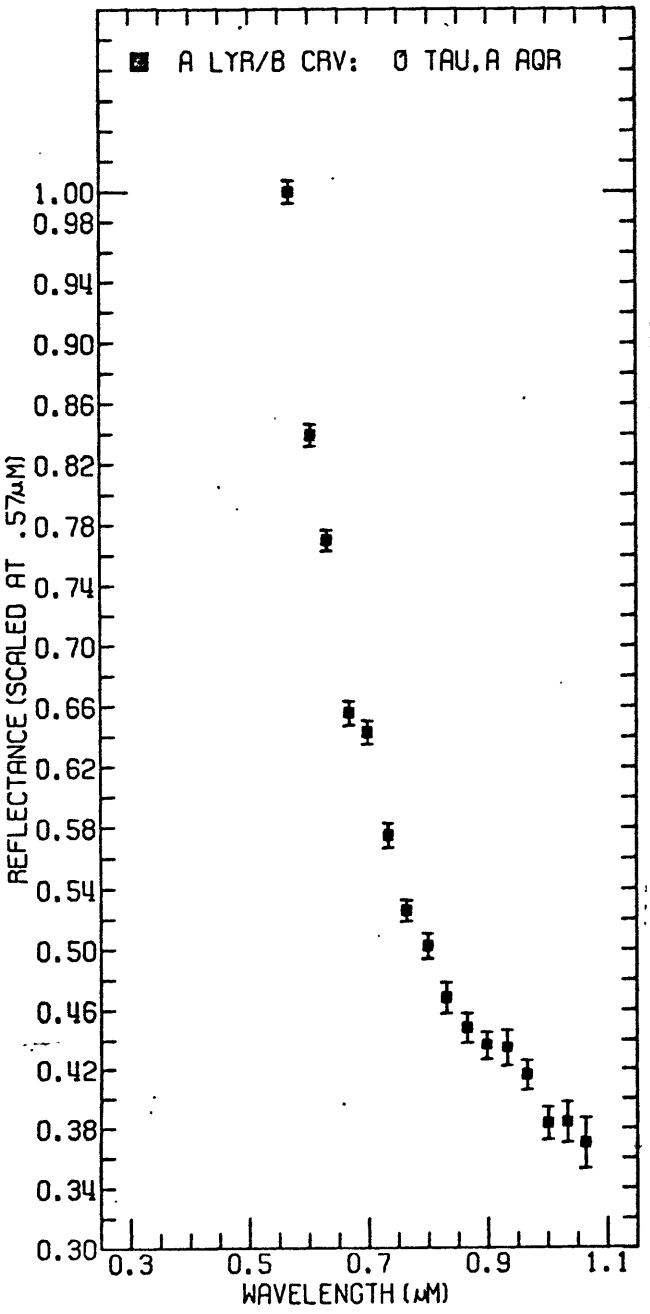

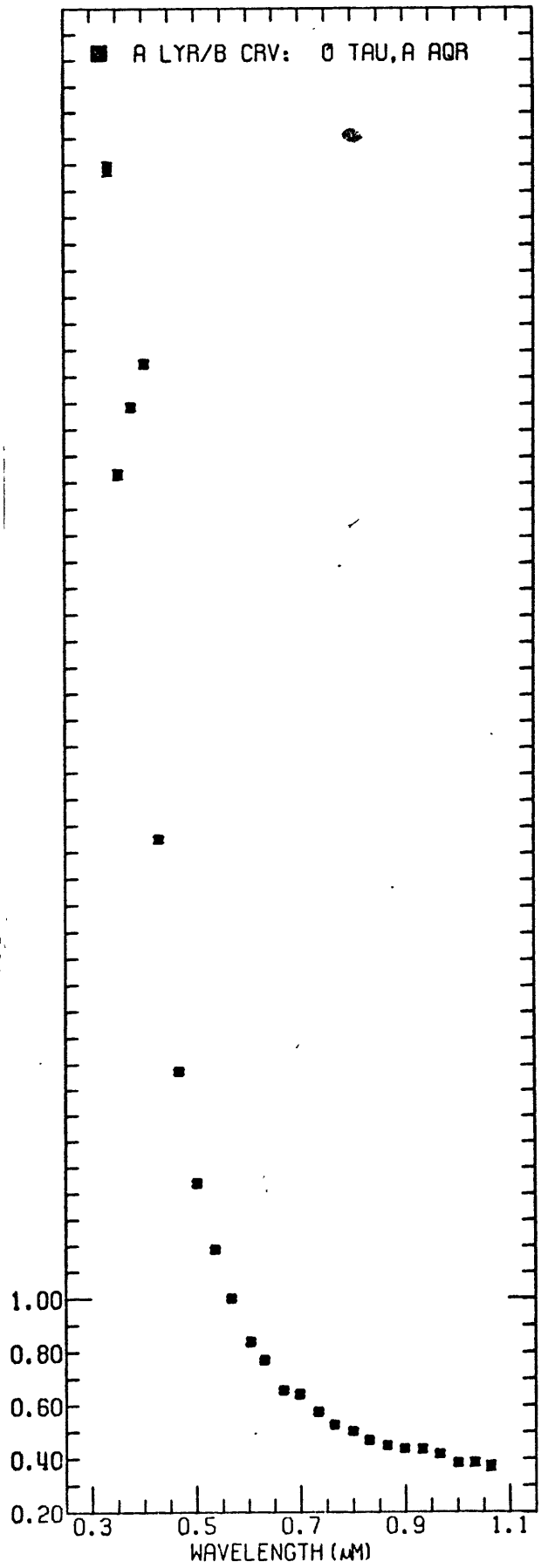

144-145

Figure IV-9,10

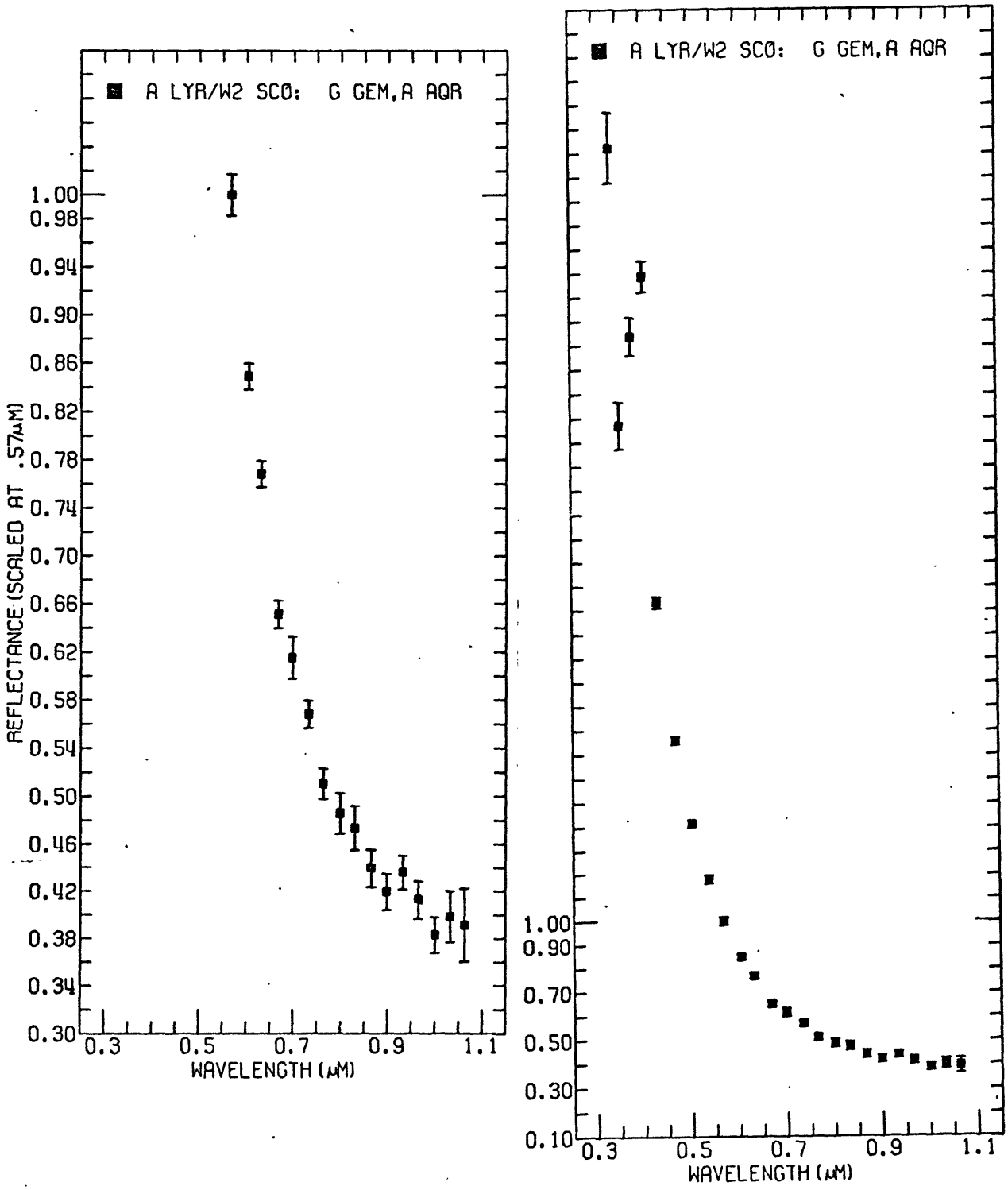

Figure IV-11,12

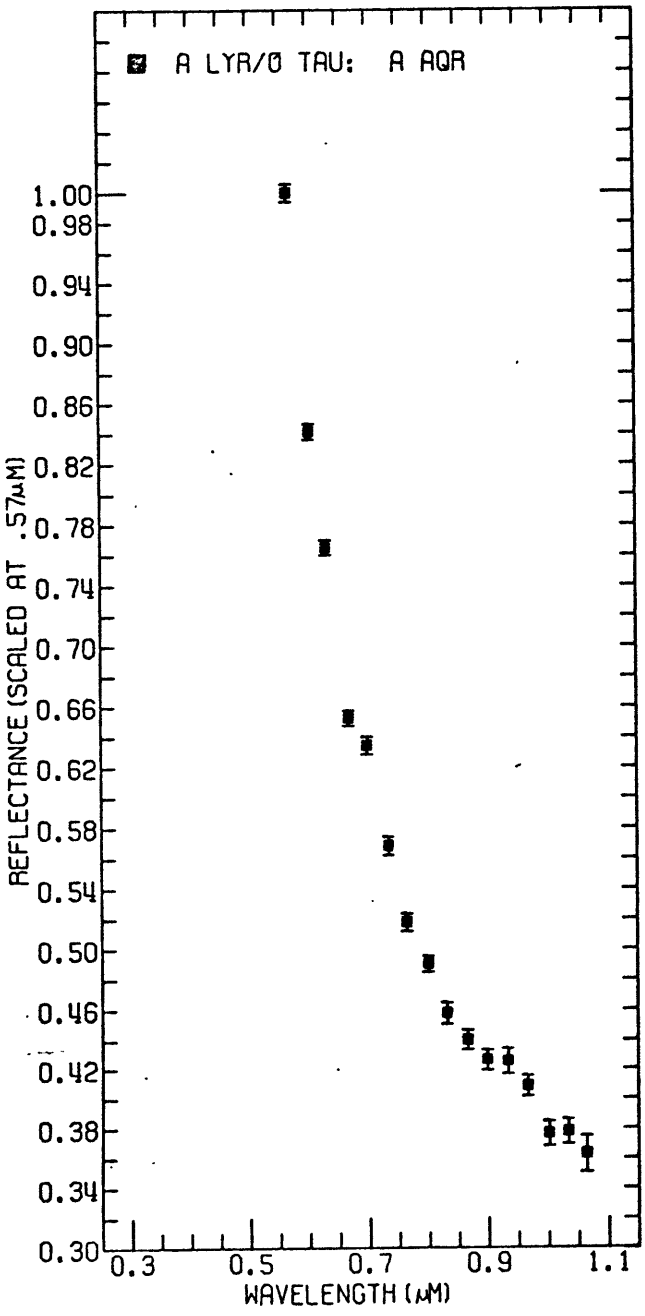

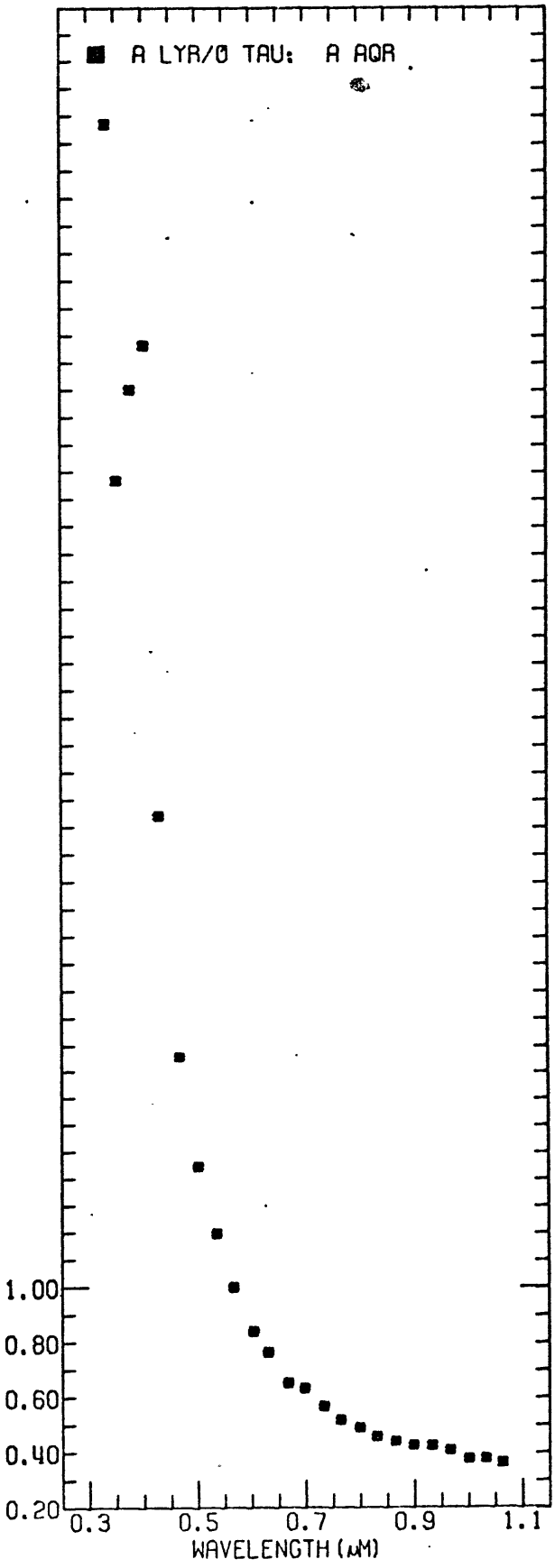

148-149

Figure IV-13

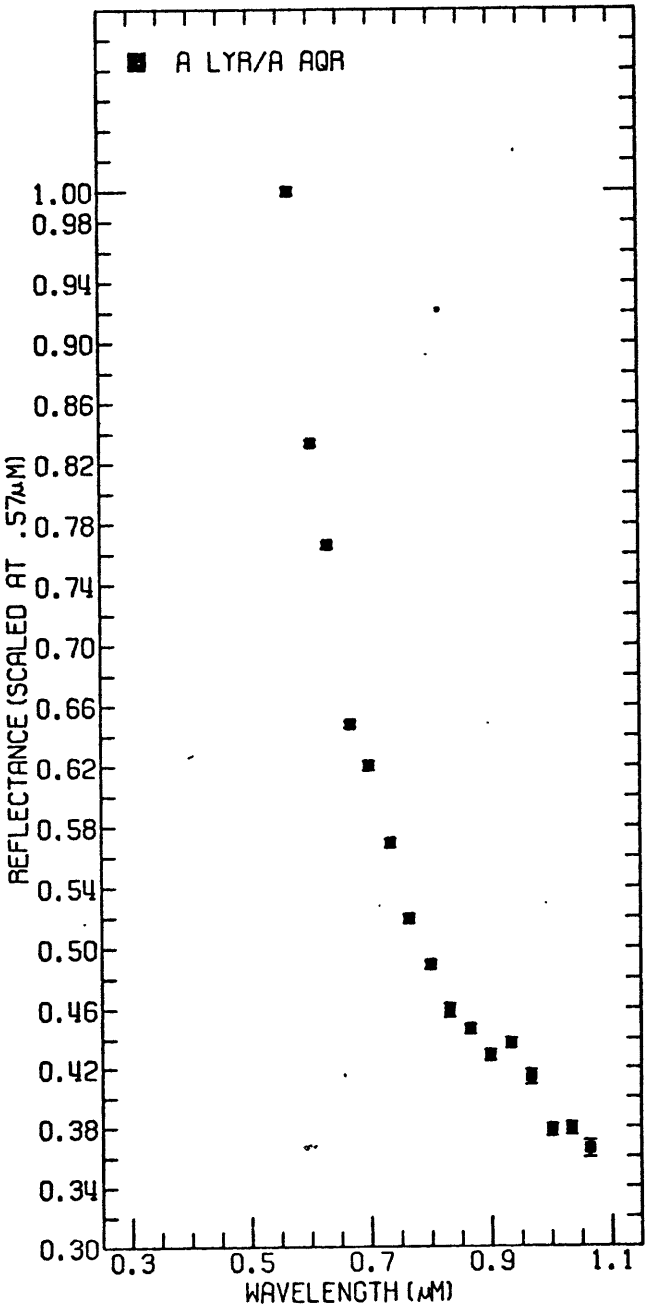
A LYR/A AQR
1.00
0.98
0.94
0.90
0.86
0.82
0.78
0.74
0.70
0.66
0.62
0.58
0.54
0.50
0.46
0.42
0.38
0.34
0.30
REFLECTANCE (SCALED AT .57μM)
0.3
0.5
0.7
0.9
1.1
WAVELENGTH (μM)

A LYR/61 VIR: G GEM,A AQR

WAVELENGTH	AVE.FLUX	STND.ERROR	PERCENT
0.3347	0.25983E 01	0.90518E-01	3.48
0.3534	0.21817E 01	0.68147E-01	3.12
0.3784	0.27121E 01	0.63864E-01	2.35
0.4041	0.30790E 01	0.57101E-01	1.85
0.4299	0.21582E 01	0.20513E-01	0.95
0.4677	0.16393E 01	0.21957E-01	1.34
0.5019	0.13946E 01	0.14483E-01	1.04
0.5366	0.11741E 01	0.19745E-01	1.68
0.5674	0.10000E 01	0.20269E-01	2.03
0.6041	0.87719E 00	0.13250E-01	1.51
0.6312	0.80691E 00	0.14178E-01	1.76
0.6679	0.70128E 00	0.14317E-01	2.04
0.6986	0.66556E 00	0.23010E-01	3.46
0.7339	0.62529E 00	0.17379E-01	2.78
0.7645	0.57018E 00	0.20641E-01	3.62
0.7999	0.55028E 00	0.19720E-01	3.58
0.8310	0.52293E 00	0.21361E-01	4.08
0.8653	0.50289E 00	0.20189E-01	4.01
0.8987	0.49582E 00	0.15657E-01	3.16
0.9329	0.51612E 00	0.24651E-01	4.78
0.9660	0.48690E 00	0.22507E-01	4.62
1.0008	0.45997E 00	0.25640E-01	5.57
1.0330	0.46955E 00	0.27657E-01	5.89
1.0637	0.43990E 00	0.39062E-01	8.88

A LYR/XI1 ORI: OMI TAU:A AQR

WAVELENGTH	AVE.FLUX	STND.ERROR	PERCENT
0.3347	0.19325E 01	0.13364E-01	0.69
0.3534	0.17025E 01	0.12475E-01	0.73
0.3784	0.20836E 01	0.11776E-01	0.57
0.4041	0.27032E 01	0.12585E-01	0.47
0.4299	0.19863E 01	0.11994E-01	0.60
0.4677	0.15534E 01	0.88820E-02	0.57
0.5019	0.12960E 01	0.84760E-02	0.65
0.5366	0.11302E 01	0.99730E-02	0.88
0.5674	0.10000E 01	0.12314E-01	1.23
0.6041	0.88114E 00	0.95140E-02	1.08
0.6312	0.81158E 00	0.10108E-01	1.25
0.6679	0.71922E 00	0.80040E-02	1.11
0.6986	0.71470E 00	0.12576E-01	1.76
0.7339	0.65005E 00	0.10177E-01	1.57
0.7645	0.60955E 00	0.92810E-02	1.52
0.7999	0.57968E 00	0.11352E-01	1.96
0.8310	0.55053E 00	0.12550E-01	2.28
0.8653	0.54369E 00	0.12052E-01	2.22
0.8987	0.54532E 00	0.11939E-01	2.19
0.9329	0.54429E 00	0.14841E-01	2.73
0.9660	0.53090E 00	0.19290E-01	3.63
1.0008	0.49961E 00	0.14683E-01	2.94
1.0330	0.51108E 00	0.16951E-01	3.32
1.0637	0.50244E 00	0.25392E-01	5.05

Table IV-2

A LYR/10 TAU: A AQR

WAVELENGTH	AVE.FLUX	STND.ERROR	PERCENT
0.3347	0.19568E 01	0.95790E-02	0.49
0.3534	0.16796E 01	0.99560E-02	0.59
0.3784	0.20081E 01	0.87830E-02	0.44
0.4041	0.25449E 01	0.90460E-02	0.36
0.4299	0.18647E 01	0.97940E-02	0.53
0.4677	0.15138E 01	0.73450E-02	0.49
0.5019	0.12835E 01	0.73530E-02	0.57
0.5366	0.11241E 01	0.66670E-02	0.59
0.5674	0.10000E 01	0.62360E-02	0.62
0.6041	0.87855E 00	0.58360E-02	0.66
0.6312	0.81978E 00	0.63840E-02	0.78
0.6679	0.73342E 00	0.52960E-02	0.72
0.6986	0.72189E 00	0.89800E-02	1.24
0.7339	0.66722E 00	0.76450E-02	1.15
0.7645	0.62528E 00	0.85010E-02	1.36
0.7999	0.59647E 00	0.87810E-02	1.47
0.8310	0.56794E 00	0.10512E-01	1.85
0.8653	0.56483E 00	0.75720E-02	1.34
0.8987	0.56487E 00	0.76600E-02	1.36
0.9329	0.55640E 00	0.94600E-02	1.70
0.9660	0.54922E 00	0.10108E-01	1.84
1.0008	0.51662E 00	0.96220E-02	1.86
1.0330	0.52617E 00	0.11190E-01	2.13
1.0637	0.51402E 00	0.17244E-01	3.35

A LYR/B CRV: 0 TAU,A AQR

WAVELENGTH	AVE.FLUX	STND.ERROR	PERCENT
0.3347	0.52859E 01	0.25173E-01	0.48
0.3534	0.41317E 01	0.17976E-01	0.44
0.3784	0.43883E 01	0.13955E-01	0.32
0.4041	0.45518E 01	0.13397E-01	0.29
0.4299	0.27501E 01	0.10740E-01	0.39
0.4677	0.18727E 01	0.86630E-02	0.46
0.5019	0.14401E 01	0.84310E-02	0.59
0.5366	0.11863E 01	0.88850E-02	0.75
0.5674	0.10000E 01	0.73370E-02	0.73
0.6041	0.83928E 00	0.72890E-02	0.87
0.6312	0.76983E 00	0.67850E-02	0.88
0.6679	0.65550E 00	0.79020E-02	1.21
0.6986	0.64300E 00	0.76460E-02	1.19
0.7339	0.57475E 00	0.80400E-02	1.40
0.7645	0.52560E 00	0.69550E-02	1.32
0.7999	0.50226E 00	0.83650E-02	1.67
0.8310	0.46806E 00	0.10167E-01	2.17
0.8653	0.44814E 00	0.96720E-02	2.16
0.8987	0.43636E 00	0.93090E-02	2.13
0.9329	0.43461E 00	0.12330E-01	2.84
0.9660	0.41595E 00	0.99570E-02	2.39
1.0008	0.38317E 00	0.11042E-01	2.88
1.0330	0.38410E 00	0.13736E-01	3.58
1.0637	0.37001E 00	0.16937E-01	4.58

Table IV-3

A LYR/OMG2 SCO:G GEM;A AQR

WAVELENGTH	AVE.FLUX	STND.ERROR	PERCENT
0.3347	0.42262E 01	0.14601E 00	3.45
0.3534	0.30720E 01	0.98209E-01	3.20
0.3784	0.34404E 01	0.79562E-01	2.31
0.4041	0.36911E 01	0.64803E-01	1.76
0.4299	0.23337E 01	0.24465E-01	1.05
0.4677	0.17605E 01	0.15937E-01	0.91
0.5019	0.14150E 01	0.14158E-01	1.00
0.5366	0.11785E 01	0.17089E-01	1.45
0.5674	0.10000E 01	0.17416E-01	1.74
0.6041	0.84894E 00	0.10612E-01	1.25
0.6312	0.76815E 00	0.10764E-01	1.40
0.6679	0.65139E 00	0.11237E-01	1.73
0.6986	0.61523E 00	0.17486E-01	2.84
0.7339	0.56814E 00	0.11397E-01	2.01
0.7645	0.51066E 00	0.12619E-01	2.47
0.7999	0.48588E 00	0.16799E-01	3.46
0.8310	0.47363E 00	0.18327E-01	3.87
0.8653	0.43950E 00	0.16012E-01	3.64
0.8987	0.41941E 00	0.15162E-01	3.62
0.9329	0.43615E 00	0.14608E-01	3.35
0.9660	0.41255E 00	0.15678E-01	3.80
1.0008	0.38303E 00	0.15150E-01	3.96
1.0330	0.39863E 00	0.21507E-01	5.40
1.0637	0.39122E 00	0.30887E-01	7.90

A LYR/OMI TAU: A AQR

WAVELENGTH	AVE.FLUX	STND.ERROR	PERCENT
0.3347	0.52721E 01	0.13315E-01	0.25
0.3534	0.39694E 01	0.12560E-01	0.32
0.3784	0.43026E 01	0.97650E-02	0.23
0.4041	0.44664E 01	0.10055E-01	0.23
0.4299	0.27408E 01	0.84970E-02	0.31
0.4677	0.18567E 01	0.65470E-02	0.35
0.5019	0.14448E 01	0.55150E-02	0.38
0.5366	0.11970E 01	0.62180E-02	0.52
0.5674	0.10000E 01	0.57250E-02	0.57
0.6041	0.84143E 00	0.52600E-02	0.63
0.6312	0.76502E 00	0.49160E-02	0.64
0.6679	0.65260E 00	0.49620E-02	0.76
0.6986	0.63436E 00	0.58220E-02	0.92
0.7339	0.56820E 00	0.60280E-02	1.06
0.7645	0.51779E 00	0.58570E-02	1.13
0.7999	0.49021E 00	0.52500E-02	1.07
0.8310	0.45757E 00	0.69610E-02	1.52
0.8653	0.44009E 00	0.63920E-02	1.45
0.8987	0.42617E 00	0.69360E-02	1.63
0.9329	0.42534E 00	0.88360E-02	2.08
0.9660	0.40824E 00	0.69290E-02	1.70
1.0008	0.37620E 00	0.81270E-02	2.16
1.0330	0.37762E 00	0.81660E-02	2.16
1.0637	0.36274E 00	0.12073E-01	3.33

Table IV-4

A LYR/A AQR

WAVELENGTH	AVE.FLUX	STND.ERROR	PERCENT
0.3347	0.68346E 01	0.95000E-02	0.14
0.3534	0.49449E 01	0.64430E-02	0.13
0.3784	0.50107E 01	0.48700E-02	0.10
0.4041	0.51988E 01	0.46110E-02	0.09
0.4299	0.29857E 01	0.44820E-02	0.15
0.4677	0.19369E 01	0.37810E-02	0.20
0.5019	0.14972E 01	0.27250E-02	0.18
0.5366	0.12240E 01	0.25790E-02	0.21
0.5674	0.10000E 01	0.28090E-02	0.28
0.6041	0.83360E 00	0.21810E-02	0.26
0.6312	0.76591E 00	0.21510E-02	0.28
0.6679	0.64767E 00	0.21120E-02	0.33
0.6986	0.62022E 00	0.29800E-02	0.48
0.7339	0.56894E 00	0.27340E-02	0.48
0.7645	0.51907E 00	0.28640E-02	0.55
0.7999	0.48885E 00	0.25560E-02	0.52
0.8310	0.45892E 00	0.43890E-02	0.96
0.8653	0.44671E 00	0.27150E-02	0.61
0.8987	0.42874E 00	0.39030E-02	0.91
0.9329	0.43717E 00	0.36460E-02	0.83
0.9660	0.41376E 00	0.48830E-02	1.18
1.0008	0.37815E 00	0.40780E-02	1.08
1.0330	0.37910E 00	0.41520E-02	1.10
1.0637	0.36536E 00	0.55510E-02	1.52

Table IV-5

V. Conclusions and Recommendations

Of the three methods used in this thesis, the Alf Lyr/Sun calibration done by using the known reflectivity of the lunar sample was the most reliable. The difference in the flux ratios, due to slope differences, for the 20° and 40° reference phase angles was a maximum of 4% in the ultraviolet (0.37μM) and was about 2% throughout the 0.56-1.10μM region. The relative accuracy of the flux ratios filter to filter was much better than 1%. The Gaffey model Alf Lyr/Sun flux values fell between these two limits, indicating that the model flux ratio for the 0.40μM filter was too low by 7-11%, the 0.87μM filter was too high by 6.7-9.6% and that systematic errors of 1-3% existed throughout the 0.37-1.06μM region (see Figure (V-1)). The Alf Lyr/Sun flux values using the Kurucz Alpha Lyrae model also fell between the two limits of the lunar calibration. The results using the lunar sample indicated that the 0.90μM and 0.93μM filters were 2-4% too high in the Kurucz calibration. The 0.87μM filter, which was suspected to be too low since the Alpha Lyrae flux value for the Kurucz model was 3-4% lower than the telescopic flux measurement at that wavelength, did not appear anomalous when compared to the lunar-derived Alf Lyr/Sun flux ratios. The flux ratios calculated from telescopic measurements of Alf Lyr and solar-type stars were not of sufficient quality or quantity to be used in deriving a final Alf Lyr/Sun calibration.

Correction factors are given in Table (V-1) to correct data reduced using the old Gaffey model Alf Lyr/Sun flux ratios to new values using the lunar-derived Alf Lyr/Sun flux ratios. A set of correction factors are given for each of the five reference phase angles used. Not enough data existed to carry out this lunar calibration for the Wallace filters. Hence, the new Alf Lyr/Sun flux ratios derived for the Spectrum filters were assumed to also be correct for the Wallace filters. Thus, the new Alf Lyr/Sun flux ratios for the Spectrum filters were divided by the old model Alf Lyr/Sun flux ratios for the Wallace filters to obtain correction factors for data reduced using Wallace filters. A set of correction factors for each of the five reference phase angles for the Wallace filters are given in Table V-2. A more thorough investigation of the differences between the Wallace and Spectrum filter sets is presently in progress.

In conclusion, the best method to calculate the Alf Lyr/Sun flux ratios for the Spectrum filter sets was to use the known reflectivity of a lunar sample. It is suggested that this method be used for future calibration work with other instruments. Further work needs to be done to determine more precisely which phase angle should be used as the reference phase in this analysis.

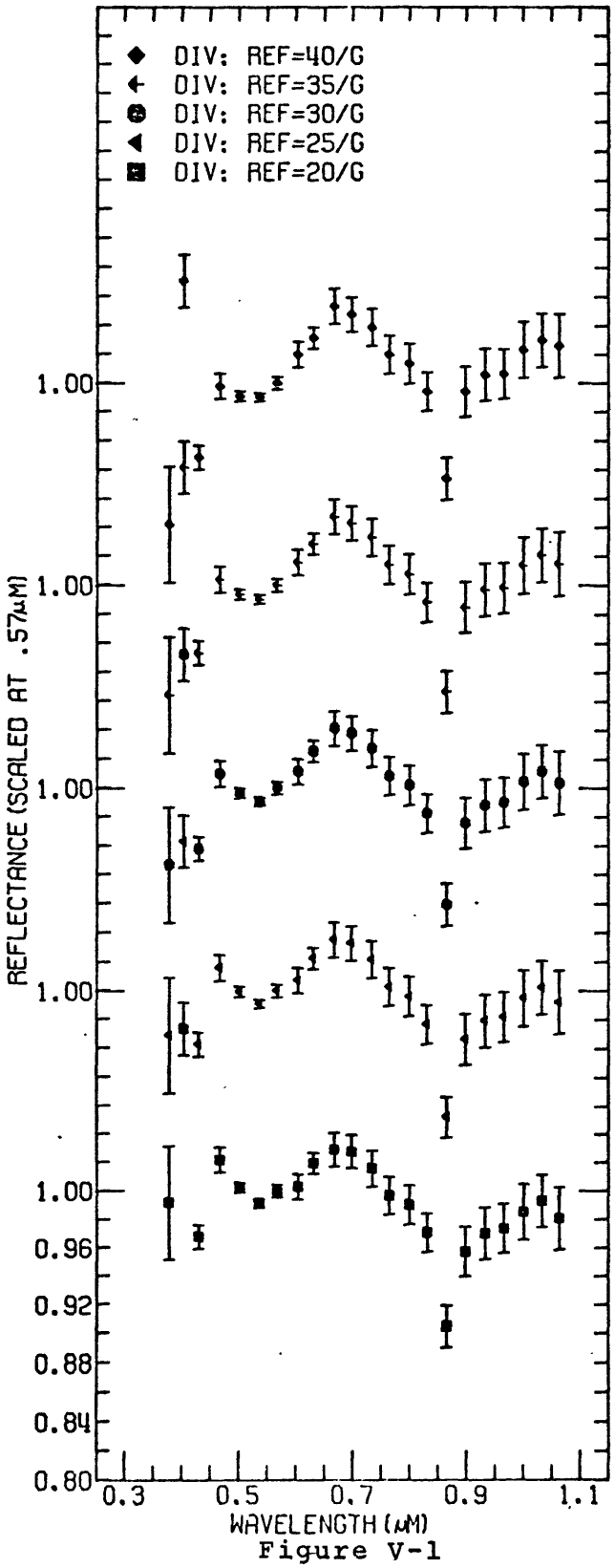
DIV: REF=40/G
DIV: REF=35/G
DIV: REF=30/G
DIV: REF=25/G
DIV: REF=20/G
REFLECTANCE (SCALED AT .57μM)
1.00
1.00
1.00
1.00
1.00
0.96
0.92
0.88
0.84
0.80
0.3
0.5
0.7
0.9
1.1
WAVELENGTH (μM)

Figure V-1

DIV: REF=20/G

WAVELENGTH	RATIO
0.3784	0.99174E 00
0.4041	C.11139E 01
0.4299	0.96770E 00
0.4677	0.10219E 01
0.5019	C.10021E 01
0.5366	0.99112E 00
0.5674	0.10000E 01
0.6041	0.10030E 01
0.6312	0.10195E 01
0.6679	0.10292E 01
0.6986	0.10277E 01
0.7339	C.10158E 01
0.7645	0.99668E 00
0.7999	0.99005E 00
0.8310	0.97059E 00
0.8653	0.90464E 00
0.8987	0.95727E 00
0.9329	0.97023E 00
0.9660	C.97366E 00
1.0008	0.98522E 00
1.0330	0.99293E 00
1.0637	0.98054E 00

DIV: REF=25/G

WAVELENGTH	RATIO
0.3784	0.96929E 00
0.4041	C.11031E 01
0.4299	0.96288E 00
0.4677	0.10159E 01
0.5019	0.99919E 00
0.5366	0.99088E 00
0.5674	0.10000E 01
0.6041	0.10073E 01
0.6312	C.10225E 01
0.6679	0.10353E 01
0.6986	0.10327E 01
0.7339	C.10216E 01
0.7645	0.10025E 01
0.7999	0.99589E 00
0.8310	0.97646E 00
0.8653	C.91189E 00
0.8987	0.96643E 00
0.9329	0.97914E 00
0.9660	0.98184E 00
1.0008	C.99470E 00
1.0330	0.10022E 01
1.0637	0.99189E 00

DIV: REF=30/G

WAVELENGTH	RATIO
0.3784	0.94683E 00
0.4041	0.10923E 01
0.4299	C.95806E 00
0.4677	0.10099E 01
0.5019	0.99633E 00
0.5366	0.99064E 00
0.5674	C.10000E 01
0.6041	0.10115E 01
0.6312	0.10256E 01
0.6679	0.10414E 01
0.6986	C.10378E 01
0.7339	0.10274E 01
0.7645	0.10083E 01
0.7999	0.10017E 01
0.8310	0.98233E 00
0.8653	0.91915E 00
0.8987	0.97560E 00
0.9329	C.98806E 00
0.9660	0.99002E 00
1.0008	0.10042E 01
1.0330	C.10115E 01
1.0637	0.10032E 01

DIV: REF=35/G

WAVELENGTH	RATIO
0.3784	0.92438E 00
0.4041	0.10815E 01
0.4299	0.95325E 00
0.4677	C.10039E 01
0.5019	0.99347E 00
0.5366	0.99040E 00
0.5674	C.10000E 01
0.6041	0.10157E 01
0.6312	C.10286E 01
0.6679	0.10474E 01
0.6986	0.10428E 01
0.7339	C.10332E 01
0.7645	0.10141E 01
0.7999	0.10076E 01
0.8310	0.98820E 00
0.8653	0.92640E 00
0.8987	0.98476E 00
0.9329	C.99697E 00
0.9660	0.99821E 00
1.0008	0.10137E 01
1.0330	C.10208E 01
1.0637	0.10146E 01

Table V-1

DIV: REF=40/G

WAVELENGTH	RATIO
0.3784	0.90193E 00
0.4041	0.10706E 01
0.4299	0.94843E 00
0.4677	0.99789E 00
0.5019	0.99061E 00
0.5366	0.99017E 00
0.5674	0.10000E 01
0.6041	0.10199E 01
0.6312	0.10317E 01
0.6679	0.10535E 01
0.6986	0.10478E 01
0.7339	0.10390E 01
0.7645	0.10199E 01
0.7999	0.10134E 01
0.8310	0.99406E 00
0.8653	0.93366E 00
0.8987	0.99392E 00
0.9329	0.10059E 01
0.9660	0.10064E 01
1.0008	0.10232E 01
1.0330	0.10300E 01
1.0637	0.10259E 01

Table V-1 (cont.)

DIV: REF=20/E

WAVELENGTH	RATIO
0.3784	0.14220E 01
0.4041	0.10899E 01
0.4299	0.10247E 01
0.4677	0.10618E 01
0.5019	0.10085E 01
0.5366	0.10053E 01
0.5674	0.10000E 01
0.6041	0.10144E 01
0.6312	0.10467E 01
0.6679	0.10322E 01
0.6986	0.10485E 01
0.7339	0.10240E 01
0.7645	0.10123E 01
0.7999	0.99706E 00
0.8310	0.99074E 00
0.8653	0.91409E 00
0.8987	0.93085E 00
0.9329	0.10268E 01
0.9660	0.97692E 00
1.0008	0.96886E 00
1.0330	0.99739E 00
1.0637	0.10194E 01

DIV: REF=25/E

WAVELENGTH	RATIO
0.3784	0.13898E 01
0.4041	0.10793E 01
0.4299	0.10196E 01
0.4677	0.10555E 01
0.5019	0.10056E 01
0.5366	0.10051E 01
0.5674	0.10000E 01
0.6041	0.10186E 01
0.6312	0.10498E 01
0.6679	0.10383E 01
0.6986	0.10537E 01
0.7339	0.10299E 01
0.7645	0.10182E 01
0.7999	0.10029E 01
0.8310	0.99673E 00
0.8653	0.92142E 00
0.8987	0.93976E 00
0.9329	0.10362E 01
0.9660	0.98513E 00
1.0008	0.97819E 00
1.0330	0.10067E 01
1.0637	0.10311E 01

DIV: REF=30/E

WAVELENGTH	RATIO
0.3784	0.13576E 01
0.4041	0.10687E 01
0.4299	0.10145E 01
0.4677	0.10493E 01
0.5019	0.10027E 01
0.5366	0.10049E 01
0.5674	0.10000E 01
0.6041	0.10229E 01
0.6312	0.10529E 01
0.6679	0.10444E 01
0.6986	0.10588E 01
0.7339	0.10357E 01
0.7645	0.10241E 01
0.7999	0.10088E 01
0.8310	0.10027E 01
0.8653	0.92875E 00
0.8987	0.94867E 00
0.9329	0.10457E 01
0.9660	0.99334E 00
1.0008	0.98752E 00
1.0330	0.10160E 01
1.0637	0.10429E 01

DIV: REF=35/E

WAVELENGTH	RATIO
0.3784	0.13254E 01
0.4041	0.10581E 01
0.4299	0.10094E 01
0.4677	0.10431E 01
0.5019	0.99981E 00
0.5366	0.10046E 01
0.5674	0.10000E 01
0.6041	0.10272E 01
0.6312	0.10560E 01
0.6679	0.10505E 01
0.6986	0.10639E 01
0.7339	0.10416E 01
0.7645	0.10300E 01
0.7999	0.10147E 01
0.8310	0.10087E 01
0.8653	0.93608E 00
0.8987	0.95758E 00
0.9329	0.10551E 01
0.9660	0.10016E 01
1.0008	0.99685E 00
1.0330	0.10253E 01
1.0637	0.10547E 01

Table V-2

DIV: REF=40/E

WAVELENGTH	RATIO
0.3784	0.12932E 01
0.4041	C.10475E 01
0.4299	0.10043E 01
0.4677	0.10368E 01
0.5019	0.99693E 00
0.5366	0.10044E 01
0.5674	C.10000E 01
0.6041	0.10314E 01
0.6312	0.10592E 01
0.6679	0.10566E 01
0.6986	C.10690E 01
0.7339	0.10474E 01
0.7645	0.10359E 01
0.7999	C.10206E 01
0.8310	0.10147E 01
0.8653	0.94341E 00
0.8987	0.96649E 00
0.9329	0.10645E 01
0.9660	C.10098E 01
1.0008	0.10062E 01
1.0330	0.10347E 01
1.0637	0.10665E 01

Table V-2 (cont.)

References

1. Adams, J.B. and McCord, T.B., "Remote sensing of lunar surface mineralogy: Implications from visible and near-infrared reflectivity of apollo 11 samples", Proceedings of the Apollo 11 Lunar Science Conference, Vol. 3, 1937-1945, (1970).

2. Adams, J.B. and McCord, T.B., "Vitrification darkening in the lunar highlands and identification of descartes material at the Apollo 16 site", Proceedings of the Fourth Lunar Science Conference, Geochimica Et Cosmochimica Acta, Supplement 4, Vol. 1, 163-177, (1973).

3. Arvesen, J.C., Griffin, R.N. and Pearson, B.D., Jr., "Determination of extraterrestrial solar spectral irradiance from a research aircraft", Applied Optics, Vol. 8, No. 11, 2215-2232, (November 1969).

4. Bass, L., "PHOTOM Manual", unpublished, MIT Remote Sensing Laboratory, Cambridge, Mass., (1975).

5. Elias, J.H., "Calibration of standard stars for planetary reflectivity studies", M.S. Thesis MIT, Department of Physics and Department of Earth and Planetary Sciences, (September 1972).

6. Gaffey, M.J., personal communication, 1975.

7. Hayes, D.S., "An absolute spectrophotometric calibration of the energy distribution of twelve standard stars", The Astrophysical Journal, Vol. 159, 165-176, (January 1970).

8. Hayes, D.S. and Latham, D.W., "A rediscussion of the atmospheric extinction and the absolute spectral-energy distribution of vega", The Astrophysical Journal, Vol. 197, 593-601, (May 1, 1975).

9. Hayes, D.S., Latham, D.W. and Hayes, S.H.,"Measurements of the monochromatic flux from vega in the near-infrared", The Astrophysical Journal, Vol. 197, 587-592, (May 1, 1975).

10. Hoffleit, D., ed. Yale Bright Star Catalogue, Yale University Observatory, New Haven, Conn., (1964).

11. Iriarte, B., Johnson, H.L., Mitchell, B.I. and Wisniewski, W., Arizona-Tonantzintla Catalogue, Sky and Telescope, 24-31, (July 1965).

12. Kurucz, R.L., "A progress report on theoretical four-dimensional photometry of F, A, and B Stars", Presented

at Conference on Multicolor Photometry and the Theoretical HR Diagram, State University of New York at Albany, October 26, 1974, Preprint Series No. 234 of the Center for Astrophysics, Cambridge, Mass.

13. Kurucz, R.L., personal communication, 1975.

14. Labs, D. "The energy flux of the sun (A critical discussion of standard values for the solar irradiance)", Problems in Stellar Atmospheres and Envelopes, ed. B. Baschek, W.H. Kegel, and G. Traving, 1-19, New York: Springer-Verlag, 1975.

15. Labs, D. and Neckel, H., "The radiation of the solar photosphere from 2000Å to 100μ", Zeitschrift für Astrophysik, Vol. 69, 1, (1968).

16. Labs, D. and Neckel, H., "The solar constant (A compilation of recent measurenents)", Solar Physics, Vol. 19, 3-15, (1971).

17. Labs, D. and Neckel, H., "Remarks on the convergence of photospheric model conceptions and the solar quasi-continuum", Solar Physics, Vol. 22, 64-69, (1972).

18. Lane, A.P. and Irvine, W.M., "Monochromatic phase curves and albedos for the lunar disk", The Astronomical Journal, Vol. 78, No. 3, 267-277, (April 1973).

19. McCord, T.B. and Adams, J.B., "Progress in remote optical analysis of lunar surface composition", The Moon, Vol. 7, 453-474, (1973).

20. McCord, T.B. and Pieters, C., personal communication, 1975.

21. Motz, L. and Duveen, A., Essentials of Astronomy, Belmont, California: Wadsworth Publishing Company, Inc., (1966).

22. Oke, J.B., "Photoelectric spectrophotometry of stars suitable for standards", The Astrophysical Journal, Vol. 140, 689-693, (1964).

23. Oke, J.B. and Schild, R.E., "The absolute spectral energy distribution of alpha lyrae", The Astrophysical Journal, Vol. 161, 1015-1023, (September 1970).

24. Schild, R., personal communication, 1975.

25. Schild, R., Peterson, D.M. and Oke, J.B., "Effective

temperatures of B- and A- type stars", The Astrophysical Journal, Vol. 166, 95-108, (May 15, 1971).

26. Thekaekara, M.P. and Drummond, A.J., "Standard values for the solar constant and its spectral components", Nature Physical Science, Vol. 229, 6-9, (January 4, 1971).

Appendix A Data Reduction Programs

PHOTOM is a series of computer programs developed at the MIT Remote Sensing Laboratory to analyze data from the two-beam filter photometer. The basic programs used in section II of this thesis were Kilroy, Moonray, Subtract, Mumpit, Mushkin, Reaverage, Reratio, and Dataplot. Only those functions actually used for data reduction in this thesis are described.

Kilroy: This program accepts photometer data as input and outputs object intensity for each filter in photon counts/second. The sky data (beam two) is automatically subtracted from the object data. The output is then used as Mumpit input.

Moonray: This program is a variation of Kilroy for use with lunar data where the two beams of the photometer must be treated independently. The program accepts photometer data as input and outputs two object intensities for each filter in counts/second.

Subtract: This program subtracts scattered light observations in counts/second for each filter from the object reflectance for that filter in counts/second. Scattered light observations are necessary when making lunar observations. The observations are made with a metal slug substituted for the aperture. Any count recorded is then due to scattered light present in the photometer (see section II.B.2.).

Mumpit: The input to this program are data records produced by Moonray or Kilroy. This program stores such information as the date and sidereal time of observation, right ascension and declination of the object, and the declination of the observatory. Using this information it calculates the air mass at which the data was measured. All of this information is stored with the data as an object record. The user can also create a "starpack" which calculates the atmospheric extinction for a sequence of data records. For each wavelength a least squares fit is derived for the logarithm of the intensity versus the air mass for the observations. The resulting slope and intercept (at one air mass) for each filter is stored as a starpack to be used as a standard. The program also outputs a graph of wavelength versus the slope coefficients and a graph of wavelength versus the intercepts. If the sky is transparent, the slope coefficients should approach a maximum value of zero towards the infrared, since the Rayleigh scattering is greatly diminished.

Mushkin: This program ratios the intensity values for each filter of a run at a given air mass to the intensity values for the corresponding filter of the designated starpack or standard at that air mass (as calculated from the extinction curve). The ratios are normalized to unity at 0.57μM. A standard deviation and standard error of the mean are calculated for each inputted wavelength. The standard error is

is a statistical error defined as the error of the mean of the data points, i.e. the error bars indicate the range that the mean of the observations can be expected to vary within. (see section II.B.1. and 2.).

Reaverage: Reaverage is used to compute composite averages of Mushkin ratios. This program was used to compute the necessary star/star links to obtain Alf Lyr/MS2 as described in section II.B.1. and to average the set of Alf Lyr/Sun flux ratios for each of the reference phase angles as described in section II.B.6. It was also used to calculate MS2/standard for those nights with more than 30 runs of MS2, since 30 is the maximum number of runs accepted by Mushkin for input. Thus, for those nights two individual Mushkin ratios were calculated and then averaged using Reaverage.

Two options exist for computation of statistical errors with this program. One option is to calculate a standard error of the mean of the inputted data points. This method ignores the errors associated with each individual data point. It is reliable only for large numbers of runs. The second method averages the standard errors of the means for the inputted data points and assigns this average value as the new standard error of the mean. This gives a more reliable result when small numbers of runs are involved. This second method was used for all applications of Reaverage except averaging the Alf Lyr/Sun flux ratios reduced to a reference

phase.

Reratio: This program allows the user to multiply or divide inputted Mushkin ratios by one another, for example: $(\text{MS2/Alf Aqr})^{-1} \cdot (\text{Alf Aqr/Alf Lyr})^{-1} = \text{Alf Lyr/MS2}$. The error assigned to the new ratio is the square root of the sum of the the squares of the object error and the new standard error times the average of the new standard. Thus, for the example above, Alf Lyr is the object and MS2 is the new standard. The error assigned for a specific wavelength is:

$$\left[(\text{stnd. error of Alf Lyr})^2 + \{(\text{stnd.er. of MS2})(\text{reflec. for MS2})\}^2\right]^{1/2}$$

(see section II.B.4.).

Dataplot: Dataplot generates the instructions via magnetic tape to produce Calcomp plots of the finished spectral reflectance curves. Note that this program was used to plot star/star, moon/star, and Alf Lyr/Sun flux ratios. All such figures should be labelled as "flux ratio normalized at 0.57μM" rather than as a spectral reflectance.

Appendix B Converting m_ν to F_λ for the Data from Kurucz

λ_2=wavelength of star for which F_λ is desired

λ_{st}=wavelength of star which is to be used as the reference or standard wavelength

m_2 =apparent magnitude of star at λ_2

m_{st}= apparent magnitude of star at λ_{st}

F_{ν_2} =flux in frequency space of star at λ_2

$F_{\nu_{st}}$ =flux in frequency space of star at λ_{st}

F_{λ_2} =flux in wavelength space of star at λ_2

$F_{\lambda_{st}}$=flux in wavelength space of star at λ_{st}

Let λ_{st}=0.8260μM. Then m_{st}=9.852 (from model by Kurucz(12))

Using the basic equation:

$$m_2 - m_{st} = -2.5 \log (F_2/F_{st})$$

$$\log(F_2/F_{st}) = (m_2 - m_{st})/-2.5$$

$$(F_2/F_{st}) = 10^{(m_2 - m_{st})/-2.5} = 10^{-m_2/2.5} \cdot 10^{m_{st}/2.5}$$

$$= (8725.7) \cdot 10^{-m_2/2.5}$$

To convert from frequency space to wavelength space:

$$\nu\lambda = c; \quad \nu = c/\lambda$$

$$1/d\nu = (\lambda^2/c)(1/d\lambda)$$

$$F_\nu \equiv dF/d\nu = (\lambda^2/c)\, dF/d\lambda \equiv (\lambda^2/c) F_\lambda$$

Thus,

$$F_{\nu_2} = (\lambda_2^2/c) \cdot F_{\lambda_2} \; ; \quad F_{\nu_{st}} = (\lambda_{st}^2/c) \cdot F_{\lambda_{st}}$$

And ratioing to the reference:

$$(F_{\nu_2} / F_{\nu_{st}}) = (\lambda_2 / \lambda_{st})^2 \cdot (F_{\lambda 2} / F_{\lambda st})$$

$$(F_{\lambda_2} / F_{\lambda_{st}}) = (\lambda_{st} / \lambda_2)^2 \cdot (F_{\nu 2} / F_{\nu_{st}})$$

The converted fluxes of Kurucz were then compared to those of Elias at several wavelengths in continuum areas to check the calculations. The values agreed to within $\pm$0.5% (see section III).